

UNIVERSITE DU QUEBEC A MONTREAL

LA TAPHONOMIE DES CORAUX PROFONDS DES CIMETIÈRES SOUS-
MARINS D'ORPHAN KNOLL ET DE FLEMISH CAP, UNE ÉTUDE
PRÉLIMINAIRE AUX ANALYSES GÉOCHIMIQUES

MÉMOIRE

PRÉSENTÉ

COMME EXIGENCE PARTIELLE

DE LA MAÎTRISE EN SCIENCES DE LA TERRE

PAR

BLÉNET AURÉLIEN

FEVRIER 2016

UNIVERSITÉ DU QUÉBEC À MONTRÉAL
Service des bibliothèques

Avertissement

La diffusion de ce mémoire se fait dans le respect des droits de son auteur, qui a signé le formulaire *Autorisation de reproduire et de diffuser un travail de recherche de cycles supérieurs* (SDU-522 – Rév.07-2011). Cette autorisation stipule que «conformément à l'article 11 du Règlement no 8 des études de cycles supérieurs, [l'auteur] concède à l'Université du Québec à Montréal une licence non exclusive d'utilisation et de publication de la totalité ou d'une partie importante de [son] travail de recherche pour des fins pédagogiques et non commerciales. Plus précisément, [l'auteur] autorise l'Université du Québec à Montréal à reproduire, diffuser, prêter, distribuer ou vendre des copies de [son] travail de recherche à des fins non commerciales sur quelque support que ce soit, y compris l'Internet. Cette licence et cette autorisation n'entraînent pas une renonciation de [la] part [de l'auteur] à [ses] droits moraux ni à [ses] droits de propriété intellectuelle. Sauf entente contraire, [l'auteur] conserve la liberté de diffuser et de commercialiser ou non ce travail dont [il] possède un exemplaire.»

[Cette page a été laissée intentionnellement blanche]

REMERCIEMENTS

Je tiens tout d'abord à remercier mes deux superviseurs : M. Claude Hillaire-Marcel et M. Evan Edinger. Sans leur aide, leurs conseils, leur expérience et leur patience, jamais cette étude n'aurait abouti à la conclusion matérialisée par le présent mémoire. Plus particulièrement je remercie Claude Hillaire-Marcel pour m'avoir donné la chance d'être son étudiant ainsi que l'opportunité et les moyens d'effectuer cette recherche. Je remercie Evan Edinger pour m'avoir offert l'opportunité de venir travailler au Canada, pour la transmission de son savoir et pour son amitié.

Je remercie également toute ma famille qui a su me soutenir dans les choix que j'ai pu faire et qui a toujours été là dans les bons comme dans les mauvais moments. À mes parents à qui je dois mon intérêt pour les sciences naturelles, à mes soeurs pour leurs encouragements qui même distant de plusieurs milliers de kilomètres ont su me pousser de l'avant et à mes grands parents qui savent me rappeler que si le passé est important l'avenir l'est tout autant.

Je remercie tous mes collègues et amis du GÉOTOP et du département des sciences de la Terre de l'UQAM. Dans ce genre de liste il y a généralement beaucoup d'oubliés aussi je vais les remercier d'abord, car toutes les interactions, discussions et autres moments de détente ont contribué à l'achèvement de ce travail. Merci donc à tous les oubliés. Je tiens à remercier Antoine Thibault pour sa franche camaraderie, Mathieu Chevalier, Florianne Moreira, Marie-Michelle Ouellet-Bernier et Geneviève Vautour pour leur amitié et grâce à qui j'ai vraiment apprécié mon temps passer à travailler à l'UQAM. Aurélie Aubry et Nicolas Pujol pour m'avoir supporté dans le bureau.

Laurence Nuttin pour son empathie. J.B. Poulihneec pour nos discussions à batons rompus. Un grand merci également à Bassam Ghaleb pour sa gentillesse et son intelligence. Merci à André Poirier pour sa franchise et sa bonne camaraderie. Je remercie toutes les personnes qui de près ou de loin ont participé à ce projet : Pauline Méjean, Lucie Ménabréaz, Jenny Maccali, Nicolas Van Neuwenhove, Quentin Simon, Audrey Limoges.

Je tiens également à remercier Michel Lamothe, Daniele Pinti et Anne de Vernal qui m'ont permis d'enseigner pendant ma maîtrise.

Je remercie aussi Pierre-Olivier Bruna, Florianne Bruna et Antoine Faure pour leur bons conseils géologiques ou non. Je tiens également à remercier Marc Floquet et Loïc Villier, mes anciens maîtres, pour m'avoir introduit dans le monde de la recherche scientifique.

Je remercie enfin DFO et NSERC pour avoir financé la mission du ROPOS sur l'Hudson au large de TerreNeuve en 2010.

AVANT-PROPOS

"Here lies one whose name was writ in water."

John Keats (1795 - 1821)

Je prie le lecteur de ne pas considérer seulement cette épitaphe comme de simples élans romantiques, mais bien comme l'expression du poète John Keats exprimant la brièveté des traces que laisse un être vivant à sa mort. Cette seule phrase exprime la raison d'être de la taphonomie. Car en effet si la vie d'un homme se résumait à un livre biographique, il en manquerait bien des pages. Celles que d'autres ou lui-même auraient oublié. Il en va de même pour l'histoire de la vie. Les lacunes stratigraphiques sont autant de pages manquantes que les organismes non préservés par la fossilisation sont de mots effacés.

Notre compréhension de l'évolution des paléo-environnements au cours du temps se heurte à ce problème majeur. Et malheureusement c'est un problème qui va croissant au fur et à mesure que l'on remonte dans le temps. Quantifier cette perte d'information est l'un des buts de la taphonomie expérimentale. C'est ainsi, par exemple, que le groupe du SSETI (pour Shelf and Slope Experimental Taphonomy Initiative) travaille sur la dégradation de coquilles de mollusques dans le golfe du Mexique depuis 1997. L'intérêt de ce type de recherche étant de comprendre, grâce au principe de l'actualisme, comment dans des environnements similaires, les restes organiques se sont dégradés par le passé.

Cette recherche s'inscrit dans la droite ligne de ces travaux de taphonomie expérimentale. En effet l'opportunité nous est ici donnée d'observer la dégradation de restes organiques, sur une longue période de temps, dans un environnement très particulier qu'est le milieu marin profond. Nous nous proposons ainsi de contribuer à la compréhension de ces phénomènes qui dégradent l'information au cours du temps. Nous tâchons de proposer les outils adaptés afin de permettre de recoller une partie des pages manquantes et retrouver une partie des mots effacés.

TABLE DES MATIERES

| | |
|---|------|
| REMERCIEMENTS..... | v |
| AVANT-PROPOS..... | vii |
| LISTE DES FIGURES..... | xiii |
| LISTE DES TABLEAUX..... | xvii |
| RÉSUMÉ..... | xix |
| INTRODUCTION..... | 1 |
| 0 . 1 Références..... | 9 |
| CHAPITRE I | |
| DEEP-SEA CORALS FROM ORPHAN KNOLL: TAPHONOMIC PROCESSES IN A LOW BURIAL RATE ENVIRONMENT SINCE 180 000 YEAR..... | 17 |
| 1.1 Abstract..... | 17 |
| 1.2 Introduction..... | 18 |
| 1.3 Methods..... | 21 |
| 1.3.1 Location..... | 21 |
| 1.3.2 ROPOS equipment..... | 22 |
| 1.3.3 Sampling..... | 23 |
| 1.3.4 Videos analysis..... | 23 |
| 1.3.5 Sample selection for taphonomic studies..... | 23 |
| 1.3.6 Analyses of corals preservation..... | 24 |
| 1.3.7 Taphonomic ranks description..... | 26 |
| 1.3.8 Statistical description of taphonomic variables..... | 28 |
| 1.3.9 Sample selection for dating..... | 28 |

| | |
|---|----|
| 1.3.10 Radiocarbon dating..... | 29 |
| 1.3.11 U-series dating..... | 30 |
| 1.3.12 Statistics for distribution curve..... | 31 |
| 1.3.13 Relationship between taphonomic index and sample age..... | 32 |
| 1.3.14 Relationship among taphonomic variables..... | 32 |
| 1.4 Results..... | 33 |
| 1.4.1 Sample area description..... | 33 |
| 1.4.2 Taphonomic description..... | 34 |
| 1.4.3 Radiocarbon and U-series dating..... | 40 |
| 1.4.4 Taphonomic parameters vs sample age..... | 45 |
| 1.4.5 Relation between taphonomic parameters..... | 50 |
| 1.5 Discussion..... | 54 |
| 1.5.1 Effect of burial..... | 54 |
| 1.5.2 Taphonomy processes through time in deep-sea..... | 56 |
| 1.5.3 Shallow marine and deep-sea environment comparison..... | 58 |
| 1.5.4 Paleooceanographic implications of coral age distribution..... | 60 |
| 1.6 Conclusion..... | 64 |
| 1.7 References..... | 65 |
| CHAPITRE II | |
| CONCLUSION..... | 77 |
| 2.1 Références..... | 80 |
| APPENDICE A | |
| SÉLECTION DES ÉCHANTILLONS GRÂCE À DES CRITÈRES TAPHONOMIQUES..... | 81 |
| A.1 Description des paramètres..... | 81 |
| A.2 Enregistrement des données..... | 87 |
| A.3 Discrimination des différentes populations..... | 87 |

APPENDICE B

| | |
|---|----|
| MÉTHODE DE NETTOYAGE ET DATATION U/Th..... | 89 |
| B.1 Nettoyage..... | 89 |
| B.1.1 Nettoyage physique..... | 89 |
| B.1.2 Nettoyage chimique..... | 89 |
| B.2 Datation U/Th..... | 90 |
| B.2.3 Préparation du traceur..... | 90 |
| B.2.4 Récupération chimique de l'Uranium et du Thorium..... | 90 |
| B.2.5 Séparation de l'Uranium et du Thorium..... | 91 |
| B.2.6 Mesure au spectromètre de masse..... | 91 |
| B.3 Références..... | 92 |
| BIBLIOGRAPHIE..... | 93 |

LISTE DES FIGURES

| Figure | Page |
|--|------|
| Figure 0.1 profondeur des environnements des études taphonomique en relation avec la durée de dégradation des restes organiques..... | 3 |
| Figure 0.2 Photos de la zone d'échantillonnage prises avec la caméra HD du ROPOS. A) Vue de la falaise de Flemish cap et du cimetière. B) communauté de <i>Desmophyllum dianthus</i> vivants sur la falaise de Flemish cap. C) assemblage de coraux fossiles dans le cimetière de Flemish cap. D) Vue de la falaise d'Orphan Knoll, l'échelle est centrée sur le milieu de l'image. E) Vue de la falaise Orphan Knoll. F) Assemblage de coraux profond fossiles dans le cimetière sous la falaise d'Orphan Knoll | 8 |
| Figure 1.1 Location of two deep-sea graveyards (red stars) investigated during the 2010 Hudson mission off the coast of Newfoundland. A) Map of North-Eastern American margin. B) Map of Newfoundland and the location of Orphan Knoll and Flemish cap. C) Bathymetric map of Orphan and Flemish cap and the location of the deep-sea corals graveyards, the interval between the level lines is 500 meter. D) Detail of the bathymetric map focused on Orphan knoll and the position of the graveyard. E) Detail of the bathymetric map focused on Flemish cap and the position of the graveyard. | 22 |
| Figure 1.2 Taphonomic parameters and ranks. Pictures A to E) absence of encrustation to high level of encrustation mostly caused by Serpulids. Pictures F to J) absence of macrobioerosion to high level mostly caused by action of lithophagous organisms and sea urchins. Pictures K to O) fully clear details to complete loss of details on whole parts of the skeleton. Pictures P to T) well preserved skeleton to heavily broken skeleton..... | 25 |
| Figure 1.3 Total of degraded specimen by rank of each taphonomic processes in function of the location where they have been collected. A) Macrobioerosion rank distribution in function of the number of specimen. B) Loss of details rank distribution in function of the number of specimen. C) Encrustation rank distribution in function of the numbers of specimen. D) Breakage ranks distribution in fuction of the number of specimen..... | 35 |

- Figure 1.4 Pictures of the different type of encrustation (scale bar = 2mm). A) Serpulid calcite tube. B) Bryozan disc. C) Branching bryozoan. D) Sponge spicules. E) Juvenile *D. dianthus*. F) Tunicate. 36
- Figure 1.5 Number of specimen degraded by the different type of encrustation, sponges and tunicate are soft bodied organisms. Total *D. dianthus* population n=142, collected in Orphan Knoll and Flemish Cap. 37
- Figure 1.6 Pictures of different type of macrobioerosion (scale bar = 2mm). A) *Entobia* made by endolithic sponges. B) Grazing traces made by sea urchins. C) Gallery in *D. dianthus* skeleton made by endolithic worm. 37
- Figure 1.7 Number of specimen degraded by the different type of macrobioerosion. Total *D. dianthus* population n=142, collected in Orphan Knoll and Flemish Cap. 38
- Figure 1.8 Pictures of colour diversity of *D. dianthus* mostly caused by precipitation of Mn oxide coating (scale bar = 1cm). A) D39 sample. B) D14 sample. C) D5 sample. D) D59 sample. 38
- Figure 1.9 Scatter diagram of PCA result on colour data from *D. dianthus* population collected in O.K. The first axis is strongly related with dark/fair difference and explain 80.79% of the data dispersion. The second axis explain 16.1% of the total population variance and is strongly related to red gradient. This diagram was realized using R software on a total *D. dianthus* population n=142m. Triangles are for Flemish Cap specimens, dots for Orphan Knoll specimens. 39
- Figure 1.10 age distribution diagram and predicted distribution curves using equation 1 on Orphan Knoll samples, h represent the smoothing parameter and n the number of samples the density function calculated with equation 1 is the probability density function of the sample distribution. A) Distribution for the full length of time represented by our sample suite (n = 17, h = 2.981e4) age bins 2,000 years. B) Detail of the distribution for the Holocene and associated density curve (n = 7, h = 2227), age bins 500 years. C) Detail of the distribution for the MIS 5 with the associated density curve (n = 9, h = 672.6) age bins 500 years. 43
- Figure 1.11 Cluster analysis of the total specimen population using the taphonomic rank level. Aged specimen are colored marked in function of their age. The four groups were determined by the software using the height. Triangles are for Flemish Cap specimens, dots for Orphan Knoll specimens. 44

Figure 1.12 Taphonomic ranks distribution for aged samples (n=18), with logarithmic regression curves, horizontal error bar were acquired during experimentation. Because of the horizontal scale some dot are overlapped, green are for Orphan Knoll samples and dark grey for Flemish cap samples. All the ages are cal. BP. A) Macrobiosion distribution B) Loss of details distribution. C) Encrustation distribution. D) Breakage distribution..... 46

Figure 1.13 Detailed taphonomic ranks distribution for aged samples (n=18), horizontal error bar were acquired during experimentation. Because of the horizontal scale some dot are overlapped, green are for Orphan Knoll samples and dark grey for Flemish cap samples. All the ages are cal. BP. A) Sponges macroboring distribution B) Encrustation of serpulids tubes distribution. C) Encrustation of sponges distribution. D) Sea urchin grazing traces distribution..... 48

Figure 1.14 Dispersion diagramm using colour PCA data and dated specimen. The first axis wich is strongly related to dark/fair difference explain 81.95% of the data dispersion. Green colour marked live collected specimen, orange and red the Holocene specimen, purple for the MIS 5 specimen and blue for MIS 7 specimen. Triangles are for Flemish Cap specimens, dots for Orphan Knoll specimens..... 49

Figure 1.15a taphonomic rank distribution the left column is for samples collected at Orphan Knoll the right column for samples collected at Flemish cap. A) Loss of details rank distribution in function of macrobioerosion index. B) Encrustation rank distribution in function of macrobioerosion index. C) Breakage rank distribution in function of macrobioerosion index. D) Same as A for Flemish cap. E) Same as B for Flemish cap. F) Same as C for Flemish cap. 51

Figure 1.15b taphonomic rank distribution the left column is for samples collected at Orphan Knoll the right column for samples collected at Flemish cap. A) Breakage rank distribution in function of loss of details index. B) Encrustation rank distribution in function of loss of details index. C) Encrustation rank distribution in function of breakage index. D) Same as A for Flemish cap. E) Same as B for Flemish cap. F) Same as C for Flemish cap. 52

Figure 1.16 Dispersion diagramm using colour PCA data and the other taphonomic processes ranks. A) Macrobioerosion ranks dispersion. B) Loss of details ranks dispersion. C) Encrustation ranks dispersion. D) Breakage ranks

| | |
|---|----|
| dispersion. Triangles are for Flemish Cap specimens, dots for Orphan Knoll specimens..... | 53 |
| Figure 1.17 model for taphonomic processes recording through realtive time. The saturation value represent the highest value on the semi-quantitative scale.. | 57 |
| Figure 1.18 position of the polar front during Last Glacial period modified from Thiagarajan et al. (2013) and the actual position of the polar front in the Labrador Sea, data from Montserrat et al. (2011). Zone where <i>D. dianthus</i> were collected are pointed with red plots. New England and Corner Rise seamounts were investigated by Thiagarajan et al. (2013), Orphan Knoll and Flemish cap deep-sea corals graveyards were investigated during Hudson cruise in 2010..... | 62 |
| Figure A.1 Clichés de <i>D. dianthus</i> , scale barr = 0.5 mm. A) Septa de l'échantillon D57 comprenant : C=cassure de niveau 1 et R= rugosité. B) Epithéca de l'échantillon D47 comprenant : O=ornementation. C) Vue d'ensemble de l'échantillon D57 montrant les différentes parties du corail : S=Septa, E=épithéca et B=base..... | 82 |

LISTE DES TABLEAUX

| Tableau | Page |
|--|------|
| Tableau 1.1 Number of taphonomically studied specimens from each location and the number alive or subfossils analyzed for age distribution by ^{14}C or U-series from each locations (total = 19). | 24 |
| Tableau 1.2 Number of specimen from each taphonomic category. Those category are the result of the evaluation of different parameters as colour (Mn oxide), macro-boring, encrustation , breakage and loss of details. | 29 |
| Tableau 1.3 $\delta^{13}\text{C}$, $\delta^{18}\text{O}$ and ages obtained on deep-sea corals samples * = live-collected specimen, ** = Flemish cap specimen. $\delta^{13}\text{C}$ and radiocarbon datation for Isidids D22 and D23 were run at ANU lab, with $\delta^{18}\text{O}$ analyzed separately at GEOTOP laboratory therefore not really a split sample. For the other radiocarbon dating samples, datation were run in CEA Saclay center and stable isotopes in GEOTOP laboratory on the same sub-sample. For the U-series dating samples analyses, including stable isotopes, were made in GEOTOP laboratory on the same sub-sample. | 41 |
| Tableau 1.4 U-series ages measured by TIMS. Half-lives of ^{234}U and ^{230}Th used in the calculations are $245,250 \pm 490$ yr and $75,690 \pm 230$ yr respectively (Cheng et al., 2000). The decay constant for ^{238}U is $1.551 \times 10^{-10} \text{ year}^{-1}$ (Jaffey et al., 1971). Ages are calculated according to equation defined by Edwards (1978) with no correction for initial ^{230}Th . All errors are 2σ | 42 |
| Tableau 1.5 Kruskal Wallis rank sum test differentiating each population (Holocene vs Pleistocene) for each parameter. | 47 |
| Tableau 1.6 Kendall correlation rank test results between the different parameters. T represent the strength of association for each parameter in row with the one in column. A value of 1 is for a perfect association and 0 the absence of association. | 50 |
| Tableau 1.7 Kendall coefficient test between colour and taphonomic parameters. W is Kendall's coefficient of concordance, $F = W*(m-1)/(1-W)$ where m is the number of judges, Prob.F is the probability associated with F statistic, the | |

| | |
|---|----|
| Chi ² is Friedman's Chi ² statistic and Prob.perm is the permutation probability..... | 54 |
| Tableau B.1 procédures de nettoyage chimique..... | 90 |

RÉSUMÉ

Le but principal de cette recherche est d'étudier la dégradation de coraux azooxanthelles dans un environnement marin profond et de comprendre l'occurrence des fossiles de *Desmophyllum dianthus* basée sur leur datation dans les cimetières sous-marin d'Orphan Knoll et de Flemish cap. 19 squelettes de coraux ont été datés en utilisant la méthode du radiocarbone et 11 de ces spécimens ont été daté par la méthode U/Th. Trois différentes populations de coraux ont été identifiées : une population Holocène (73 à 10000 ans BP) , une population du Stade Marin Isotopique 5 (97000 à 112000 ans BP) et un spécimen datant du Stade Marin Isotopique 7 (181000 années BP). Cette distribution a été reliée au déplacement Nord/Sud du front polaire entre les périodes interglaciaire et glaciaires. 142 spécimens de coraux de la mer du Labrador ont été analysés taphonomiquement et les différents processus taphonomiques ont été identifiés. Ces processus ont été quantifiés en utilisant une échelle semi-quantitative. Il a été démontré que dans cet environnement de basse vitesse de sédimentation, l'échantillon reste sur le fond de la mer sur une longue période de temps. Le taux d'enfouissement lent explique les principales différences observées entre milieu marin profond et peu profond. L'utilisation de tests statistiques a montré que la plupart des processus taphonomiques liés à l'âge des spécimens sont causés par la micro et la macro bioerosion issue de l'action d'éponges, d'oursins et de micro-organismes. Une valeur de saturation du signal taphonomique a été définie pour chaque processus. Cette valeur est atteinte à différents moments selon le processus taphonomique étudié. Ces différences, illustrées par des analyses multivariées, sont les clefs pour comprendre les relations entre les processus de dégradation et leur enregistrement sur le squelette d'un organisme en milieu marin profond.

Mots clefs : paléontologie, taphonomie, milieu profond, radiocarbone, U/Th, mer du Labrador

INTRODUCTION

L'étude et la compréhension du monde qui nous entoure passe par l'étude de son passé et par la compréhension des changements qui sont intervenus depuis lors. Les témoignages de ces changements laissent des traces analysables dans les enregistrements fossiles que sont les roches sédimentaires et les assemblages fossiles qu'elles contiennent. Cependant plus loin on remonte dans le passé, plus ces archives sont incomplètes (Allison et Bottjer, 2011). En effet au cours des temps géologiques de nombreux facteurs, faisant partie de la télogénèse, de la diagenèse tardive ou du métamorphisme, dégradent les enregistrements fossiles (Andrews, P., 1995 ; Powell, W., 2003). Ces processus se produisent longtemps après l'enfouissement et la fossilisation des restes organiques. D'autres facteurs interviennent eux directement après la mort des organismes et perdurent jusqu'à leur fossilisation. Ces facteurs concernent les passages de biocénose à thanatocénose et de thanatocénose à taphocénose (Fürsich et Pandey, 1999). Leur étude, qui vise à comprendre la dégradation des restes organiques au cours du temps, est appelée taphonomie (Efremov, 1940).

En milieu marin les processus taphonomiques qui affectent les assemblages de restes organiques commencent au cours du vivant de l'organisme, comme l'encrouement, la bioérosion ou la lithification (Friedman, 1964 ; Ginsburg, 1954 ; Nothdurft et Webb, 2009 ; Strasser et Strohmenger, 1997). Ces processus ont un impact sur la préservation des coquilles dans les enregistrements fossiles et influent sur les reconstitutions des conditions environnementales passées (Efremov, 1940). En préservant les organismes préférentiellement squelettiques en fonction de la minéralogie de leur squelette ou leur résistance, les processus taphonomiques

introduisent un biais dans les archives fossiles pour la reconstruction de la biodiversité passé (Cherns et Wright, 2009). Certains de ces processus sont causés par des organismes qui ont utilisé les squelettes comme habitat ou sources d'alimentation. Ces organismes comme les algues et les cyanobactéries qui corrodent squelette sont restreints à la zone photique et ne peuvent pas vivre sur la pente ou en environnement marin profond. De plus certaines espèces bioérodeuses comme certains oursins dépendent de ces organismes pour s'alimenter. Le panel d'organismes corrodeurs va donc lui aussi dépendre de l'environnement et être plus restreint en environnement profond. Les processus taphonomiques sont dépendant de l'environnement de dépôt des assemblages des restes organiques.

Les processus de dégradation des environnements marins peu profonds sont de plus en plus documentés ces dernières décennies, notamment par Shelf and Slope Experimental Taphonomy Initiative group (SSETI). Leurs études ont permis de quantifier les processus de dégradation dans divers milieux marins (Parsons, Powell, Brett, Walker et Callender, 1997). Des études à court terme - ± 10 ans - (Fig.0.1) ont été réalisées sur plateau continental et la rampe carbonatée des Bahamas (Cai, Chen, Powell, Walker, Parsons-Hubbard, Staff, Wang, Ashton-Alcox, Callender et Brett, 2006 ; Powell, Eric N, Parsons-Hubbard, Callender, Staff, Rowe, Brett, Walker, Raymond, Carlson et White, 2002 ; Powell, Eric N., Parsons-Hubbard, Callender, Staff, Rowe, Brett, Walker, Raymond, Carlson, White et Heise, 2002 ; Walker, Parsons Hubbard, Powell et Brett, 1998). Selon ces études l'influence des cycles d'inhumation et d'exhumation est le phénomène permettant d'expliquer les processus taphonomiques observés (Parsons-Hubbard, Callender, Powell, Brett, Walker, Raymond et Staff, 1999 ; Staff, Callender, Powell, Parsons-Hubbard, Brett, Walker, Carlson, White, Raymond et Heise, 2002). Le taux de dégradation sur le plateau continental est plus rapide que sur la rampe et est lié au taux d'enfouissement des restes organiques. Dans un environnement plus profond et en particulier en bas de pente, le taux de dégradation doit être plus lent en raison des conditions

hydrodynamiques faibles, de l'absence d'organismes encroûtants photosynthétiques comme les algues et les cyanobactéries et la baisse de l'activité des organismes corrodeurs (Walker, Parsons-Hubbard, Powell et Brett, 2002). L'échelle de temps et le taux d'enfouissement sont donc les paramètres les plus importants afin de comprendre les processus taphonomiques.

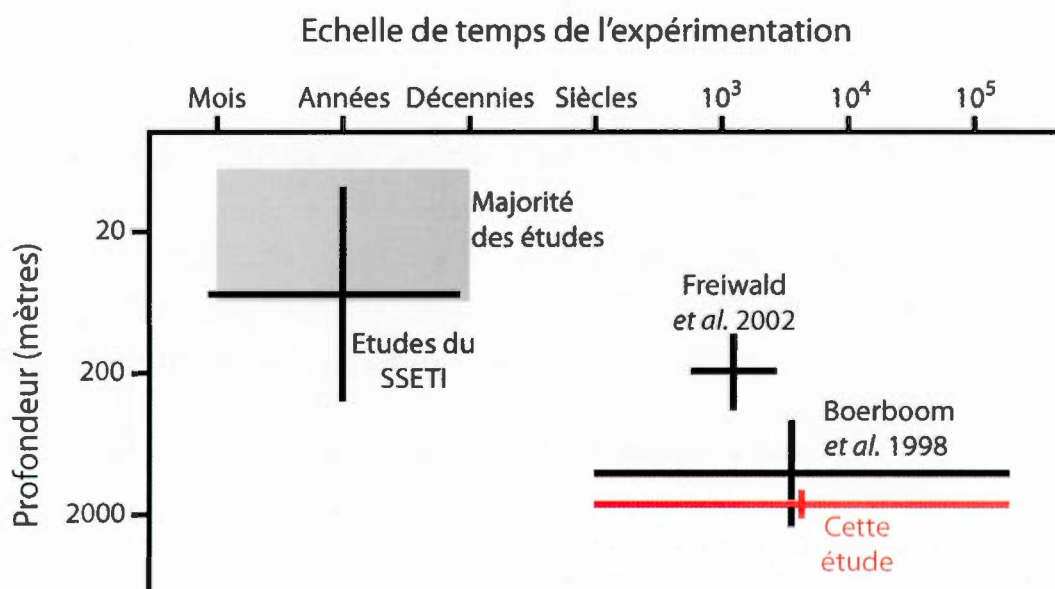


Figure 0.1 profondeur des environnements des études taphonomique en relation avec la durée de dégradation des restes organiques.

Le rapport entre le taux de sédimentation et le taux d'accumulation de coquilles va déterminer le temps moyen pendant lequel les restes organique vont demeurer à l'interface eau sédiment et la rapidité avec laquelle ils seront enfouis. Plus le temps de résidence au fond de la mer des coquilles augmentent plus leur dégradation augmente (Flessa, Cutler et Meldahl, 1993). De plus des variations de ce temps de résidence provoquent des pertes d'informations stratigraphiques en associant des assemblages fossiles qui n'étaient contemporains (Kowalewski, Michał, 1996 ; Kowalewski, Michał et Bambach, 2008 ; Kowalewski, M, Carroll, Casazza, Gupta, Hannisdal, Hendy, Krause Jr, LaBarbera, Lazo et Messina, 2003 ; Kowalewski, Michał et

Hoffmeister, 2003), faussant les interprétations paléo-écologiques issues de l'analyse des assemblages fossiles. Ce temps de résidence peut-être déduit grâce à l'étude de la distribution des âges des coquilles composant les assemblages fossiles (Bambach, 1977 ; Fursich et Aberhan, 1990). Les dépôts de fossiles perturbés par ces variations sont dits *time averaged*. Dans un environnement marin profond, notamment dans le cas d'un cimetière à corail, malgré le faible taux d'accumulation de squelettes, le faible taux de sédimentation, peut provoquer la formation d'une zone à fort taux de résidence. C'est dépôt peuvent donc être *time averaged*.

Cette étude porte donc sur la compréhension des processus taphonomiques en milieu marin profond et sur leur influence quant à la préservation de l'information paléo-environnementale que peuvent fournir les squelettes de *Desmophyllum dianthus*. L'étude des coraux profonds a gagné beaucoup d'importance ces dernières décennies. Depuis leur découverte au 18ème siècle par Linné (1758), leur importance pour la pérennité des écosystèmes marins profonds à été mis en évidence (Auster, 2005 ; Auster, Moore, Heinonen et Watling, 2005 ; Costello, McCrea, Freiwald, Lundälv, Jonsson, Bett, van Weering, de Haas, Roberts et Allen, 2005 ; Mortensen, Pål Buhl, Rapp et Båmstedt, 1998). À l'heure d'importants changements environnementaux, leur protection est devenue une priorité pour la communauté scientifique (Costello *et al.*, 2005 ; Edinger, Evan N, Wareham et Haedrich, 2007 ; Mortensen, P. B., Buhl-Mortensen, Gordon Jr., Fader, McKeown et Fenton, 2005). Leur étude a permis de comprendre le fonctionnement de ces écosystèmes profonds (Auster *et al.*, 2005) mais donne aussi de précieux renseignements sur l'évolution du climat et les changements environnementaux au cours de ces derniers milliers d'années notamment par le biais de l'analyse géochimique de leur squelette (Roberts, J. M., Wheeler, Freiwald et Cairns, 2009).

Afin d'étudier ces changements environnementaux, une attention particulière a été accordée à la composition isotopique de leurs squelettes. En effet en raison de leur

longévité (Andrews, A., Stone, Lundstrom et DeVogelaere, 2009 ; Roark, E. B., Guilderson, Dunbar et Ingram, 2006 ; Roark, E. Brendan, Guilderson, Flood-Page, Dunbar, Ingram, Fallon et McCulloch, 2005 ; Sherwood, O. A. et Edinger, 2009 ; Tracey, Neil, Marriott, Andrews, Cailliet et Sanchez, 2007) ces organismes représentent un enregistrement continu sur plusieurs décennies des conditions environnementales prévalant lors de leur croissance. L'analyse des rapports en isotopes stables du carbone et de l'oxygène (Adkins, Boyle, Curry et Lutringer, 2003 ; Sherwood, Owen A, Heikoop, Scott, Risk, Guilderson et McKinney, 2005) ainsi que l'étude des rapports Sr/Ca (Cohen, Owens, Layne et Shimizu, 2002 ; Hill, LaVigne, Spero, Guilderson, Gaylord et Clague, 2012) et Mg/Ca (Gagnon, Adkins, Fernandez et Robinson, 2007) ont fourni des renseignements notamment pour estimer les paléotempératures. Les changements de conditions hydrographiques ont elles aussi pu être étudiées notamment grâce à l'utilisation des isotopes du Nd (Colin, Frank, Copard et Douville, 2010 ; López Correa, Montagna, Joseph, Rüggeberg, Fietzke, Flögel, Dorschel, Goldstein, Wheeler et Freiwald, 2012 ; Montagna, McCulloch, Mazzoli, Silenzi et Odorico, 2007 ; van de Flierdt, Robinson et Adkins, 2010). Les méthodes de datation U/Th (Eisele, Frank, Wienberg, Hebbeln, López Correa, Douville et Freiwald, 2011 ; Frank, Freiwald, Correa, Wienberg, Eisele, Hebbeln, Van Rooij, Henriët, Colin et van Weering, 2011) et C^{14} (Thiagarajan, Gerlach, Roberts, Burke, McNichol, Jenkins, Subhas, Thresher et Adkins, 2013) ont permis de relier leurs occurrences aux changements de productivité primaire liées aux changements climatiques globaux et aux déplacements du front polaire. La réponse de ces organismes aux changements environnementaux actuels et notamment à l'acidification des océans a elle aussi été étudiée (Form et Riebesell, 2012 ; Foster, Ragazzola, Wall, Form et Freiwald, 2012 ; Guinotte, Orr, Cairns, Freiwald, Morgan et George, 2006 ; Roberts, J Murray, Wheeler et Freiwald, 2006). Toutes ces études ont permis de mettre en évidence l'intérêt de l'étude géochimique des squelettes des

coraux profonds pour la compréhension des changements environnementaux passés et futurs.

Les récentes problématiques liées aux changements climatique ont amené la communauté scientifique à adopter une approche globale des interactions entre atmosphère, système terre et océan. L'analyse de ces interactions est cruciale pour comprendre notamment les cycles climatiques notamment dans l'hémisphère Nord. Cela passe par la compréhension du cycle du carbone, de l'évolution de la productivité primaire et des conditions hydrographiques des océans. Ainsi les projets VITALS et Past4Future étudient l'évolution de ces systèmes afin de comprendre l'évolution des conditions climatiques et paléocéanographiques dans l'Atlantique Nord. Des études notamment sur des carottes sédimentaires (Hillaire-Marcel, C, Vernal, Bilodeau et Wu, 1994 ; Hillaire-Marcel, Claude, Vernal, Lucotte, Mucci, Bilodeau, Rochon, Vallières et Wu, 1994 ; Simon, Hillaire-Marcel, St-Onge et Andrews, 2013 ; Solignac, de Vernal et Hillaire-Marcel, 2004) et des assemblages de foraminifères (de Vernal, Hillaire-Marcel, Peltier et Weaver, 2002) dans la Baie de Baffin et en mer du Labrador ont permis de reconstituer les conditions paléocéanographiques au cours de l'Holocène et de confirmer leur intérêt pour la compréhension globale du système climatique terrestre. La mission de l'Hudson en 2010 au large de Terre-Neuve financée par (DFO, NSERC), s'inscrit dans la compréhension de ces problématiques (Edinger, Evan N. et al., 2010).

Un des buts de cette mission était d'explorer les mounds découverts lors de précédentes missions (Keen, 1978 ; Ruffman, 1989 ; Smith, Risk, Schwarcz et McConnaughey, 1997) à Orphan Knoll et Flemish cap, situé au large de Terre-Neuve. Deux cimetières à coraux profonds ont ainsi été localisés (O.K. : 50°N - 33.12', 46°W - 11.59' et F.c. : 46°N - 20.02', 44°W - 33') respectivement à 1740 mètres et 2200 mètres de profondeur. Des spécimens de coraux profonds appartenant principalement à l'espèce *Desmophyllum dianthus* ont été récoltés par le ROV scientifique canadien

(ROPOS pour Remotely Operated Platform for Ocean Science). Ces cimetières sous-marins se sont formés par l'accumulation de squelettes de *D. dianthus* provenant des falaises (Fig.0.2) surplombants ces formations (Meredyk, Piper, Edinger et Ruffman, 2012b). Considérant le faible taux de sédimentation dans cette zone (Andrews, J., Tedesco, Briggs et Evans, 1994 ; Hillaire-Marcel, C *et al.*, 1994), les squelettes coralliens ne sont pas enfouis rapidement mais restent exposés à l'interface eau/sédiment sur de longue période de temps.

Ces cimetières à coraux profonds trouvés au large de Terre-Neuve, sont donc le résultat d'une accumulation sur le long terme de squelettes aragonitiques de *Desmophyllum dianthus*. Dans un tel contexte la dégradation de ces restes organiques au cours du temps est à considérer afin de mieux aborder l'étude géochimique de ces squelettes à des fins de reconstitutions paléo-environnementales. Les objectifs de cette étude sont : 1) de comprendre en combien de temps et dans quelles conditions ont pu se former ces cimetières, 2) d'analyser la taphonomie dans ce milieu particulier à faible taux d'enfouissement et 3) de proposer une méthode pour aborder l'étude géochimique de ces restes organiques en tenant compte de leur dégradation.

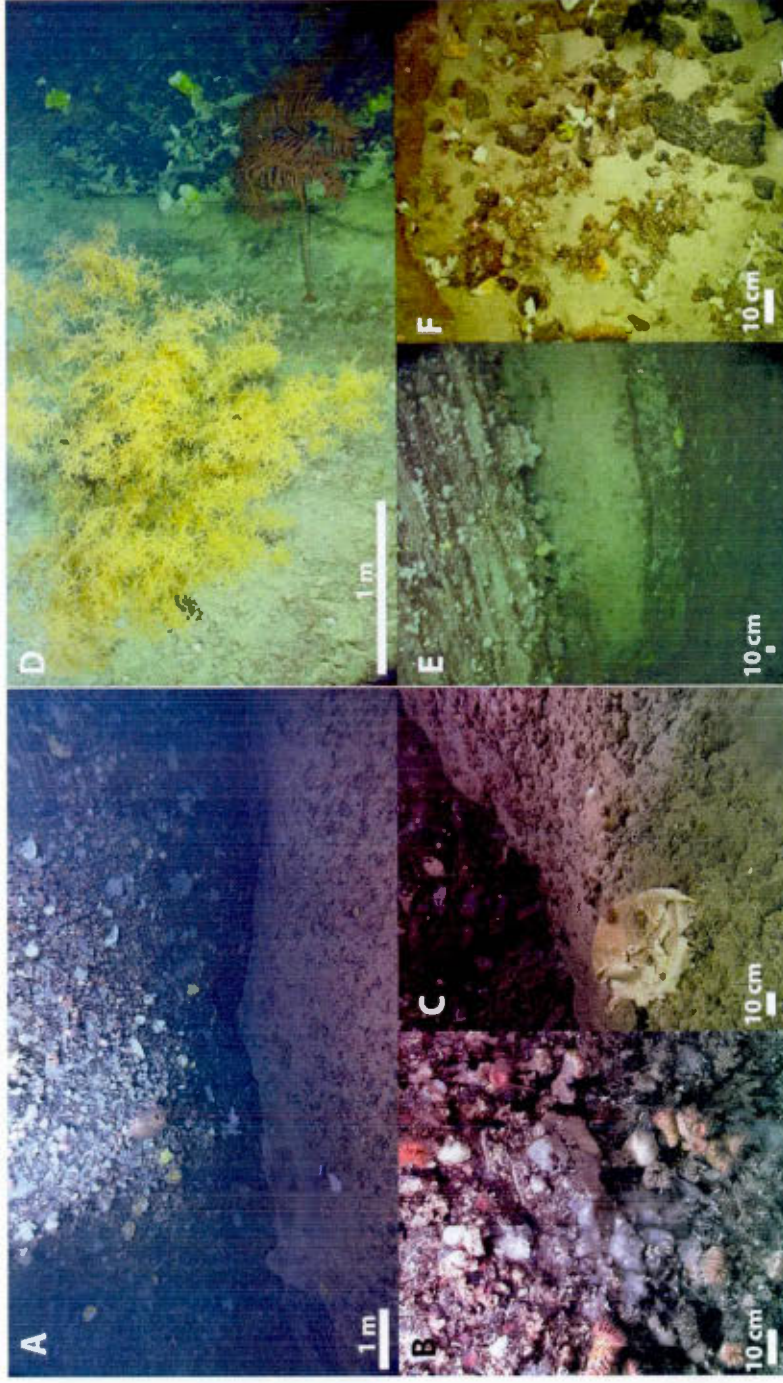


Figure 0.2 Photos de la zone d'échantillonnage prises avec la caméra HD du ROPOS. A) Vue de la falaise de Flemish cap et du cimetière. B) communauté de *Desmophyllum dianthus* vivants sur la falaise de Flemish cap. C) assemblage de coraux fossiles dans le cimetière de Flemish cap. D) Vue de la falaise d'Orphan Knoll, l'échelle est centrée sur le milieu de l'image. E) Vue de la falaise Orphan Knoll. F) Assemblage de coraux profond fossiles dans le cimetière sous la falaise d'Orphan Knoll

0.1 Références

- Adkins, J., Boyle, E., Curry, W. et Lutringer, A. (2003). Stable isotopes in deep-sea corals and a new mechanism for “vital effects”. *Geochimica et Cosmochimica Acta*, 67(6), 1129-1143.
- Allison, P.A. et Bottjer, D.J. (2011). Taphonomy: bias and process through time *Taphonomy* (p. 1-17) : Springer.
- Andrews, A., Stone, R., Lundstrom, C. et DeVogelaere, A. (2009). Growth rate and age determination of bamboo corals from the northeastern Pacific Ocean using refined ²¹⁰Pb dating. *Marine Ecology Progress Series*, 397, 173-185.
<http://dx.doi.org/10.3354/meps08193>
- Andrews, J., Tedesco, K., Briggs, W. et Evans, L. (1994). Sediments, sedimentation rates, and environments, southeast Baffin Shelf and northwest Labrador Sea, 8-26 ka. *Canadian Journal of Earth Sciences*, 31(1), 90-103.
- Andrews, P. (1995). Experiments in taphonomy. *Journal of Archaeological Science*, 22(2), 147-153.
- Auster, P.J. (2005). Are deep-water corals important habitats for fishes? *Cold-water corals and ecosystems* (p. 747-760) : Springer.
- Auster, P.J., Moore, J., Heinonen, K.B. et Watling, L. (2005). A habitat classification scheme for seamount landscapes: assessing the functional role of deep-water corals as fish habitat *Cold-water corals and ecosystems* (p. 761-769) : Springer.
- Bambach, R.K. (1977). Species richness in marine benthic habitats through the Phanerozoic. *Paleobiology*, 152-167.
- Cai, W.-J., Chen, F., Powell, E.N., Walker, S.E., Parsons-Hubbard, K.M., Staff, G.M., Wang, Y., Ashton-Alcox, K.A., Callender, W.R. et Brett, C.E. (2006). Preferential dissolution of carbonate shells driven by petroleum seep activity in the Gulf of Mexico. *Earth and Planetary Science Letters*, 248(1), 227-243.

- Cherns, L. et Wright, V.P. (2009). Quantifying the impact of early diagenetic aragonite dissolution on the fossil record. *Palaios*, 24, 756-771.
- Cohen, A.L., Owens, K.E., Layne, G.D. et Shimizu, N. (2002). The Effect of Algal Symbionts on the Accuracy of Sr/Ca Paleotemperatures from Coral. *Science*, 296(5566), 331-333. <http://dx.doi.org/10.1126/science.1069330>
- Colin, C., Frank, N., Copard, K. et Douville, E. (2010). Neodymium isotopic composition of deep-sea corals from the NE Atlantic: implications for past hydrological changes during the Holocene. *Quaternary Science Reviews*, 10.1016, 1-9.
- Costello, M.J., McCrea, M., Freiwald, A., Lundälv, T., Jonsson, L., Bett, B.J., van Weering, T.C., de Haas, H., Roberts, J.M. et Allen, D. (2005). Role of cold-water *Lophelia pertusa* coral reefs as fish habitat in the NE Atlantic *Cold-water corals and ecosystems* (p. 771-805) : Springer.
- de Vernal, A., Hillaire-Marcel, C., Peltier, W.R. et Weaver, A.J. (2002). Structure of the upper water column in the northwest North Atlantic: Modern versus Last Glacial Maximum conditions. *PALEOCEANOGRAPHY*, 17(4), 1050.
- Edinger, E.N. et al., e. (2010). *NSERC ship-time cruise report; ROPOS mission onboard the CCGS Hudson*.
- Edinger, E.N., Wareham, V.E. et Haedrich, R.L. (2007). Patterns of groundfish diversity and abundance in relation to deep-sea coral distributions in Newfoundland and Labrador waters. *Bulletin of Marine Science*, 81(Supplement 1), 101-122.
- Efremov, I. (1940). Taphonomy : new branch of paleontology. *Pan-American Geologist*, 74, 81-93.
- Eisele, M., Frank, N., Wienberg, C., Hebbeln, D., López Correa, M., Douville, E. et Freiwald, A. (2011). Productivity controlled cold-water coral growth periods during the last glacial off Mauritania. [doi: 10.1016/j.margeo.2010.12.007]. *Marine Geology*, 280(1-4), 143-149.

- Flessa, K.W., Cutler, A.H. et Meldahl, K.H. (1993). Time and taphonomy: quantitative estimates of time-averaging and stratigraphic disorder in a shallow marine habitat. *Paleobiology*, 266-286.
- Form, A.U. et Riebesell, U. (2012). Acclimation to ocean acidification during long-term CO₂ exposure in the cold-water coral *Lophelia pertusa*. *Global Change Biology*, 18(3), 843-853.
- Foster, L.C., Ragazzola, F., Wall, M., Form, A.U. et Freiwald, A. (2012). The biomineralisation response of the cold-water coral *Lophelia pertusa* to ocean acidification.
- Frank, N., Freiwald, A., Correa, M.L., Wienberg, C., Eisele, M., Hebbeln, D., Van Rooij, D., Henriët, J.-P., Colin, C. et van Weering, T. (2011). Northeastern Atlantic cold-water coral reefs and climate. *Geology*, 39(8), 743-746.
- Friedman, G.M. (1964). Early diagenesis and lithification in carbonate sediments. *Journal of Sedimentary Research*, 34(4), 777-813.
- Fürsich, F. et Pandey, D. (1999). Genesis and environmental significance of Upper Cretaceous shell concentrations from the Cauvery Basin, southern India. *Palaeogeography, Palaeoclimatology, Palaeoecology*, 145(1), 119-139.
- Fursich, F.T. et Aberhan, M. (1990). Significance of time-averaging for palaeocommunity analysis. *Lethaia*, 23(2), 143-152.
- Gagnon, A.C., Adkins, J.F., Fernandez, D.P. et Robinson, L.F. (2007). Sr/Ca and Mg/Ca vital effects correlated with skeletal architecture in a scleractinian deep-sea coral and the role of Rayleigh fractionation. *Earth and Planetary Science Letters*, 261(1), 280-295.
- Ginsburg, R.N. (1954). *Early diagenesis and lithification of shallow-water carbonate sediments in south Florida*. : SEPM.
- Guinotte, J.M., Orr, J., Cairns, S., Freiwald, A., Morgan, L. et George, R. (2006). Will human-induced changes in seawater chemistry alter the distribution of

- deep-sea scleractinian corals? *Frontiers in Ecology and the Environment*, 4(3), 141-146.
- Hill, T., LaVigne, M., Spero, H., Guilderson, T., Gaylord, B. et Clague, D. (2012). Variations in seawater Sr/Ca recorded in deep-sea bamboo corals. *PALEOCEANOGRAPHY*, 27(3)
- Hillaire-Marcel, C., Vernal, A.d., Bilodeau, G. et Wu, G. (1994). Isotope stratigraphy, sedimentation rates, deep circulation, and carbonate events in the Labrador Sea during the last~ 200 ka. *Canadian Journal of Earth Sciences*, 31(1), 63-89.
- Hillaire-Marcel, C., Vernal, A.d., Lucotte, M., Mucci, A., Bilodeau, G., Rochon, A., Vallières, S. et Wu, G. (1994). Productivité et flux de carbone dans la mer du Labrador au cours des derniers 40 000 ans. *Canadian Journal of Earth Sciences*, 31(1), 139-158. <http://dx.doi.org/doi:10.1139/e94-012>
- Keen, C. (1978). Cruise Report CSS Hudson 78 020, June 27 to July 19, 1978. *Atl. Geosc. Centre, Bedford Inst. Oceanogr., Int. Rep. 1*, 15.
- Kowalewski, M. (1996). Time-averaging, overcompleteness, and the geological record. *Journal of Geology*, 104(3), 317-326. Récupéré de geh
- Kowalewski, M. et Bambach, R.K. (2008). *The limits of paleontological resolution*. : Springer.
- Kowalewski, M., Carroll, M., Casazza, L., Gupta, N., Hannisdal, B., Hendy, A., Krause Jr, R., LaBarbera, M., Lazo, D. et Messina, C. (2003). Quantitative fidelity of brachiopod-mollusk assemblages from modern subtidal environments of San Juan Islands, USA. *Journal of Taphonomy*, 1(1), 43-65.
- Kowalewski, M. et Hoffmeister, A.P. (2003). Sieves and fossils: Effects of mesh size on paleontological patterns. *PALAIOS*, 18(4-5), 460-469.
- López Correa, M., Montagna, P., Joseph, N., Rüggeberg, A., Fietzke, J., Flögel, S., Dorschel, B., Goldstein, S.L., Wheeler, A. et Freiwald, A. (2012). Preboreal onset of cold-water coral growth beyond the Arctic Circle revealed by coupled

- radiocarbon and U-series dating and neodymium isotopes. [doi: 10.1016/j.quascirev.2011.12.005]. *Quaternary Science Reviews*, 34(0), 24-43.
- Meredyk, S., Piper, D., Edinger, E. et Ruffman, A. (2012b). *Composition, probable origin, and recent coral fauna of enigmatic mounds on Orphan Knoll, Northwest Atlantic Ocean. GAC-MAC annual meeting, Actes du colloque, 2012b, St. John's, NL*
- Montagna, P., McCulloch, M., Mazzoli, C., Silenzi, S. et Odorico, R. (2007). The non-tropical coral *Cladocora caespitosa* as the new climate archive for the Mediterranean: high-resolution (~weekly) trace element systematics. [doi: 10.1016/j.quascirev.2006.09.008]. *Quaternary Science Reviews*, 26(3-4), 441-462.
- Mortensen, P.B., Buhl-Mortensen, L., Gordon Jr., D.C., Fader, G.B.J., McKeown, D.L. et Fenton, D.G. (2005). Effects of fisheries on deep water gorgonian corals in the Northeast Channel. *NovaScotia.Am.Fish.Soc.Symp*, 41, 369-382.
- Mortensen, P.B., Rapp, H.T. et Båmstedt, U. (1998). Oxygen and carbon isotope ratios related to growth line patterns in skeletons of *Lophelia pertusa* (L) (Anthozoa, Scleractinia): Implications for determination of linear extension rate. [doi: 10.1080/00364827.1998.10413702]. *Sarsia*, 83(5), 433-446.
<http://dx.doi.org/10.1080/00364827.1998.10413702>
- Nothdurft, L. et Webb, G. (2009). Earliest diagenesis in scleractinian coral skeletons: implications for palaeoclimate-sensitive geochemical archives. *Facies*, 55(2), 161-201. <http://dx.doi.org/10.1007/s10347-008-0167-z>
- Parsons-Hubbard, K.M., Callender, W.R., Powell, E.N., Brett, C.E., Walker, S.E., Raymond, A.L. et Staff, G.M. (1999). Rates of burial and disturbance of experimentally-deployed molluscs; implications for preservation potential. *PALAIOS*, 14(4), 337-351.
- Parsons, K.M., Powell, E.N., Brett, C.E., Walker, S.E. et Callender, W.R. (1997). *Shelf and slope experimental taphonomy initiative (SSETI) : Bahamas and gulf of Mexico. Proc 8th Int Coral Reef Sym, Actes du colloque, 1997,*

- Powell, E.N., Parsons-Hubbard, K.M., Callender, W.R., Staff, G.M., Rowe, G.T., Brett, C.E., Walker, S.E., Raymond, A., Carlson, D.D. et White, S. (2002). Taphonomy on the continental shelf and slope: two-year trends—Gulf of Mexico and Bahamas. *Palaeogeography, Palaeoclimatology, Palaeoecology*, 184(1), 1-35.
- Powell, E.N., Parsons-Hubbard, K.M., Callender, W.R., Staff, G.M., Rowe, G.T., Brett, C.E., Walker, S.E., Raymond, A., Carlson, D.D., White, S. et Heise, E.A. (2002). Taphonomy on the continental shelf and slope: two-year trends – Gulf of Mexico and Bahamas. [doi: 10.1016/S0031-0182(01)00457-6]. *Palaeogeography, Palaeoclimatology, Palaeoecology*, 184(1–2), 1-35.
- Powell, W. (2003). Greenschist-facies metamorphism of the Burgess Shale and its implications for models of fossil formation and preservation. *Canadian Journal of Earth Sciences*, 40(1), 13-25.
- Roark, E.B., Guilderson, T.P., Dunbar, R.B. et Ingram, B.L. (2006). Radiocarbon-based ages and growth rates of Hawaiian deep-sea corals. *Marine Ecology Progress Series*, 327, 1–14.
- Roark, E.B., Guilderson, T.P., Flood-Page, S., Dunbar, R.B., Ingram, B.L., Fallon, S.J. et McCulloch, M. (2005). Radiocarbon-based ages and growth rates of bamboo corals from the Gulf of Alaska. *Geophysical Research Letters*, 32(4)
- Roberts, J.M., Wheeler, A., Freiwald, A. et Cairns, S. (2009). *Cold-water corals: the biology and geology of deep-sea coral habitats*. : Cambridge University Press,.
- Roberts, J.M., Wheeler, A.J. et Freiwald, A. (2006). Reefs of the deep: the biology and geology of cold-water coral ecosystems. *Science*, 312(5773), 543-547.
- Ruffman, A. (1989). *Devonian Shelf-depth Limestone Dredged from Orphan Knoll: A 1971 Discovery and A Reassessment of the Hudson 78-020 Dredge Hauls from Orphan Knoll*. : G.S.C.

- Sherwood, O.A. et Edinger, E.N. (2009). Ages and growth rates of some deep-sea gorgonian and antipatharian corals of Newfoundland and Labrador. *Can. J. Fish. Aquat. Sci.*, 66, 142–152.
- Sherwood, O.A., Heikoop, J.M., Scott, D.B., Risk, M.J., Guilderson, T.P. et McKinney, R.A. (2005). Stable isotopic composition of deep-sea gorgonian corals *Primnoa* spp.: a new archive of surface processes. *Marine Ecology Progress Series*, 301, 135–148.
- Simon, Q., Hillaire-Marcel, C., St-Onge, G. et Andrews, J.T. (2013). North-eastern Laurentide, western Greenland and southern Innuitian ice stream dynamics during the last glacial cycle. *Journal of Quaternary Science*
- Smith, J.E., Risk, M.J., Schwarcz, H.P. et McConnaughey, T.A. (1997). Rapid climate change in the North Atlantic during the Younger Dryas recorded by deep-sea corals. [10.1038/386818a0]. *Nature*, 386(6627), 818–820.
- Solignac, S., de Vernal, A. et Hillaire-Marcel, C. (2004). Holocene sea-surface conditions in the North Atlantic—Contrasted trends and regimes in the western and eastern sectors (Labrador Sea vs. Iceland Basin). *Quaternary Science Reviews*, 23(3), 319–334.
- Staff, G.M., Callender, W.R., Powell, E.N., Parsons-Hubbard, K.M., Brett, C.E., Walker, S.E., Carlson, D.D., White, S., Raymond, A. et Heise, E.A. (2002). Taphonomic Trends Along a Forereef Slope: Lee Stocking Island, Bahamas. II. Time. *PALAIOS*, 17(1), 66–83.
- Strasser, A. et Strohmenger, C. (1997). Early diagenesis in Pleistocene coral reefs, southern Sinai, Egypt: response to tectonics, sea-level and climate. *Sedimentology*, 44(3), 537–558.
- Thiagarajan, N., Gerlach, D., Roberts, M.L., Burke, A., McNichol, A., Jenkins, W.J., Subhas, A.V., Thresher, R.E. et Adkins, J.F. (2013). Movement of deep-sea coral populations on climatic timescales. *PALEOCEANOGRAPHY*

- Tracey, D.M., Neil, H., Marriott, P., Andrews, A.H., Cailliet, G.M. et Sanchez, J.A. (2007). Age and growth of two genera of deep-sea bamboo corals (Family Isididae) in New Zealand waters. *Bulletin of Marine Science*, 81(3), 393-408.
- van de Flierdt, T., Robinson, L.F. et Adkins, J.F. (2010). Deep-sea coral aragonite as a recorder for the neodymium isotopic composition of seawater. [doi: 10.1016/j.gca.2010.08.001]. *Geochimica et Cosmochimica Acta*, 74(21), 6014-6032.
- Walker, S.E., Parsons-Hubbard, K., Powell, E. et Brett, C.E. (2002). Predation on experimentally deployed molluscan shells from shelf to slope depths in a tropical carbonate environment. *PALAIOS*, 17(2), 147-170.
- Walker, S.E., Parsons Hubbard, K., Powell, E.N. et Brett, C.E. (1998). Bioerosion or bioaccumulation? Shelf-slope trends for EPI-and endobionts on experimentally deployed gastropod shells. *Historical Biology*, 13(1), 61-72.

CHAPITRE I

Deep-sea corals from Orphan Knoll: taphonomic processes in a low burial rate environment since 180000 years

Blénet, Aurélien¹; Edinger, Evan²; Hillaire-Marcel, Claude¹; Ghaleb, Bassam¹

1. GEOTOP-UQAM CP 8888, Montreal (Qc) H3C 3P8 Canada

2. Dept. of Geography and Dept. of Biology, Memorial University, St. John's, NL, A1B 3X9 Canada.

1.1 **Abstract**

Modern deep sea coral graveyards provide a unique opportunity to evaluate bioclast degradation in a deep-water low sedimentation rate environment. The aim of this study is to understand the degradation process of an assemblage of 145 *Desmophyllum dianthus* collected from two deep-sea graveyards off the coast of Newfoundland, 123 in Orphan Knoll and 22 in Flemish Cap. We used radiocarbon and u-series method to date 19 samples. We described 2 main populations of samples, the first from the Holocene, another in the MIS 5 and single specimen in the MIS 7. We proposed hypothesis for this non randomly distributed ages taking into account of the environmental difference between glacial and interglacial periods. We isolated four main taphonomic parameters and have described their action on skeletons using a semi-quantitative scale separately for each location. Encrustation and breakage is more important on samples between thousand and two thousand years old. Macro-boring is very important for samples older than 5 000 years old. Loss of details is very important for the older samples. We found a relation between macro-boring and

loss of details process and the age of our sample and non random distribution of the breakage and encrustation process during time. We explained that non random distribution by the action of macro-boring and loss of details that should have degrade the record of the two others process.

1.2 **Introduction**

In shallow marine environment taphonomic processes affecting marine assemblages begin during the life of the organism, as encrustation, bioerosion or lithification (Friedman, 1964 ; Ginsburg, 1954 ; Nothdurft et Webb, 2009 ; Strasser et Strohmenger, 1997). Those processes have an impact on shell preservation in the fossil records and influence the reconstitutions of past environmental conditions (Efremov, 1940). Effect of taphonomic processes have been studied in order to reconstruct paleoenvironment and paleobiodiversity in paleozoic (Cherns et Wright, 2009 ; Wood, 2011), understand preservation processes (Tomasovych et Schlogl, 2008) and interpret fossils records (Fürsich et Pandey, 1998). In actual environment many of those degradations, like fragmentation, abrasion, loss of details and encrustation, are originally caused by the action of bioencrusters and bioeroders (Parsons-Hubbard, Callender, Powell, Brett, Walker, Raymond et Staff, 1999 ; Parsons, Karla M et Brett, 1991 ; Powell, E., Staff, Davies et Callender, 1989 ; Zuschin, Stachowitsch et Stanton, 2003). Those organisms differ from an environment to another. In shallow marine environment the predominant bioeroders and bioencrusters are algae and cyanobacteria (Walker, Parsons Hubbard, Powell et Brett, 1998). Those organisms are restricted to the photic zone. In the deep-sea this role must be played by other organisms.

Degradation processes in actual shallow marine environment have been documented those last decades by the Shelf and Slope Experimental Taphonomy Initiative group (SSETI), in order to quantify those degradation processes (Parsons, K. M., Powell, Brett, Walker et Callender, 1997). Short term studies (2 -4 years) have been

performed with shell deposits in various environments on Bahamas shelf and slope (Cai, Chen, Powell, Walker, Parsons-Hubbard, Staff, Wang, Ashton-Alcox, Callender et Brett, 2006 ; Powell, Eric N, Parsons-Hubbard, Callender, Staff, Rowe, Brett, Walker, Raymond, Carlson et White, 2002 ; Powell, Eric N., Parsons-Hubbard, Callender, Staff, Rowe, Brett, Walker, Raymond, Carlson, White et Heise, 2002 ; Walker *et al.*, 1998). Studies according to the influence of rapid burial and exhumation events on taphonomic characteristics (Parsons-Hubbard *et al.*, 1999 ; Staff, Callender, Powell, Parsons-Hubbard, Brett, Walker, Carlson, White, Raymond et Heise, 2002). The predominant described processes are discoloration and dissolution (Callender, Staff, Parsons-Hubbard, Powell, Rowe, Walker, Brett, Raymond, Carlson et White, 2002). Degradation rate in the shelf is clearly quicker than in the slope and related to the burial rate. In deeper environment and especially in the deep-sea, degradation rate must be slower because of the low hydrodynamic conditions, the absence of light-dependent bioeroders like algae and cyanobacteria and the lower activity of predators (Walker, Parsons-Hubbard, Powell et Brett, 2002). Others short term studies focused on shallow marine environment taphonomy (Estrada Alvarez, Edinger et Pandolfi, 2004 ; Lescinsky, Edinger et Risk, 2002).

In an ideal geological record every event would be preserved in correspondence with its chronology. A taphonomic phenomenon could induce a gap in the fossil record and disturb the chronological record. This phenomenon is the time averaging and is describe as a temporal mixing of chronological events (Fürsich et Aberhan, 1990 ; Kidwell et Bosence, 1991) that affects every geological records depending of the studied scale. Caused by incompleteness and stratigraphic disorder (Kowalewski, Michal, 1996) it can induce that organisms that have lived in different periods of time, will be fossilized in the same stratigraphic unit and appears to have lived in synchronicity. The age distribution of a fossil population will be the result of this time averaging. Age distribution curve of a fossil assemblage are usually used to characterize time averaging (Flessa, Cutler et Meldahl, 1993). In the deep sea, the

slow burial rate can provoke a faunal condensation that can mixed benthic organisms skeletons (Fürsich, 1978).

Deep-sea corals communities provide habitat, food for a large amount of deep marine species (Freiwald, André et Wilson, 1998) and are essential especially for deep fish species as juvenile habitats, feeding area or refuges from predation (Auster, 2005 ; Auster, Moore, Heinonen et Watling, 2005 ; Costello, McCrea, Freiwald, Lundälv, Jonsson, Bett, van Weering, de Haas, Roberts et Allen, 2005 ; Edinger, Evan N, Wareham et Haedrich, 2007). Those communities are important biodiversity hotspot (Edinger, E. N. *et al.*, 2007 ; Freiwald, A. et Roberts, 2005 ; Roberts, J. M., Wheeler, Freiwald et Cairns, 2009 ; Roberts, J Murray, Wheeler et Freiwald, 2006). The accumulation of dead corals skeletons, over long period of time, formed graveyards. Those graveyards, that can be used to understand environmental changes (Colin, Frank, Copard et Douville, 2010 ; Copard, Colin, Henderson, Scholten, Douville, Sicre et Frank, 2012 ; Edinger, E., Burr, Pandolfi et Ortiz, 2007 ; Eisele, Frank, Wienberg, Hebbeln, López Correa, Douville et Freiwald, 2011 ; Frank, Freiwald, Correa, Wienberg, Eisele, Hebbeln, Van Rooij, Henriët, Colin et van Weering, 2011 ; Hill, LaVigne, Spero, Guilderson, Gaylord et Clague, 2012 ; Rollion-Bard, Blamart, Cuif et Juillet-Leclerc, 2003 ; Sherwood, Owen A, Heikoop, Scott, Risk, Guilderson et McKinney, 2005 ; Sherwood, Owen A., Jamieson, Edinger et Wareham, 2008 ; Smith, Jodie E., Risk, Schwarcz et McConnaughey, 1997 ; Thiagarajan, Gerlach, Roberts, Burke, McNichol, Jenkins, Subhas, Thresher et Adkins, 2013), represent a unique opportunity to study long term degradation of skeleton in the deep-sea and quantify taphonomic degradations in this particular environment.

Desmophyllum dianthus communities in Atlantic Canada have been registered of the coast of Newfoundland, in Orphan Knoll and Flemish cap (Edinger, Evan N. et al., 2010 ; Meredyk, Piper, Edinger et Ruffman, 2012b). Those scleractinians corals produced an aragonite skeleton that can be easily dated using U-series methods. That

characteristic make them good records of paleoceanic conditions (Anagnostou, Sherrell, Gagnon, LaVigne, Field et McDonough, 2011 ; Foerster, Beuck, Haeussermann et Freiwald, 2005 ; Smith, J. E., 1993). Furthermore their post-mortem persistence on the sea-floor compared with gorgonian and antipatharian (Edinger, Evan N et Sherwood, 2012) made them good records for long periods of time.

In this study, using samples collected in a deep-sea graveyard off the coast of Newfoundland, we will 1) understand the environmental conditions that lead to the accumulation of deep-sea coral graveyards, 2) describe the rates of taphonomic processes in a cold, deep, low sedimentation rate environment, 3) determine which taphonomic processes are most related to age, 4) study the extent to which different taphonomic processes are correlated with one another. Our results indicate the unity of taphonomic processes in shallow and deep-water environments, despite radical differences in rates.

1.3 **Methods**

1.3.1 Location

In 2010 a cruise off the coast of Newfoundland with the CCGS Hudson and ROV ROPOS documented and collected samples from two coral graveyards. Samples from the coral graveyard at Orphan Knoll at 1740 meters depth had been previously collected by rock dredge in 1978 (Keen, 1978 ; Ruffman, 1989 ; Smith, Jodie E. *et al.*, 1997). A second graveyard was discovered and sampled on the south side of the Flemish Cap at about 2200 meters depth (Edinger, Evan N. *et al.*, 2010) (see Fig.1.1).

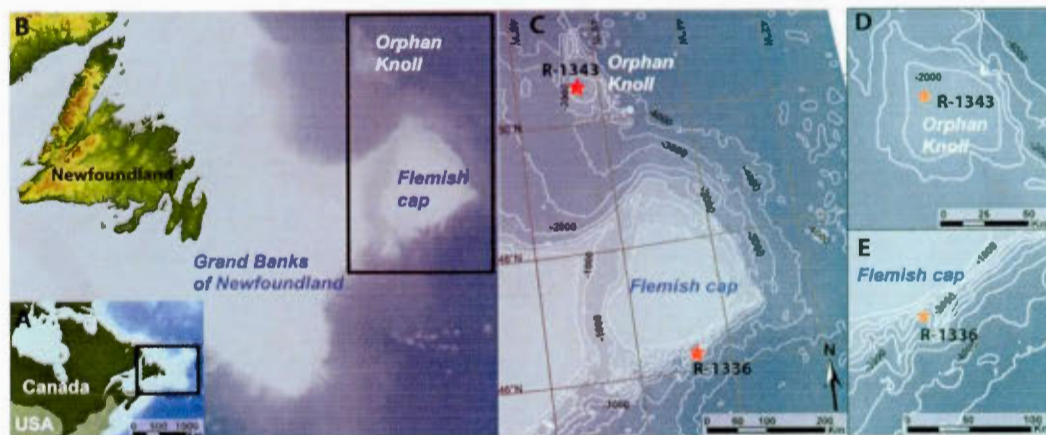


Figure 1.1 Location of two deep-sea graveyards (red stars) investigated during the 2010 Hudson mission off the coast of Newfoundland. A) Map of North-Eastern American margin. B) Map of Newfoundland and the location of Orphan Knoll and Flemish cap. C) Bathymetric map of Orphan and Flemish cap and the location of the deep-sea corals graveyards, the interval between the level lines is 500 meter. D) Detail of the bathymetric map focused on Orphan knoll and the position of the graveyard. E) Detail of the bathymetric map focused on Flemish cap and the position of the graveyard.

1.3.2 ROPOS equipment

The ROV used, Remotely Operated Platform for Ocean Science (ROPOS), was equipped with two video cameras and a still camera. The forward-looking high definition camera (Pacific Zeus Plus), mostly used to recording the ROPOS dives (see <http://www.ropos.com/> for instruments specificity) and a downward-looking high-definition video camera (Pacific Mini-Zeus). To measure the cliffs and graveyards dimension, the used scale was given by the laser pointers 10 cm apart on the pictures. ROV Position data determined by USBL acoustic telemetry encoded on the audio track of the mpeg files. ROPOS is also equipped with 2 manipulator arms (Kraft Predator) used to collect samples and manipulate other sampling tools as the plastic scoop, used for sampling.

1.3.3 Sampling

Both graveyards are accumulations of the solitary scleractinian coral *Desmophyllum dianthus* accumulated at the base of small vertical cliffs. Fossilised corals were sampled using ROPOS. Live specimens were observed and collected on the cliffs above the graveyards. Live samples were removed from cliffs using the ROV manipulator arms, while dead samples were collected from the bottom using a plastic scoop of ~ 1.5 litres volume.

1.3.4 Videos analysis

Pictures and videos from this device have been analysed on computer in the laboratory at Memorial University. To determine the density of live coral specimens on the cliffs we randomly stopped the video and counted the number of corals per meter square we repeated this 25 times and calculated the average of the number of corals per m² on the cliff.

1.3.5 Sample selection for taphonomic studies

Specimens D22 and D24 have been excluded from the colours analysis because of the impossibility to use the copy stand to take the pictures. Three others specimens (D20, D82 and D91) have been excluded from taphonomical and colour analysis because their fragmentation caused an impossibility to be individualized.

Tableau 1.1 Number of taphonomically studied specimens from each location and the number alive or subfossils analyzed for age distribution by ^{14}C or U-series from each locations (total = 19).

| | Dive number | Total number of collected specimen | Samples taphonomically analyzed | Samples analyzed for age | Dated <i>Desmophyllum dianthus</i> | Dated Isidid | Live samples collected | Live samples collected analyzed for age |
|------------------------|-------------|------------------------------------|---------------------------------|--------------------------|------------------------------------|--------------|------------------------|---|
| Orphan Knoll graveyard | R-1343 | 123 | 120 | 17 | 14 | 3 | 3 | 1 |
| Flemish cap | R-1336 | 22 | 22 | 2 | 2 | 0 | 6 | 2 |

1.3.6 Analyses of Corals Preservation

Five taphonomic variables were measured using visual inspection and magnifying glass (x20) on selected samples: degree of encrustation, degree of macrobioerosion, degree of fragmentation, loss of surface detail, and discolouration. Encrustation, macrobioerosion, fragmentation, and loss of surface detail were ranked on a scale, from 0 for non-degraded to 4 for much degraded (see Fig.1.2). Encrustation refers to the presence of encrusting organisms attached to coral skeleton (Fig.1.2 photos A to E). Soft bodied encrusters like sponges and tunicates and skeletal encrusters such as serpulid worms, bryozoans and juvenile *D. dianthus* were separated in the observations.

Macrobioerosion refers to the presence of macroboring caused by the action of endolithic invertebrates as describe by (Boerboom, Smith et Risk, 1998 ; Freiwald, André et Wilson, 1998) (Fig.1.2 photos F to J). Macrobioerosion traces have been observed using visual inspection, magnifying glass (x20) and microscope (x40). The different traces found on the skeletons were distinguished on their shape and inferring the identity of the organisms that produced them. Loss of detail refers to the loss of ornamentation and septa on coral skeleton (Fig.1.2 photos K to O).

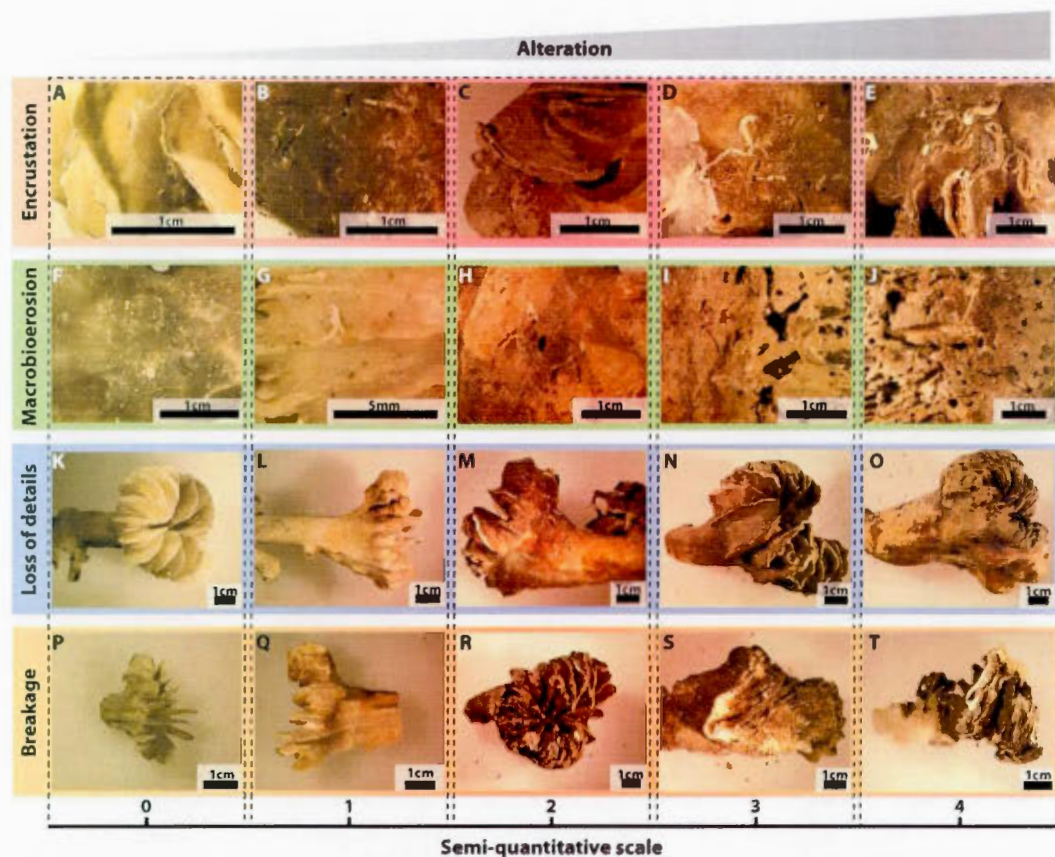


Figure 1.2 Taphonomic parameters and ranks. Pictures A to E) absence of encrustation to high level of encrustation mostly caused by Serpulids. Pictures F to J) absence of macrobioerosion to high level mostly caused by action of lithophagous organisms and sea urchins. Pictures K to O) fully clear details to complete loss of details on whole parts of the skeleton. Pictures P to T) well preserved skeleton to heavily broken skeleton.

Breakage refers to the mechanical alteration of corals skeleton (Fig.1.2 photos P to T). Fresh breaks have not been taken into account because of the possibility that they have been made by the plastic scoop during the sampling. Those which have been covered by encrustation, manganese oxide or degraded by bio-erosion were used to evaluate mechanical degradation of the samples. Evaluation of the degradation was made separately on the different parts of the corals (septa, epitheca and base) and

when it was possible on the buried part separately from the non buried part of the skeleton

Discolouration, mostly by Mn-oxides, was measured using photographic colour analysis. Each coral was photographed using a Minolta® DiMAGE 7/5 camera on a copy stand equipped with medical and photo lamp bulb BELLAPHOT® 64607 (8V and 50W) allowing to homogenize lighting conditions between pictures. Pictures were 2560x1920 pixels size. A minimum of 4 views have been taken including a top and bottom view and a lateral view on each side of the sample.

Ten to 20 points were randomly selected on each picture, taken with a copy stand, of the most FeMn coated part of the sample. Cyan; magenta; yellow and black (CMYK) values colours of each point were measured with Adobe Illustrator™ software. The average of those points values were calculated and used to represent sample colour.

Each sample was photographed and cataloged in a database including all the information obtained about each samples. All of those information were compiled in a database built using Filemaker pro 12.0v1 software.

1.3.7 Taphonomic ranks description

For the encrustation parameter (see Fig.1.2 A - E) the null value characterizes the absence of encrusting organisms. A value of 1 characterizes a low presence of encrusting organisms. The value 2 characterizes an encrustation of a small surface of the specimen with altered centimetric serpulids tubes. The value 3 characterizes a common presence of altered encrusters. The value 4 characterizes encrusting on a large surface of the skeleton with centimeter long tubes, continuous and well preserved.

For the macrobioerosion (see Fig.1.2 F - J) the null value corresponds to the absence of macro-perforations. A value of 1 characterizes the rare presence of micro-perforations only visible under magnifying glass. The value 2 characterizes the presence of micro and macro-perforations about 2 mm diameter. The value 3 characterizes the common presence of joined and centimetric macro-perforations and the presence of macrobioerosion trace. The value 4 characterizes the presence of joined macroperforation forming galleries in the coral skeleton and dominant macrobioerosion traces.

For the loss of details parameter (see Fig.1.2 K - O) the null value corresponds to the preservation of skeletal details of *Desmophyllum dianthus*. A value of 1 corresponds to the alteration of the surface roughness of the septa and the disappearance of the ornamentation of the epitheca. The value 2 corresponds to the gradual disappearance of primary and secondary septa or ornamentation or roughnesses are visible. The value 3 corresponds to the disappearance of secondary septa, major septa are still visible but reduced by approximately 50%. The value 4 is the almost complete disappearance of the major septa.

For the breakage parameter (see Fig.1.2 P - T) the null value for this parameter is the total absence of breakage. A value of 1 corresponds to the presence of millimetric cracks on the septa. The value 2 corresponds to the presence of half centimeter or less cracks in the septa. The value 3 corresponds to the presence of centimetric breaks on all the septa. The value 4 in the presence of breaks in the entire skeleton. Fresh looking breakages have not been including in this study cause of the risk that they would be done during ROV collection.

1.3.8 Statistical description of taphonomic variables

To describe frequency of taphonomic parameters, histograms were calculated to show the number of specimens for each parameters rank. For macrobioerosion and encrustation parameters different borers and encrusters taxa have been separated.

Using R software CMYK average colours values were transformed into RGB colours using a function created for this purpose:

$$(1) \quad r = 255 \times (1 - c) \times (1 - k)$$

$$(2) \quad g = 255 \times (1 - m) \times (1 - k)$$

$$(3) \quad b = 255 \times (1 - y) \times (1 - k)$$

where c, m, y and k are the percentage of cyan, magenta, yellow and key measured using Illustrator® and r, g, b are the calculated value of red, green and blue colours. Then the colours of samples were discriminated using a Principal Component Analysis (PCA).

1.3.9 Sample selection for dating

It was not possible to determine the ages of all 142 samples in the collection. Therefore, to select a subsample of the corals that likely represented the largest possible age range, taphonomic scores described previously were used. The assumption underlying this procedure was that the oldest specimens would show the most overall taphonomic alteration.

Tableau 1.2 Number of specimen from each taphonomic category. Those category are the result of the evaluation of different parameters as colour (Mn oxide), macro-boring, encrustation, breakage and loss of details.

| | Taphonomic category 1 | Taphonomic category 2 | Taphonomic category 3 | Taphonomic category 4 | Taphonomic category 5 | Taphonomic category 6 |
|---|-----------------------|-----------------------|-----------------------|-----------------------|-----------------------|-----------------------|
| Dated specimens | 3 | 5 | 3 | 3 | 2 | 3 |
| Total of specimens | 9 | 13 | 17 | 7 | 20 | 9 |
| Proportion of aged specimen for each category (%) | 33,33 | 38,46 | 17,65 | 42,86 | 10,00 | 33,33 |

Samples were binned into five groups corresponding to their visual degradation. We then selected 19 samples for age determination by radiocarbon and U-series dating, with the number of samples from each group proportional to the number of samples in that group (see Table 1.2).

1.3.10 Radiocarbon dating

Samples were taken from 19 coral skeletons and transferred to cleaned vials. Sixteen *D. dianthus* and one isidid bamboo coral were sent to Orsay's laboratory in Paris to be analyzed by an Accelerator Mass Spectrometer (AMS). The two other bamboo corals were analyzed at Australian National University (ANU).

Graphitization of CO₂ from sample (0.75 mg for Orsay's laboratory and 0.1 mg at ANU) prepared for AMS analysis follows the method described by Vogel *et al.* (Vogel, Nelson et Southon, 1987) in Orsay's laboratory and by Fallon *et al.* (Fallon, Fifield et Chappell, 2010) in ANU laboratory. Sample preparation were done at the Département des Sciences de la Terre de la Faculté d'Orsay in Paris and at Australian National University (ANU). 17 Graphite samples are pressed into targets and measured for their ¹⁴C/¹³C ratio at centre CEA de Saclay (Gif-sur-Yvette, France) and

2 samples were analysed at ANU's radiocarbon dating centre following the same method. The corrected modern fraction (F) is reported as described by Donahue (Donahue, Jull et Toolin, 1990). The “old” oxalic acid standard is normalized to 1950 and a $\delta^{13}\text{C}$ value of -19‰ and the sample is normalized to a $\delta^{13}\text{C}$ of -25‰ . Conventional radiocarbon ages have been corrected for the isotopic fractionation, $\delta^{13}\text{C}$, by measurement of the $^{13}\text{C}/^{12}\text{C}$ ratio of the coral skeleton. Ages were then calibrated using Calib v.6.0 (Stuiver, Reimer et Reimer, 2005), using MARINE 09 calibration curve. The standard deviation 2σ was used for all the calibrated age.

1.3.11 U-series dating

U-series and stable isotope analysis were done on the same samples. First, pieces of specimens were cut. Then those sub-samples were examined under a binocular microscope and were physically cleaned using a dremel tool to remove all the visible oxide coating. Samples were ultrasonically agitated in water to removed sedimentary material, in 0.2 M nitric acid to remove residual Mn and Fe oxides coating and in a 50% bleach solution to remove remaining organic matter. Samples were dried and crushed with an agate mortar.

We selected one of the youngest sample as a test of the method and 10 samples with apparent radiocarbon ages older than 40,000 years as candidates to have the widest range of dates. The samples ($\pm 1\text{g}$) were dissolved using 15N HNO_3 in Teflon beakers, in which an amount of 0.15g of mixed spikes ^{229}Th - ^{233}U - ^{236}U was pre-weighed and pre-evaporated. U and Th were concentrated by co-precipitation with $\pm 6\text{ mg}$ of a Fe carrier, and then separated by centrifugation to form the bulk solution. Further purification was carried out using an anion exchange resin (AG 1-X8, 200 – 400 mesh). Analytical procedure for U and Th separation was that reported by (Chen, Edwards et Wasserburg, 1986 ; Edwards, Chen et Wasserburg, 1987 1987b). Isotopic compositions were measured on a Thermo™ thermal ionization mass spectrometer

(TIMS) by pick jumping mod using SEM detector. U and Th were loaded on single Re filament coated with graphite.

1.3.12 Statistics for age distribution curve

To predict the age distribution of a theoretical full population, a density curve based on the ages of our studied specimens was calculated (Scott, 1992 ; Sheather et Jones, 1991 ; Silverman, 1986). To calculate the predicted distribution of specimens along the full length of time represented by our sample suite, we used Gaussian density curves. Individual Gaussian curves are fixed on each x value. The final density curve is the sum of all the individual curves. The algorithm used to calculate this curve disperses the mass of the empirical distribution function over a regular grid of at least 512 points and then uses the fast Fourier transform to convolve this approximation with a discretized version of the kernel (see equation 4),

$$(4) \quad \hat{f}_h(x) = \frac{1}{n} \sum_{i=1}^n K_h(x - x_i) = \frac{1}{nh} \sum_{i=1}^n K\left(\frac{x - x_i}{h}\right)$$

where n is the number of samples ($n=19$), K is the kernel function, and h is the bandwidth parameter. It represents the smoothing parameter of each Gaussian curve and at least the standard deviation of the kernel ($h = 2.947e^4$). This smoothing parameter is the most important and it is fixed by the software according to the number of n to make h proportional to $n^{-1/5}$. The statistical properties of a kernel are determined by equation 5:

$$(5) \quad \sigma^2(K) = \int (t^2 K(t)) dt$$

which is fixed by R program to be = 1. Specimens have been grouped in 2,000 year intervals, and then we used R software to plot a graph of the age distribution of the samples (Fig. 1.3 A). Details of this distribution have been made for the Holocene

(Fig. 1.3 B) and for MIS 5 c-d (Fig. 1.3 C) with 500 year intervals to characterize time averaging of the graveyard.

1.3.13 Relationship between taphonomic index and sample age.

To test the link between taphonomic parameters and time, the non-parametric Kruskal Wallis sum rank test were used on data separated in two different aged populations: Holocene specimens and MIS5/7 aged specimen. The tested hypothesis was H0: based on taphonomic data for the considered parameter the two aged populations can't be isolated, H1: based on taphonomic data for the considered parameter the two aged population are statistically different. Because of the limited number of samples for which we had absolute ages, significance in the K-W tests was interpreted at $p < 0.10$). Those relations are illustrated using cross plotting diagram with age on x axis and taphonomic rank on y axis. Logarithmic and linear regressions were performed to understand the trends of our variables.

1.3.14 Relationship among taphonomic variables.

To evaluate the relationships between the taphonomic parameters, the non-parametric Kendall rank correlation test was used because of the ordinal nature of the data. The tested hypothesis were: H0: based on our data distribution, the different rank samples are not statistically correlated; H1: based on our data distribution at taphonomic variables are statistically correlated. Those relations are represented using Bar-plot diagram. Significance was interpreted at $p < 0.05$. Correlation between taphonomic variables and colour was tested using Kendall coefficient correlation test with the first axis of the PCA against the different taphonomic parameters ranks. Perfect correlation were for Kendall's correlation coefficient $W=1$ and an absence of correlation were for $W=0$. Those were illustrated using PCA colour diagram with the different ranks values plotted for each parameters separately.

To understand the relationship and the consistency between our taphonomic parameters a cluster analysis were used, with Ward's method, based on a dissimilarity matrix calculated with Gowers' distance. Groups isolated by the analysis were linked with aged specimens.

1.4 Results

1.4.1 Sample area description

At Flemish cap, 22 specimens were collected on dives R-1335 and R-1336 including 6 live specimens (Table 1.1). Live specimens were collected from a cliff made of non-stratified bedrock, with angular breakage, higher than 3 meters and longer than 10 meters (Fig.0.2). Corals were homogeneously distributed on the vertical bedrock surface (an average of 16 specimens per m²). The graveyard was just below the cliff at 2200 meters depth, located at 46°N - 20.02', 44°W - 33' and covered an area less than 40 m².

At Orphan knoll, 123 specimens were collected on the R-1343 dive including 3 live specimens (Table 1). Two isolated live *Desmophyllum dianthus* corals, and one live *Flabellum alabastrum* were observed on a cliff 9 meters high and up to 10 meters long for the area just above the graveyard. This cliff was made of stratified sedimentary rock (Fig.0.2), dipping about 25° to 45° degrees to the west (Meredyk *et al.*, 2012b). A large coral graveyard was found at 50°N - 33.12', 46°W - 11.59' at the base of the cliff at 1740 meters depth, containing a large number of sub-fossil coral specimens. Two live *Desmophyllum* were collected from this site. One hundred and twenty sub-fossil corals were collected from the base of the cliff using a plastic scoop.

1.4.2 Taphonomic description

Three deep-sea corals taxa were identified: Isididae, probably *Isidella* sp. (Octocorallia: gorgonacea) (n=3), *Flabellum alabastrum* (n=1) and *Desmophyllum dianthus* (n=141) which is the most abundant in the assemblage. A total of 142 samples (Table 1.1) were evaluated on taphonomic criteria described previously (see methods).

Four taphonomic parameters have been scaled. For each parameters we found a similar pattern between population of samples collected at Ophan Knoll and those collected at Flemish cap. Ranked distribution frequencies showed a common pattern for encrustation, loss of details and macrobioerosion (Fig.1.3). For each of those parameters, the highest frequency was for the medium rank. By contrast breakage frequencies (Fig.1.3 A) showed a log-normal distribution with highest frequencies for the rank 1 (n=63) and rank 0 (n=30). The encrustation frequencies showed an even distribution (Fig.1.3 B) with higher frequencies for the rank 2 (n=70) equal frequencies for ranks 1 and 3 (n=29) and lowest frequencies for ranks 0 and 4 (respectively n=10 and n=2). The loss of details frequencies showed a negatively skewed distribution (Fig.1.3 C). The highest frequencies were for the rank 2 (n=50) and rank 3 (n=37), frequencies increased from rank 0 to rank 1 (respectively n=20 and n=27), the lowest frequency was for rank 4 (n=6). The macrobioerosion frequencies showed a distribution similar to loss of details distribution (Fig.1.3 D). The highest frequencies were for the rank 2 (n=51) and rank 3 (n=44), frequencies increased from rank 0 to rank 1 (respectively n=16 and n=17), the lowest frequency was for rank 4 (n=11).

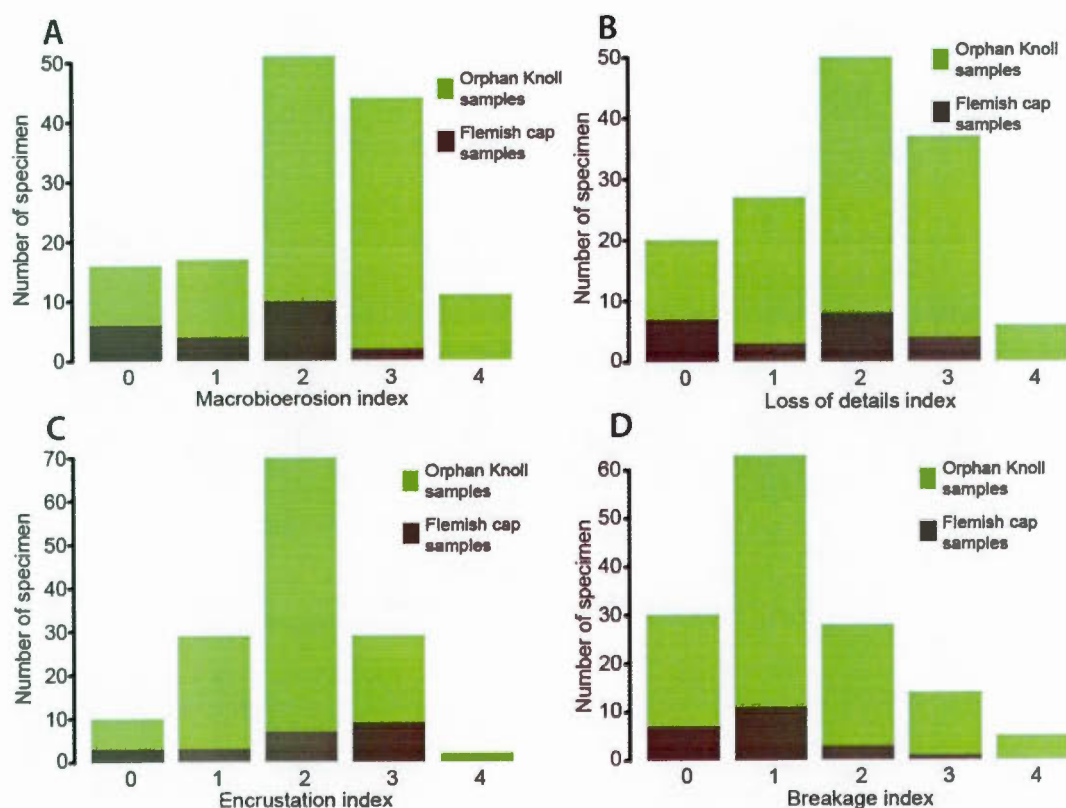


Figure 1.3 Total of degraded specimen by rank of each taphonomic processes in function of the location where they have been collected. A) Macrobioerosion rank distribution in function of the number of specimen. B) Loss of details rank distribution in function of the number of specimen. C) Encrustation rank distribution in function of the numbers of specimen. D) Breakage ranks distribution in fuction of the number of specimen.

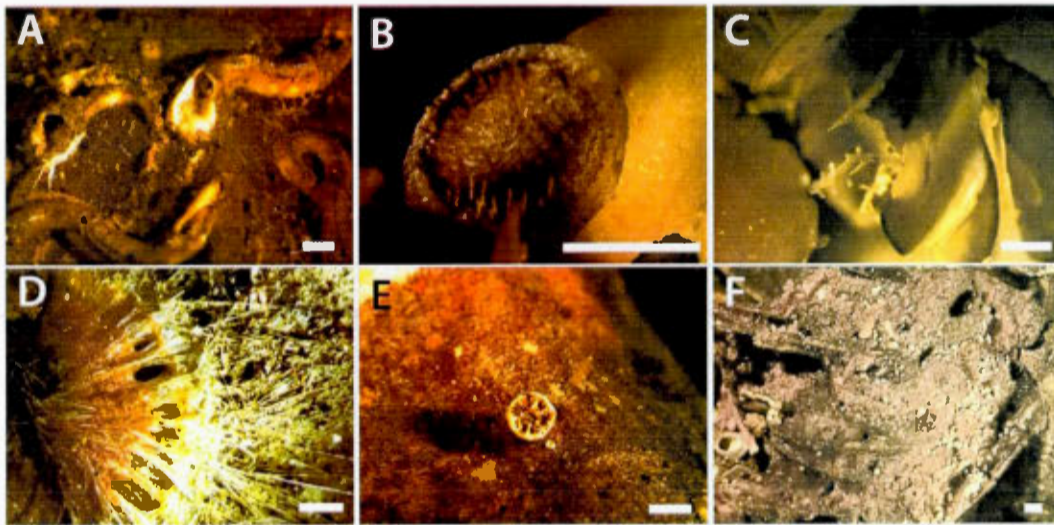


Figure 1.4 Pictures of the different type of encrustation (scale bar = 2mm). A) Serpulid calcite tube. B) Bryozan disc. C) Branching bryozoan. D) Sponge spicules. E) Juvenile *D. dianthus*. F) Tunicate.

Five encrusting organisms have been observed (Fig.1.4): Serpulid worms, characterized by the formation of calcite tubes; different forms of encrusting bryozoans; sponges, recognizable by their spicules; juvenile *D. dianthus*; and tunicates, characterized by their purple colour. The most common encruster in our population were serpulid worms, affecting 126 specimens (Fig.1.5). Sponges affected 40 specimens, bryozoans affected 36, juvenile *D. dianthus* affected 4 specimens and 3 specimen was affected by a tunicate.

Three forms of macrobioerosion degradation have been noted. Those forms were imposed on the specimens by two endolithic organisms: clionid sponges and worms, and by grazing organism like sea-urchins (Fig.1.6). Clionid sponges were identifiable by the fossils trace *Entobia* spp. they formed. Worms perforate the skeleton and create easily recognizable tunnels. Other organism participated in less proportion to the macrobioerosion process. Sponge traces affected 114 specimens (Fig.1.7), and

were the most common macrobioerosion degradation in our two collections; sea-urchin trace affected 71 specimens, and worms, 3.

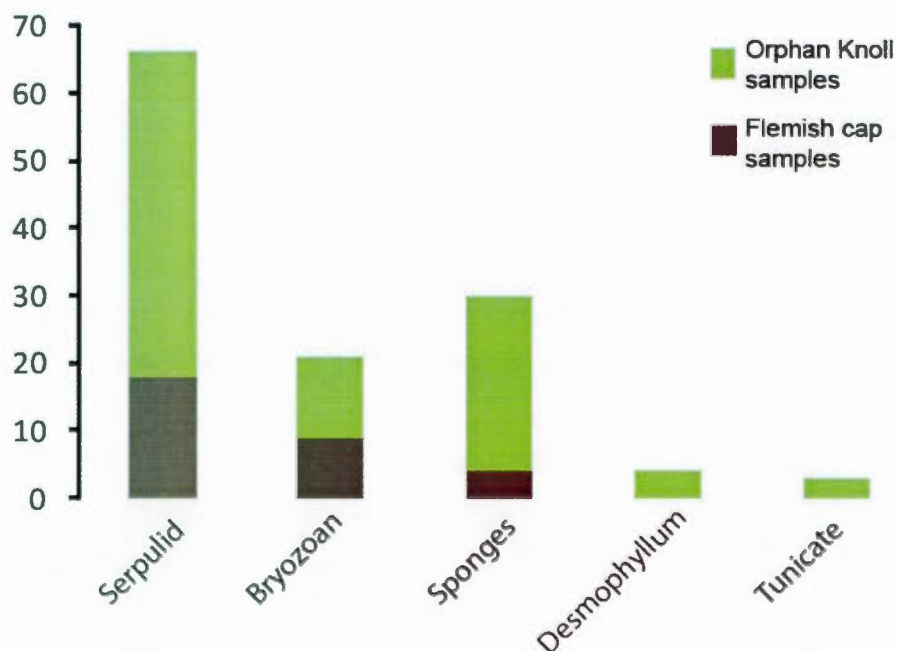


Figure 1.5 Number of specimen degraded by the different type of encrustation, sponges and tunicate are soft bodied organisms. Total *D. dianthus* population $n=142$, collected in Orphan Knoll and Flemish Cap.

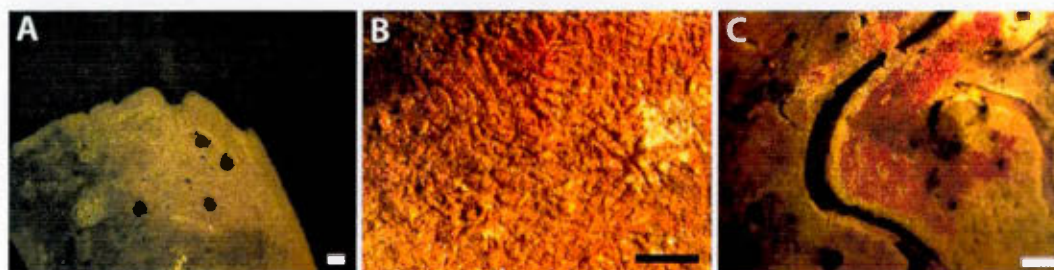


Figure 1.6 Pictures of different type of macrobioerosion (scale bar = 2mm). A) *Entobia* made by endolithic sponges. B) Grazing traces made by sea urchins. C) Gallery in *D. dianthus* skeleton made by endolithic worm.

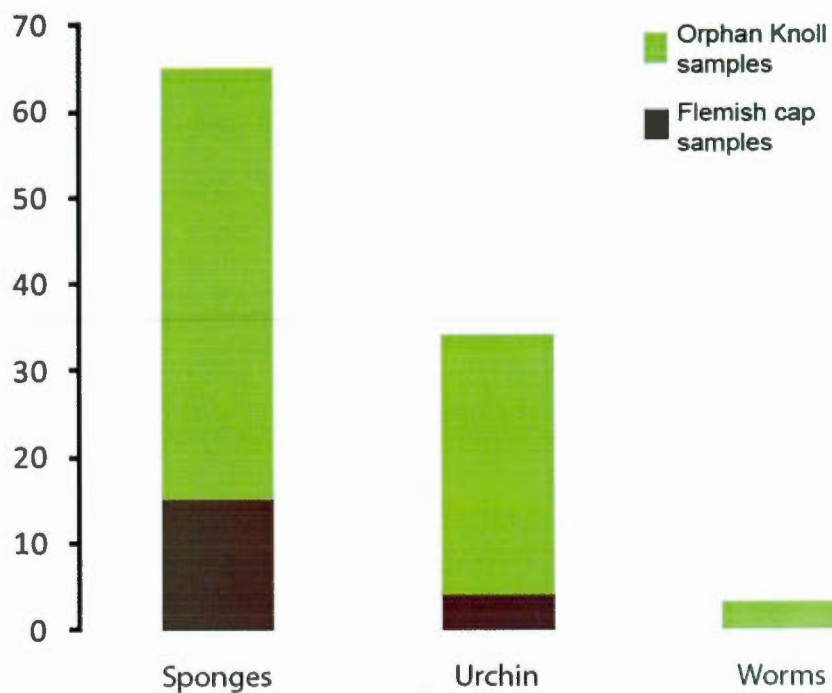


Figure 1.7 Number of specimen degraded by the different type of macrobioerosion. Total *D. dianthus* population $n=142$, collected in Orphan Knoll and Flemish Cap.

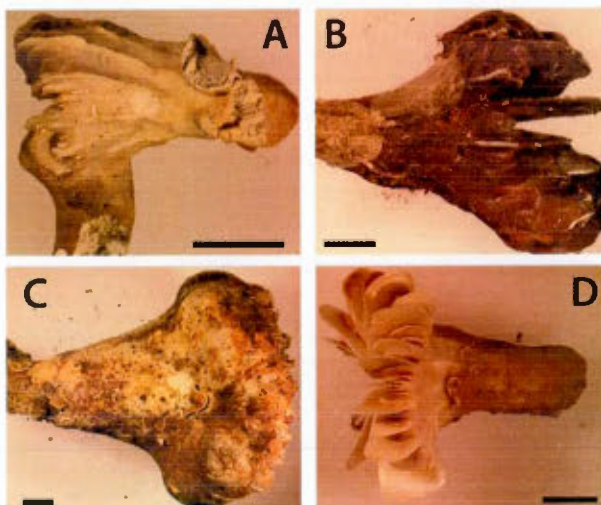


Figure 1.8 Pictures of colour diversity of *D. dianthus* mostly caused by precipitation of Mn oxide coating (scale bar = 1cm). A) D39 sample. B) D14 sample. C) D5 sample. D) D59 sample.

Specimens colours (Fig.1.8) were mostly linked with ferromanganese oxide coatings on the coral skeleton. Distribution of those colour on scatter diagram (Fig.1.9), along two axis calculated using PCA analysis, was strongly related to dark/light difference represented by the first axis, which explained 80.79% of the total variance of the sample population. The second axis explained 16.1% of the population variance. This axis is strongly related to red colour axis.

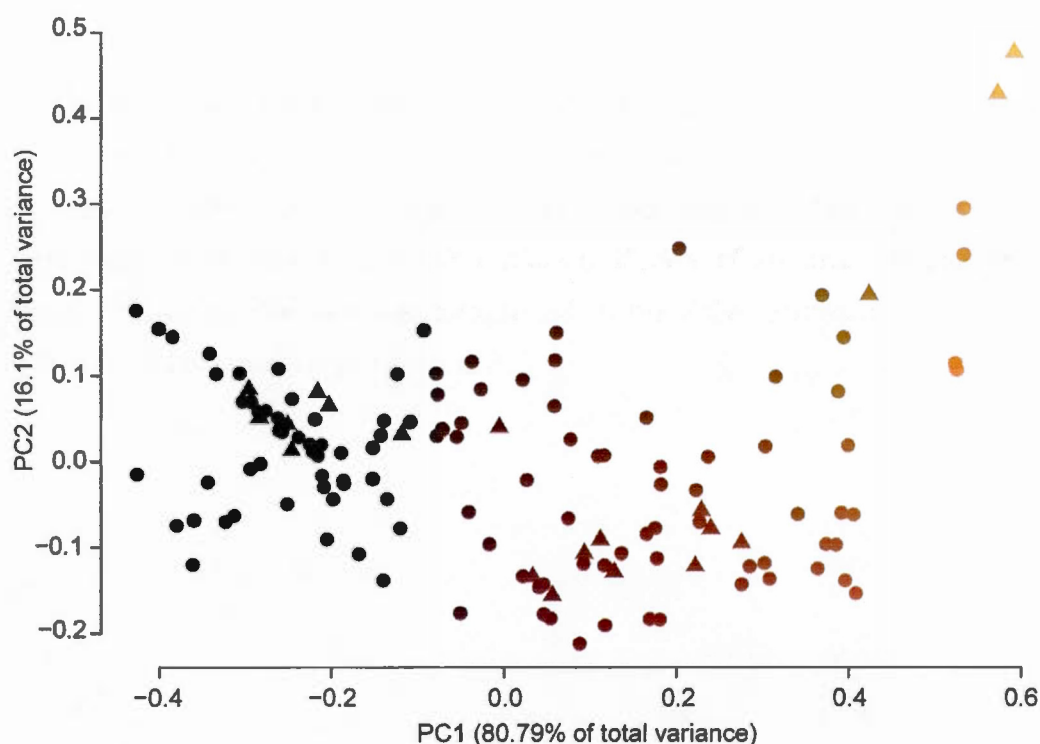


Figure 1.9 Scatter diagram of PCA result on colour data from *D. dianthus* population collected in O.K. The first axis is strongly related with dark/light difference and explain 80.79% of the data dispersion. The second axis explain 16.1% of the total population variance and is strongly related to red gradient. This diagram was realized using R software on a total *D. dianthus* population $n=142m$. Triangles are for Flemish Cap specimens, dots for Orphan Knoll specimens.

1.4.3 Radiocarbon and U-series dating

The results of the AMS-14C dating of deep-sea corals are presented in Table 1.3. Dating of D24, collected alive, with radiocarbon and U-series yielded ages of $166 \text{ years} \pm 101 \text{ cal. BP}$ and $188 \text{ years} \pm 4$, respectively (see Table 1.2). Those ages are consistent with the longevity of those organisms (Smith, Jodie E. *et al.*, 1997). Ages of the live sampled *Desmophyllum* specimens from Flemish cap (D56 and D58), ranged between $73 \text{ years} \pm 73$ and $296 \text{ years} \pm 71$ (Cal BP).

Three sub-fossil coral specimens from Orphan Knoll were aged between 611 ± 166 and $1,284 \pm 65 \text{ cal years BP}$. Three others were between $5,759 \pm 118 \text{ cal years BP}$ and $9,703 \pm 161 \text{ cal years BP}$. For the remaining 10 fossilised samples we found a radiocarbon age over 40,000 years BP, suggesting that the samples were radiocarbon dead. U-series ages were determined for the live-collected sample D24 and for all samples with radiocarbon ages $> 40\text{ka}$. Uranium and Thorium concentrations are presented in Table 4. The nine samples remaining had U-series ages between 97,000 and 107,000 years BP (Fig.1.10). One sample (D5) had an U-series age of $180,987 \pm 4,856 \text{ years}$.

Sample ages were grouped around 2 main intervals (Fig.1.10). The first group, with live-collected and sub-fossil specimens up to 9,700 years old, corresponds to the Marine Isotopic Stage 1 (MIS 1), or Holocene ages. The second group contains sub-fossil corals age between 97,000 years and 111,000 years and corresponds to the Marine Isotopic Stage 5 (MIS 5c-d), part of the last interglacial interval. The specimen D5, dated to $\sim 181,000 \text{ years}$, corresponds to MIS 7a.

Tableau 1.3 $\delta^{13}\text{C}$, $\delta^{18}\text{O}$ and ages obtained on deep-sea corals samples * = live-collected specimen, ** = Flemish cap specimen. $\delta^{13}\text{C}$ and radiocarbon datation for Isidids D22 and D23 were run at ANU lab, with $\delta^{18}\text{O}$ analyzed separately at GEOTOP laboratory therefore not really a split sample. For the other radiocarbon dating samples, datation were run in CEA Saclay center and stables isotopes in GEOTOP laboratory on the same sub-sample. For the U-series dating samples analyses, including stable isotopes, were made in GEOTOP laboratory on the same sub-sample.

| Lab number | Sample id. | Species | Skeleton composition | $\delta^{13}\text{C}$ | $\delta^{18}\text{O}$ | PMC fractionation fixing | radiocarbon age (years BP) | Cal radiocarbon age (years BP) | U-series age (year BP) |
|----------------|------------|-------------------------------|----------------------|-----------------------|-----------------------|--------------------------|----------------------------|--------------------------------|------------------------|
| I778 FB-CH-D56 | D56** | <i>Desmophyllum dianthus*</i> | aragonite | -4,55 | 1,57 | 94,47 ± 0,33 | 455 ± 30 | 73 ± 73 | |
| I782 FB-CH-D24 | D24 | <i>Desmophyllum dianthus*</i> | aragonite | -4,94 | 1,55 | 93,48 ± 0,35 | 540 ± 30 | 165 ± 100 | 188 ± 4 |
| I772 FB-CH-D58 | D58** | <i>Desmophyllum dianthus*</i> | aragonite | -5,18 | 1,29 | 92,47 ± 0,31 | 630 ± 25 | 296 ± 71 | |
| I773 FB-CH-D18 | D18 | <i>Desmophyllum dianthus</i> | aragonite | -1,61 | 2,53 | 87,68 ± 0,37 | 1055 ± 35 | 611 ± 66 | |
| I781 FB-CH-D20 | D20 | <i>Isidid</i> | calcite | 0,93 | 2,79 | 84,50 ± 0,32 | 1355 ± 30 | 883 ± 84 | |
| 30816 | D22 | <i>Isidid</i> | calcite | -0,02 | 2,59 | 80,64 ± 0,31 | 1730 ± 35 | 1284 ± 65 | |
| I775 FB-CH-D33 | D33 | <i>Desmophyllum dianthus</i> | aragonite | -4,59 | 1,51 | 51,15 ± 0,29 | 5385 ± 45 | 5759 ± 118 | |
| I776 FB-CH-D13 | D13 | <i>Desmophyllum dianthus</i> | aragonite | -4,20 | 2,00 | 50,71 ± 0,27 | 5455 ± 45 | 5818 ± 108 | |
| 30820 | D23 | <i>Isidid</i> | calcite | 0,56 | 2,36 | 32,56 ± 0,18 | 9015 ± 45 | 9703 ± 161 | |
| I780 FB-CH-D19 | D19-1 | <i>Desmophyllum dianthus</i> | aragonite | -7,22 | 1,40 | < 0,41 | > 44 100 BP | > 44 100 BP | 97426 ± 2470 |
| I783 FB-CH-D15 | D15 | <i>Desmophyllum dianthus</i> | aragonite | -4,68 | 2,68 | < 0,41 | > 44 100 BP | > 44 100 BP | 98672 ± 1782 |
| I779 FB-CH-D27 | D27 | <i>Desmophyllum dianthus</i> | aragonite | -4,76 | 2,13 | < 0,41 | > 44 100 BP | > 44 100 BP | 105100 ± 2000 |
| I787 FB-CH-D3 | D3 | <i>Desmophyllum dianthus</i> | aragonite | -5,01 | 2,37 | < 0,42 | > 44 000 BP | > 44 000 BP | 105776 ± 2617 |
| I785 FB-CH-D46 | D46 | <i>Desmophyllum dianthus</i> | aragonite | -6,09 | 1,66 | < 0,41 | > 44 100 BP | > 44 100 BP | 106535 ± 3449 |
| I786 FB-CH-D47 | D47 | <i>Desmophyllum dianthus</i> | aragonite | -6,47 | 0,46 | < 0,64 | > 40 600 BP | > 40 600 BP | 106600 ± 1900 |
| I774 FB-CH-D17 | D17-2 | <i>Desmophyllum dianthus</i> | aragonite | -5,80 | 2,07 | < 0,42 | > 44 100 BP | > 44 100 BP | 106602 ± 2614 |
| I771 FB-CH-D2 | D2 | <i>Desmophyllum dianthus</i> | aragonite | -3,74 | 2,78 | < 0,41 | > 44 100 BP | > 44 100 BP | 106817 ± 2395 |
| I784 FB-CH-D16 | D16 | <i>Desmophyllum dianthus</i> | aragonite | -7,62 | 0,99 | < 0,66 | > 40 300 BP | > 40 300 BP | 111823 ± 2586 |
| I777 FB-CH-D5 | D5 | <i>Desmophyllum dianthus</i> | aragonite | -5,98 | 2,01 | < 0,42 | > 44 100 BP | > 44 100 BP | 180987 ± 4856 |

Tableau 1.4 U-series ages measured by TIMS. Half-lives of ^{234}U and ^{230}Th used in the calculations are $245,250 \pm 490$ yr and $75,690 \pm 230$ yr respectively (Cheng et al., 2000). The decay constant for ^{238}U is $1.551 \times 10^{-10} \text{ year}^{-1}$ (Jaffey et al., 1971). Ages are calculated according to equation defined by Edwards (1978) with no correction for initial ^{230}Th . All errors are 2σ .

| Sample id. | Weight (g) | $[^{238}\text{U}]$ ppm | $[^{232}\text{Th}]$ ppb | $^{230}\text{Th}/^{232}\text{Th}$ | $^{234}\text{U}/^{238}\text{U}$ | $^{230}\text{Th}/^{234}\text{U}$ | U-series age (Year BP) |
|------------|------------|------------------------|-------------------------|-----------------------------------|---------------------------------|----------------------------------|------------------------|
| D24 | 3,805 | 3,13 \pm 0,014 | 0,40 \pm 0,002 | 47,61 \pm 1,22 | 1,154 \pm 0,007 | 0,002 \pm 0,000 | 188 \pm 4 |
| D19-1 | 1,059 | 3,29 \pm 0,014 | 1,80 \pm 0,020 | 3762,48 \pm 68,07 | 1,123 \pm 0,008 | 0,600 \pm 0,009 | 97426 \pm 2470 |
| D15 | 1,002 | 4,17 \pm 0,017 | 1,49 \pm 0,010 | 5818,05 \pm 66,42 | 1,122 \pm 0,007 | 0,605 \pm 0,006 | 98672 \pm 1782 |
| D27 | 1,017 | 3,76 \pm 0,017 | 6,94 \pm 0,036 | 1171,46 \pm 9,71 | 1,120 \pm 0,009 | 0,634 \pm 0,006 | 105100 \pm 2000 |
| D3 | 1,087 | 3,90 \pm 0,015 | 35,25 \pm 0,370 | 237,42 \pm 4,10 | 1,115 \pm 0,006 | 0,631 \pm 0,009 | 105776 \pm 2617 |
| D46 | 1,020 | 3,33 \pm 0,016 | 4,41 \pm 0,052 | 1641,57 \pm 32,90 | 1,121 \pm 0,011 | 0,634 \pm 0,012 | 106535 \pm 3449 |
| D47 | 1,005 | 4,18 \pm 0,019 | 6,93 \pm 0,040 | 1294,81 \pm 12,10 | 1,117 \pm 0,009 | 0,628 \pm 0,006 | 106600 \pm 1900 |
| D17-2 | 1,008 | 3,96 \pm 0,017 | 18,57 \pm 0,175 | 456,46 \pm 7,14 | 1,106 \pm 0,008 | 0,633 \pm 0,009 | 106602 \pm 2614 |
| D2 | 1,053 | 3,95 \pm 0,017 | 6,38 \pm 0,055 | 1335,19 \pm 18,64 | 1,113 \pm 0,008 | 0,634 \pm 0,008 | 106817 \pm 2395 |
| D16 | 1,012 | 3,18 \pm 0,012 | 11,63 \pm 0,106 | 615,37 \pm 9,47 | 1,128 \pm 0,006 | 0,653 \pm 0,008 | 111823 \pm 2586 |
| D5 | 1,073 | 3,53 \pm 0,013 | 3,79 \pm 0,026 | 2566,43 \pm 28,19 | 1,094 \pm 0,006 | 0,826 \pm 0,008 | 180987 \pm 4856 |

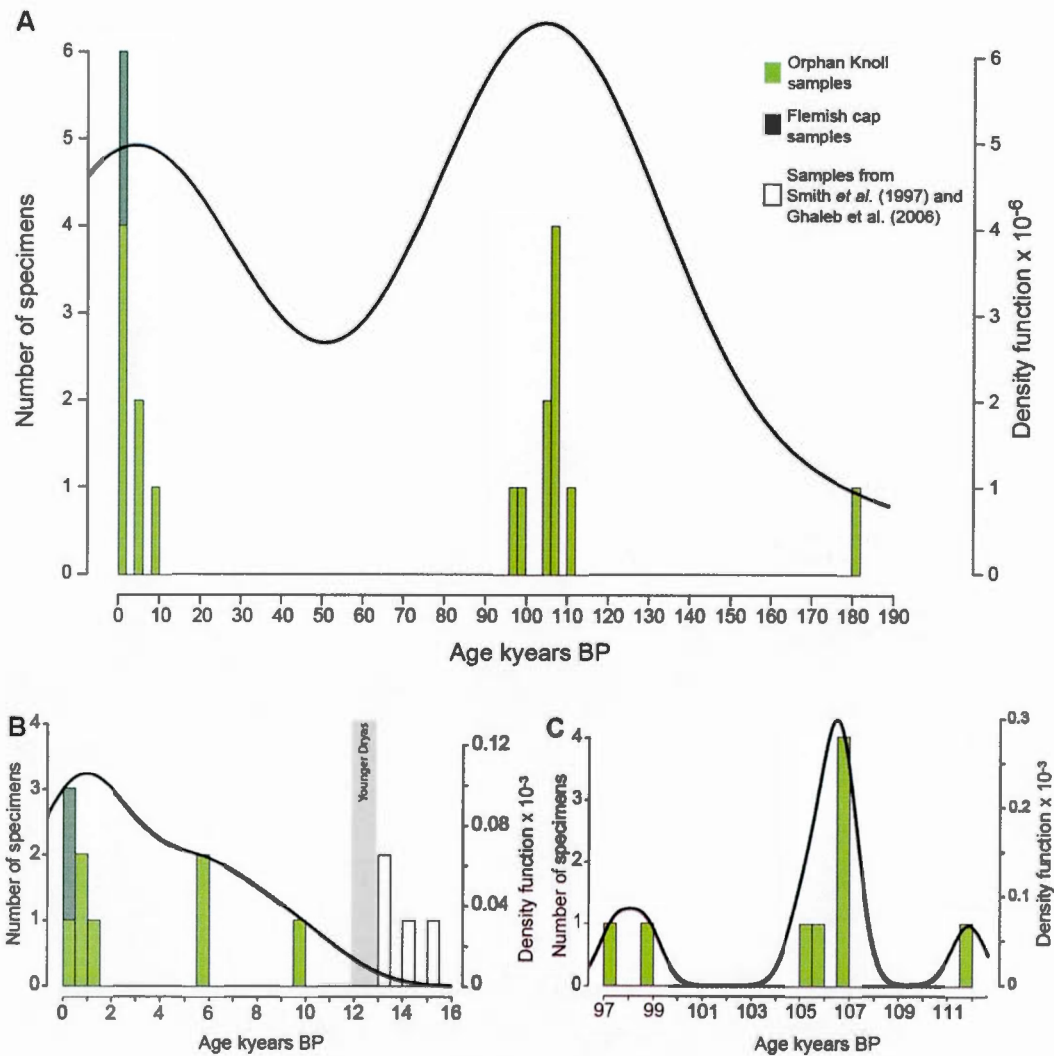


Figure 1.10 age distribution diagram and predicted distribution curves using equation 1 on Orphan Knoll samples, h represent the smoothing parameter and n the number of samples the density function calculated with equation 1 is the probability density function of the sample distribution. A) Distribution for the full length of time represented by our sample suite ($n = 17$, $h = 2.981e4$) age bins 2,000 years. B) Detail of the distribution for the Holocene and associated density curve ($n = 7$, $h = 2227$), age bins 500 years. C) Detail of the distribution for the MIS 5 with the associated density curve ($n = 9$, $h = 672.6$) age bins 500 years.

The predicted age distribution curve for the live-collected and Holocene corals (Fig.1.10.B) approximates a logarithmic shape (1-tailed distribution). By contrast, the MIS-5 age distribution approximates a 2-tailed Gaussian distribution.

1.4.4 Taphonomic parameters vs sample age

Cluster analysis based on taphonomic variables created 4 groups (Fig.1.11). One of those groups collects all the live collected samples and sample aged from 600 years to 1300 years. The other aged specimens were distributed among the 4 different groups.

The age distribution of taphonomic parameter ranks through time (Fig.1.12) showed differences between taphonomic parameters. Macrobioerosion and loss of details had higher ranks for older specimen (MIS 5 and 7) than for Holocene specimens. This were demonstrated by Kruskal-Wallis rank sum test (see Table 1.5), the Holocene population and the MIS5/7 population have been differentiated with macrobioerosion parameter ($\chi^2 = 3$, $df = 1$, $p = 0.08326$). Therefore the two populations did not differ in the loss of details parameter ($\chi^2 = 4$, $df = 3$, $p = 0.2615$). Furthermore those parameters, macrobioerosion and loss of details, had the higher logarithmic regression r^2 (respectively $r^2=0.2782$ and $r^2=0.2665$). The linear regression gave respectively $r^2=0.1403$ and $r^2=0.1867$.

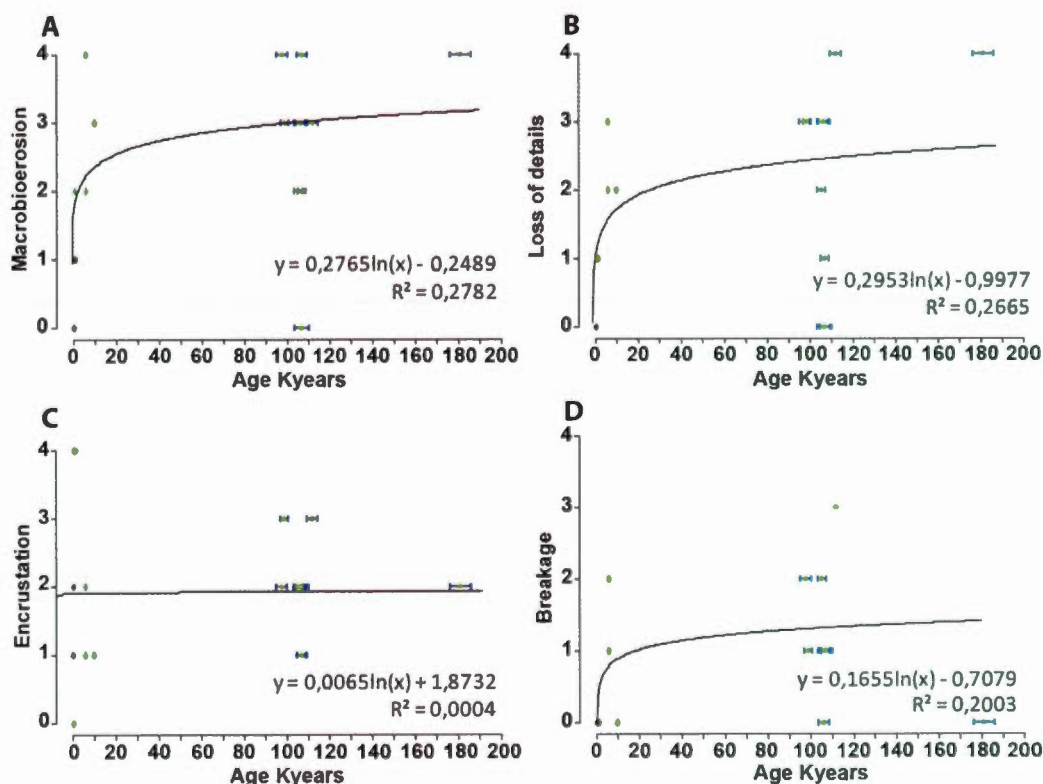


Figure 1.12 Taphonomic ranks distribution for aged samples (n=18), with logarithmic regression curves, horizontal error bar were acquired during experimentation. Because of the horizontal scale some dot are overlapped, green are for Orphan Knoll samples and dark grey for Flemish cap samples. All the ages are cal. BP. A) Macrobioerosion distribution B) Loss of details distribution. C) Encrustation distribution. D) Breakage distribution.

By contrast, the breakage parameter was not different between Holocene and Pleistocene samples (see Fig.1.12) the two population couldn't be differentiated ($\chi^2 = 3.3158$, $df = 2$, $p = 0.1905$). This parameter showed a logarithmic regression of $r^2=0.2003$. The linear regression gave a $r^2=0.0659$.

Tableau 1.5 Kruskal Wallis rank sum test differentiating each population (Holocene vs Pleistocene) for each parameter.

| Tested parameter | Chi2 | Degree of freedom | p-value |
|------------------------|--------|-------------------|---------|
| Breakage | 3,3158 | 2 | 0,1905 |
| Encrustation | 1,2778 | 3 | 0,7344 |
| Loss of details | 4 | 3 | 0,2615 |
| Macrobioerosion | 3 | 1 | 0,08326 |
| Serpulids encrustation | 1,4211 | 3 | 0,7006 |
| Sponges encrustation | 2,1333 | 2 | 0,3442 |
| Sponges macroboring | 2,4 | 2 | 0,3012 |
| Urchin macrobioerosion | 3,3333 | 2 | 0,1889 |
| Colour | 5 | 5 | 0,4159 |

Encrustation parameter showed less differences between specimens from the MIS 5/7 population and Holocene population than macrobioerosion, loss of detail, or breakage, Kruskal-Wallis test did not differentiate between the populations ($\chi^2 = 1.2778$, $df = 3$, $p = 0.7344$) and logarithmic regression vs. age had a weak r^2 value ($r^2=0.0004$). The linear regression gave a $r^2=0.0054$.

Apparent differences were noted between the main encrusters and macroborer organisms through time (Fig.1.13). Serpulids encrusters have the same attitude than total encrustation parameter.

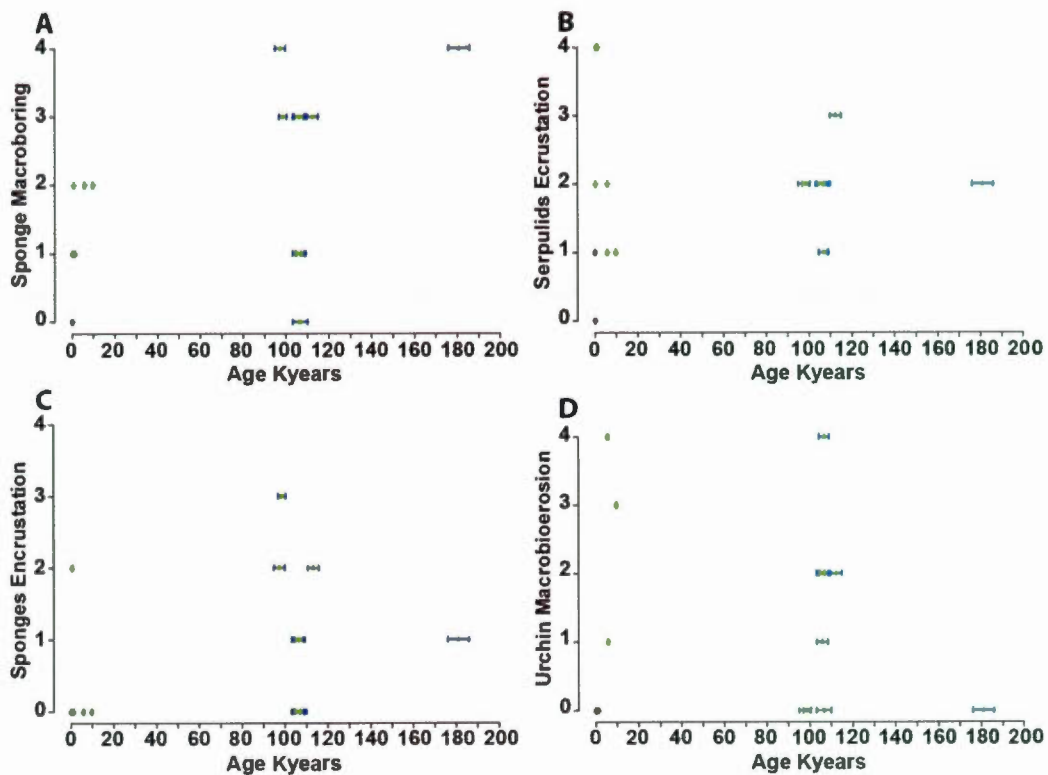


Figure 1.13 Detailed taphonomic ranks distribution for aged samples (n=18), horizontal error bar were acquired during experimentation. Because of the horizontal scale some dot are overlapped, green are for Orphan Knoll samples and dark grey for Flemish cap samples. All the ages are cal. BP. A) Sponges macroboring distribution B) Encrustation of serpulids tubes distribution. C) Encrustation of sponges distribution. D) Sea urchin grazing traces distribution.

In contrast encrusting sponges were common for MIS 5/7 population and unequal for the different specimen. Sponges macroboring traces affected more MIS 5/7 specimens than Holocene specimens. By contrast, sea-urchins grazing traces were more common in the Holocene population than in MIS 5/7 population. However, Kruskal-Wallis rank sum test found no significant differences between Holocene and MIS 5/7 populations for any of those variables.

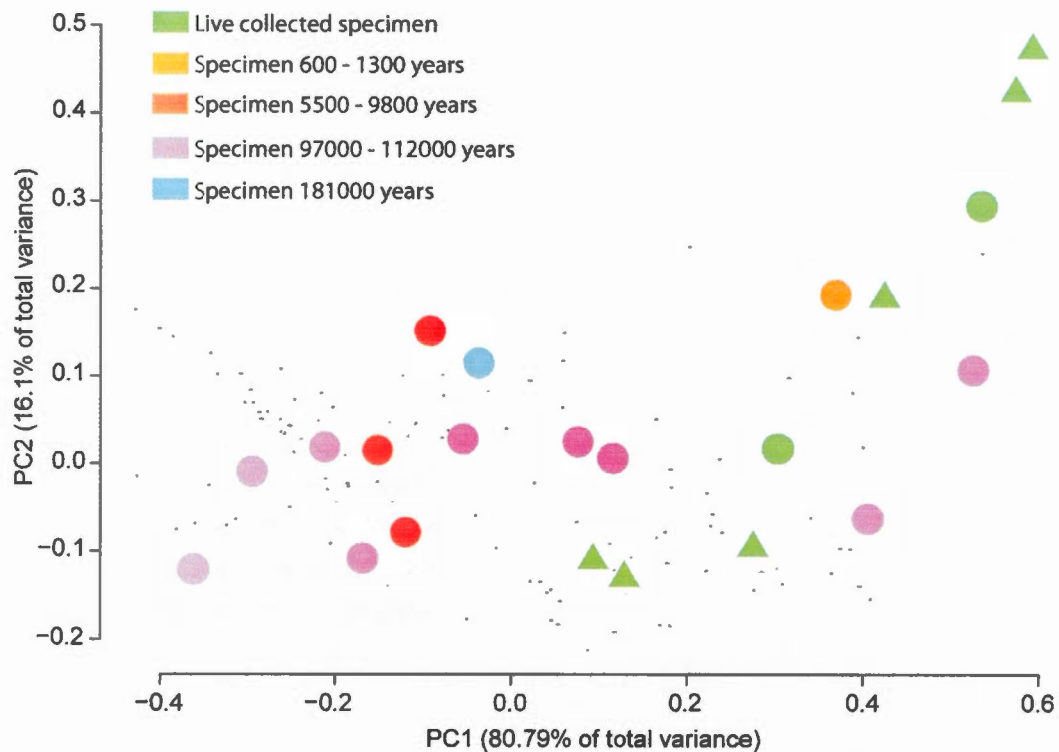


Figure 1.14 Dispersion diagram using colour PCA data and dated specimen. The first axis which is strongly related to dark/fair difference explain 81.95% of the data dispersion. Green colour marked live collected specimen, orange and red the Holocene specimen, purple for the MIS 5 specimen and blue for MIS 7 specimen. Triangles are for Flemish Cap specimens, dots for Orphan Knoll specimens.

PCA using colour data don't allow us to regroup aged specimen in specific colours (Fig.1.14). Recent specimen (live collected and younger than 1300 years cal. BP) were distributed along a vector explained both by the first (dark/fair difference) and the second axis (red colour). Those samples were concentrated in the fairest part of the diagram. The older specimen except D46 and D47, were on the darker part of the diagram. Therefore the Holocene population could not be statistically differentiated from the MIS 5/7 population ($\chi^2 = 5$, $df = 5$, $p = 0.4159$), no clear relation between the age and the colour was observed (Table 1.5). Logarithmic regression showed a $r^2=0.2151$.

1.4.5 Relation between taphonomic parameters

A strong relationship between macrobioerosion and loss of detail was observed. Kendall correlation rank test (see Table 1.6) showed a significant relationship between those parameters ($T = 0.661$, $n = 142$, $p = <2.2 \times 10^{-16}$). This was illustrated by the barplot (Fig. 1.15A), the higher loss of details ranks were correlated with the higher macrobioerosion ranks.

Tableau 1.6 Kendall correlation rank test results between the different parameters. T represent the strength of association for each parameter in row with the one in column. A value of 1 is for a perfect association and 0 the absence of association.

| | Loss of details | Macrobioerosion | Breakage | Encrustation |
|-----------------|-----------------|---------------------------|----------------|--------------|
| Loss of details | | $p < 2.2 \times 10^{-16}$ | $p = 0.004624$ | $p = 0.0036$ |
| Macrobioerosion | $T = 0.661$ | | $p = 0.04101$ | $p = 0.5251$ |
| Breakage | $T = 0.2015$ | $T = 0.14645$ | | $p = 0.8752$ |
| Encrustation | $T = 0.2092$ | $T = 0.04601$ | $T = -0.01141$ | |

Kendall correlation rank test (Table 1.6) showed a positive correlation between breakage and loss of details or macrobioerosion parameters, with: $T = 0.2015$, $p = 4.624 \times 10^{-3}$ for breakage/loss of details and $T = 0.14645$, $p = 0.04101$ for breakage/macrobioerosion. On barplots (Fig. 1.15.C and D) the higher breakage ranks were correlated with the higher macrobioerosion and loss of details ranks. We can observe an increase of breakage index concomitantly with an increase of loss of details rank. In contrast the lower breakage index were nearly equally distributed among the macrobioerosion index.

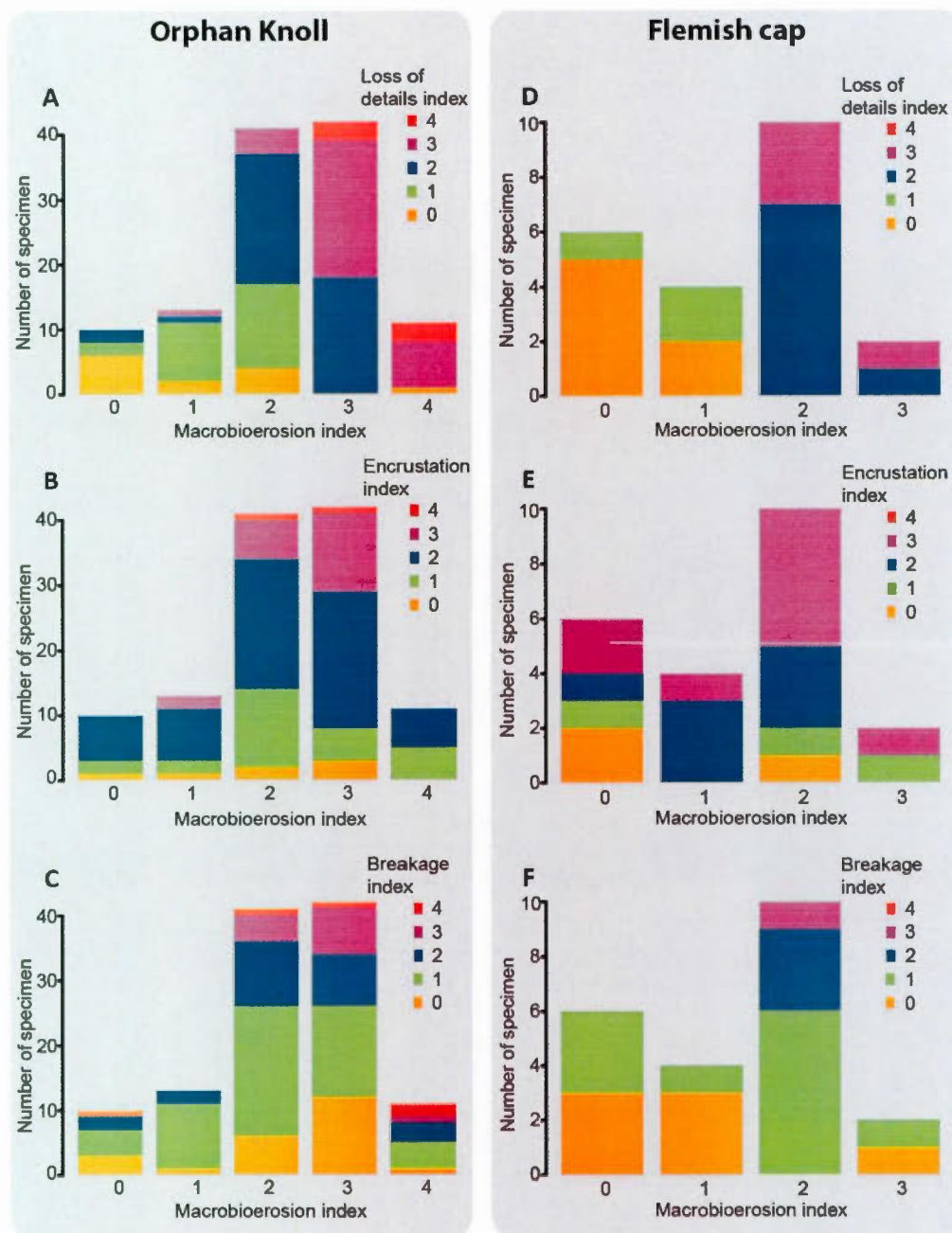


Figure 1.15a taphonomic rank distribution the left column is for samples collected at Orphan Knoll the right column for samples collected at Flemish cap. A) Loss of details rank distribution in function of macrobioerosion index. B) Encrustation rank distribution in function of macrobioerosion index. C) Breakage rank distribution in function of macrobioerosion index. D) Same as A for Flemish cap. E) Same as B for Flemish cap. F) Same as C for Flemish cap.

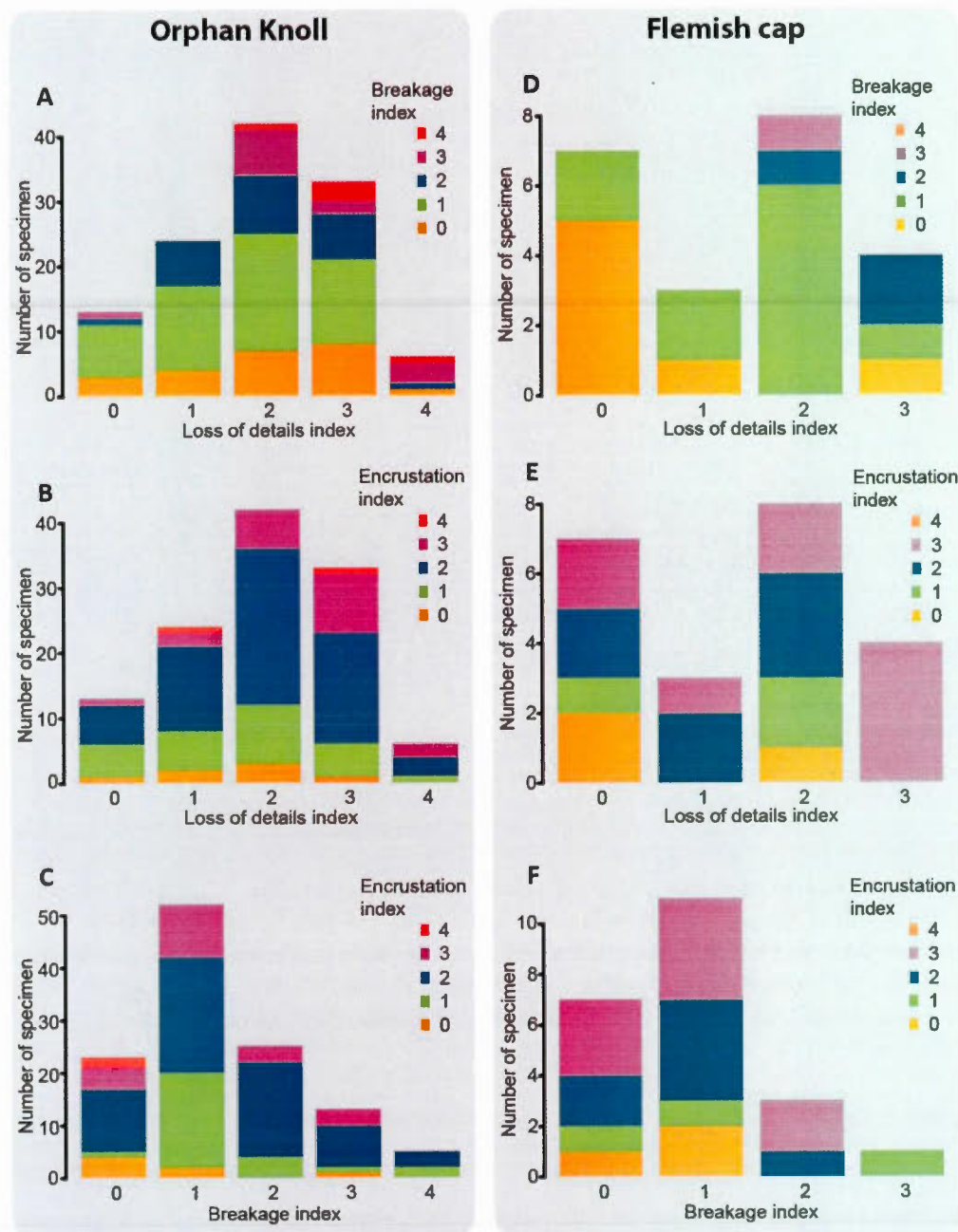


Figure 1.16b taphonomic rank distribution the left column is for samples collected at Orphan Knoll the right column for samples collected at Flemish cap. A) Breakage rank distribution in function of loss of details index. B) Encrustation rank distribution in function of loss of details index. C) Encrustation rank distribution in function of breakage index. D) Same as A for Flemish cap. E) Same as B for Flemish cap. F) Same as C for Flemish cap.

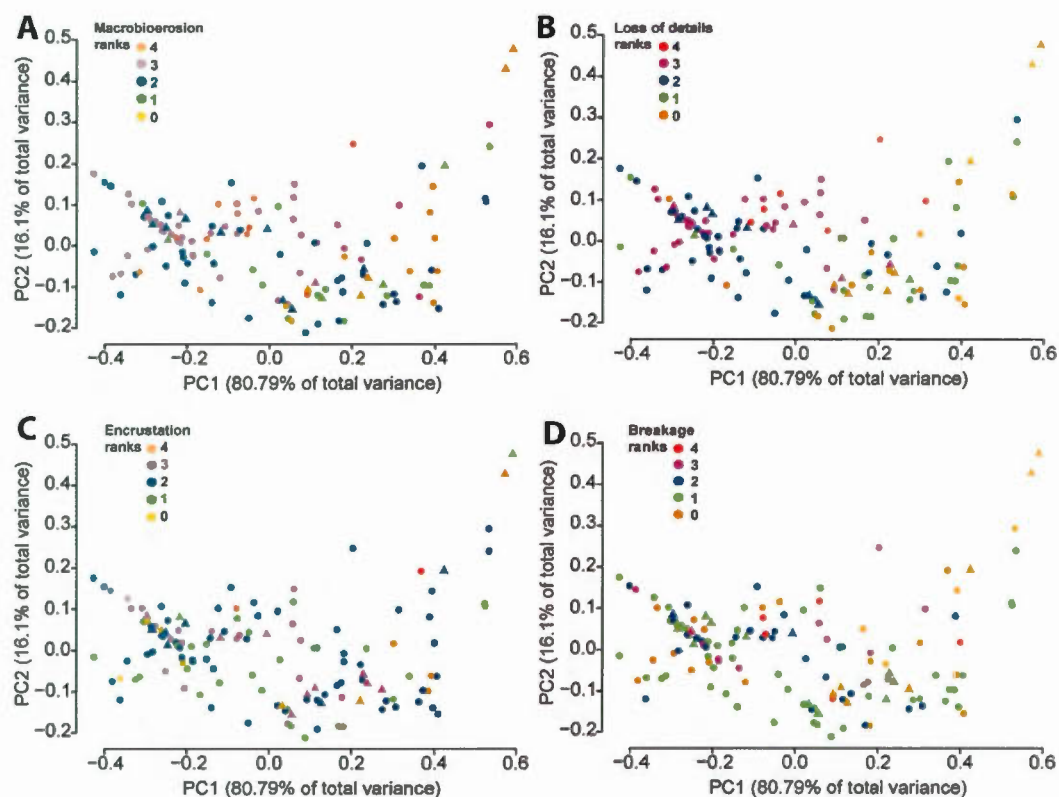


Figure 1.17 Dispersion diagram using colour PCA data and the other taphonomic processes ranks. A) Macrobioerosion ranks dispersion. B) Loss of details ranks dispersion. C) Encrustation ranks dispersion. D) Breakage ranks dispersion. Triangles are for Flemish Cap specimens, dots for Orphan Knoll specimens.

Kendall correlation rank test showed no significant parameter correlation with the encrustation index: with $T = 0.2092$, $p = 0.0036$ for encrustation/loss of details, $T = -0.04601$, $p = 0.5251$ for encrustation/macrobioerosion and $T = -0.01141$, $p = 0.8752$ for encrustation/breakage. Barplots (Fig. 1.15.B, E and F) revealed a sub-homogenous distribution between encrustation index values and the other taphonomic parameters.

No statistical relations have been identified between PCA result on samples colours and the others taphonomic parameters. However Kendall coefficient test (Table 1.7)

showed strongest correlation between sample colour and encrustation or breakage ($W=0.4549$, $p\text{-perm}=0.848$ and $W=0.4146$, $p\text{-perm}=0.978$) than for loss of details and macrobioerosion showed weak correlation with sample colours ($W=0.2558$, $p\text{-perm}=1$ and $W=0.2966$, $p\text{-perm}=1$). Ranks distribution on PCA diagram (Fig.1.16.C and D) showed a predominance of the lowest taphonomic ranks sub-homogeneously distributed for encrustation and breakage parameters, the highest ranks were restricted to the darkest part of the diagram. In contrast, for macrobioerosion and loss of details, medium ranks dominated the diagram (Fig.1.16.A and B) and were sub-homogeneously distributed while lowest and highest ranks were restricted to fairest and darkest of the diagram.

Tableau 1.7 Kendall coefficient test between colour and taphonomic parameters. W is Kendall's coefficient of concordance, $F = W*(m-1)/(1-W)$ where m is the number of judges, Prob.F is the probability associated with F statistic, the χ^2 is Friedman's χ^2 statistic and Prob.perm is the permutation probability.

| | W | F | Prob.F | χ^2 | Prob.perm |
|----------------|--------|--------|--------|----------|-----------|
| Loss of detail | 0,2558 | 0,3438 | 1 | 71,1282 | 1 |
| Macroboring | 0,2966 | 0,4218 | 0,9999 | 82,4745 | 1 |
| Encrustation | 0,4549 | 0,8347 | 0,855 | 126,48 | 0,848 |
| Breakage | 0,4146 | 0,7084 | 0,978 | 115,282 | 0,978 |

1.5 Discussion

1.5.1 Effect of burial

Fossil samples were collected at the base of the underwater cliff on which are living communities of *Desmophyllum dianthus*. In a low-current environment (Greenan, Yashayaev, Head, Harrison, Azetsu-Scott, Li, Loder et Geshelin, 2010), bioclasts are subject to virtually no transport by moving water. Under those circumstances, the loss of detail samples should not be subject to mechanical abrasion. Microboring caused

by micro-organism is the parameter that best explain this loss of detail. Macrobioerosion and loss of details mostly are the main processes that altered coral skeleton. Those processes are caused by organisms that used corals skeleton as food source or substratum. Older specimen are the most degraded by those processes, they might have stay on the water / sediment interface over a long period of time.

Two specimens could be distinguished on the PCA analysis (Fig. 14): D46 and D47. They have been dated from the MIS 5 and remain well preserved without macrobioerosion traces, loss of details or ferro-manganese oxides coating. That difference with the other MIS 5 specimen could be explained by a possible quick burial that have protected them from bioeroders and encrusters. Mn oxide (dark) will continuously precipitate on unburied deep-sea corals skeleton through time. Fe- oxide coating gives this dark red colour.

Those specimens are the only well preserved MIS 5 specimens. Their probable burial remains exceptional in that low sedimentation rate environment. This differs from shallow water environment in which organism shell or skeleton will be exhumed and buried several time before being buried and preserved as fossils (Edinger, E. *et al.*, 2007 ; Estrada Alvarez *et al.*, 2004 ; Kidwell et Flessa, 1996 ; Olszewski, 2004). In deep-sea graveyards, the low hydrodynamism will not perturb the limited sediment that has been deposited.

Skeletons still leave recognizable remains even after a long degradation period. That can be explained by the low rate of alteration despite a low rate of burial. This apparent contradiction could be explain by the lack of light and the low primary productivity that cause bioencrusters less common and less bioerosion activity.

1.5.2 Taphonomic processes through time in the deep-sea

As described by Freiwald (Freiwald, André et Wilson, 1998) on *Lophelia pertusa*, living deep-sea corals are protected from encrusters because of their mucus production. As expected, younger subfossil skeletons (from 500 to 10 000 years) seem to be more encrusted by a high diversity of organisms (Serpulids, bryozans, tunicate, etc). But in contrast older skeletons from MIS 5 and 7 are less encrusted than specimens from Holocene. Macrobioerosion, also describe by Freiwald (Freiwald, André et Wilson, 1998) as the result of sponge activity, and the loss of details resulting of the action of micro-bioeroders are correlated with the specimen age. By contrast breakage and encrustation parameters seems to be poorly related to the age of the specimen.

The non-correlation of those two parameters can be caused by what we will call the saturation value of the taphonomic index. Regressions were weak for all the taphonomic parameters, but the r^2 values were higher using a logarithmic regression than polynomial or a linear regression for macrobioerosion, loss of details, breakage and colours parameters. That means that the best trend to explain our taphonomic data distribution over time reached a maximum. However for the encrustation parameter there was no difference between logarithmic, polynomial or linear regression and the regression was weaker than for the other parameters. This could be explain by the small population of dated samples, and because each of the studied parameters is measured on a semi-quantitative scale. The highest rank can be considered as the maximum value for a parameter. Until this maximum value is reached for a parameter no additional degradation would be recorded. Over this maximum the taphonomic signal will be saturated.

This saturation of the taphonomic is a key to understand the degradation of biological remain in the deep sea. The saturation value of a taphonomic parameter can be define

as the level of degradation above which no other taphonomic informations will be recorded. The reasons for this saturation are different for each parameters we used in this study. Where encrustation parameter will be limited by the total surface of the skeleton, the other parameters will have different limitations. Breakage and loss of detail parameters reach the saturation value when pieces of skeleton are unrecognizable. Macrobioerosion index will reach the saturation value when the entire skeletons surface has been covered by grazing or boring traces. This saturation value once reached, the continued deterioration of the skeletons will not be registered even if it continues over time.

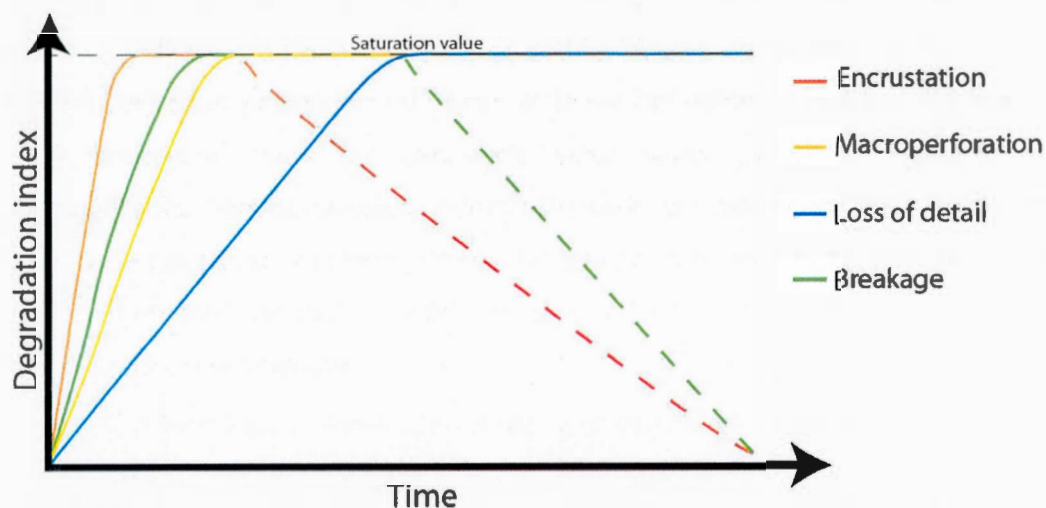


Figure 1.18 model for taphonomic processes recording through realtive time. The saturation value represent the highest value on the semi-quantitative scale.

Through time, different parameters will not reach this saturation value at the same moment (Fig.1.17). All the degradation caused by bioencrusters, bioeroders will begin soon after the death of the corals. But bioencrustation and breakage seems to reach the maximum value quicker than the corrosion caused by macro and micro-bioeroders. Specimen would be broken soon after their death by their fall from the cliff to the graveyard. Although Zuschin (Zuschin *et al.*, 2003) demonstrated the

influence of bioerosion for the fragmentation of marine shell, the absence of strong hydrodynamism in this deep sea location will preserve them from other breakage.

Evolution of degradation through time will follow a logarithmic trend and reach the saturation value at different for each parameters we used in the present study (Fig.1.17). Macroperforation and loss of detail caused by microbioerosion will stay at this level because their signal will not be degraded by the action of the other taphonomic parameters. But encrustation and breakage value of older specimen is on average lower than youngest. That's because of the corrosive action of macro and micro bioeroders. Fresh breaks will be smoothed and altered and became unrecognizable. This corrosion affect by the same way encrusters traces like serpulids tubes or bryozans skeleton. Encrustation and breakage taphonomic signal will be degraded and the observer will not be able to quantify it.

Over the long period of unburied degradation time that characterized this deep-sea environment loss of detail parameter caused by micro-bioeroders and corrosion caused by macro-bioeroders would prevail on the other taphonomic records.

1.5.3 Shallow marine and deep-sea environment comparison

Studies performed by the Shelf and Slope Experimental Taphonomy Initiative (SSETI) group in the Bahamas (Parsons, K. M. *et al.*, 1997) described taphonomy in the shallow and outer shelf as controlled by high rate of oxidation and significant burial and exhumation events (Powell, Eric N. *et al.*, 2002). In their 4 years experimental study on mollusc shell degradation they noticed that discoloration was the dominant taphonomic process in the shallow marine environment (Callender *et al.*, 2002). Furthermore, the fast shell accumulation hid the action of bioerosion (Walker *et al.*, 1998). The photic zone was characterised by quicker alteration of shells by organic processes than on the slope (Staff *et al.*, 2002). That was explained by the action of boring algae and cyanobacteria, predominant in shallow water

(Walker *et al.*, 1998). Moreover most of the encrustation was caused by soft bodied organisms like algae (Walker *et al.*, 1998).

Taphonomic processes action in shallow marine environment can be noticed in several years (Estrada Alvarez *et al.*, 2004 ; Greenstein et Pandolfi, 1997). By contrast in Orphan Knoll graveyard, degradation processes can't be noticed on specimen younger than 500 years. Because productivity and biodiversity are less important in deep marine settings, bioencrusters and bioeroders are less common. Their nature also changes. In that deep environment, because of the absence of light, algae cannot grow and cannot contribute to general taphonomic degradation. But, as in shallow marine environment, the most common bioencrusters are serpulids and bryozans. The most common bioeroders are clionid sponges and sea urchins. Because of those differences degradation in deep marine environment is slower than in shallow marine environment. In shallow marine settings, bioencrusters are often dominated soft-tissue organisms (Lescinsky *et al.*, 2002). Bioencrustation began faster but was saturated quickly and trended to be altered by bioerosion.

In shallow marine skeletons are buried quickly and exhumed several time. As the age distribution showed us Orphan Knoll graveyard is characterized by a slow burial rate. *D. dianthus* skeletons remain on the sea floor at least 180000 years. Macro-bioerosion was mostly caused by sponges and loss of detail caused by micro-bioerosion are the predominant taphonomic processes in deep marine with discoloration explained by ferromanganese oxides. Because of slow burial rates, Fe-Mn oxides have time to develop. This explain the trend of our PCA analysis mostly explained (first axis) by fair/dark differences where older specimen were darker and covered by ferromanganese oxides. In shallow marine environments, bioerosion is not generally predominant over encrustation. In the Orphan Knoll and Flemish Cap coral graveyards, bioeroders have time to graze and corrode the skeleton but also the encrusters traces. Due to the absence of algae and the exposure time on the sea floor,

bioerosion was more important in the deep-sea than in shallow marine environments. Because of the slow burial rate, taphonomic parameters don't reach the saturation value as fast in deep marine environment as in shallow marine. But in shallow marine because of importance of taphonomic processes and the shorter degradation time, taphonomic signals are not totally obliterated by other taphonomic processes. By contrast, in deep marine environment, the record of encrustation and breakage processes is degraded by macro and micro bioerosion. Those degradation and controlled by the burial rate and their actions can't be obliterated by bioerosion. In both environments taphonomic processes are controlled by the burial rate and exposure time on the sea floor.

1.5.4 *Paleoceanographic implications of coral age distribution*

The age distribution we found represents discontinuous accumulation of dead corals into the deep-sea coral graveyard. Those ages are not randomly distributed (see Fig.1.10), the young-skewed shape of the Holocene sample age distribution (Fig.1.10.B) reflects a currently accumulating statistical population, rather than a normally distributed population (Kowalewski, Michał et Bambach, 2008). In contrast the MIS 5 population is from a fossil assemblage, and has a normal distribution of ages (Fig.1.10.C), as expected for a population that is no longer accumulating individual fossils (Kowalewski, Michał et Bambach, 2008).

An understanding of deep-sea corals communities' age distribution could be informative for the reconstruction of the evolution of environmental conditions in the Labrador Sea. Because of the low sedimentation rate in the area (Andrews, J. *et al.*, 1994 ; Hillaire-Marcel, C *et al.*, 1994), corals accumulated in Orphan Knoll and Flemish Cap graveyards and stay on the sea floor for a long period of time. The observed age distribution of our corals from Orphan Knoll suggests that oceanographic conditions near Orphan Knoll were inhospitable for *D. dianthus* growth during glacial intervals. Conditions that could change between glacial and

interglacial intervals include primary productivity, temperature, turbidity, and dissolved oxygen concentration. Here we will focus on climatic parameters and environmental conditions which could explain the observed age distribution.

Working further south within the Northwest Atlantic, Thiagarajan et al. (Thiagarajan et al., 2013) found deep-sea corals communities throughout the Holocene and during the last glacial period in the New-England and Corner Rise seamounts. On the New England Seamounts, *Desmophyllum* corals were more abundant during the last glacial interval than during the interglacial. They explained this age distribution of deep-sea corals by enhanced paleoproductivity during the last glacial period in their studied area. Those observations allowed them to locate the polar front, during the last glacial period, South of Newfoundland and North of the New England Seamounts.

Similarly, previous compilations of *Lophelia pertusa* and *Madrepora oculata* age distribution data in the Northeast Atlantic found no occurrences of that coral assemblage between 50° to 70° N in Atlantic Ocean during glacial period. In contrast between 20° to 50° N, coral assemblages were continuous during the last 45 ky and appeared regularly during cold and warm periods (Frank et al., 2011). This allowed them to locate the deep-sea corals biogeographical limit, caused by the location of the polar front and paleo-productivity zone, between 50° to 70° N and controlled by climate oscillations.

Food supply is the most crucial environmental control on *D. dianthus* communities, as this species has a very wide reported temperature tolerance (Roberts, J. M. et al., 2009). Those corals are dependent of the availability of food from pelagic rain for their growth. Present day food availability for corals on Orphan Knoll is provided by primary production in the Labrador Sea and the transport of nutrient by the Labrador Coastal Current.

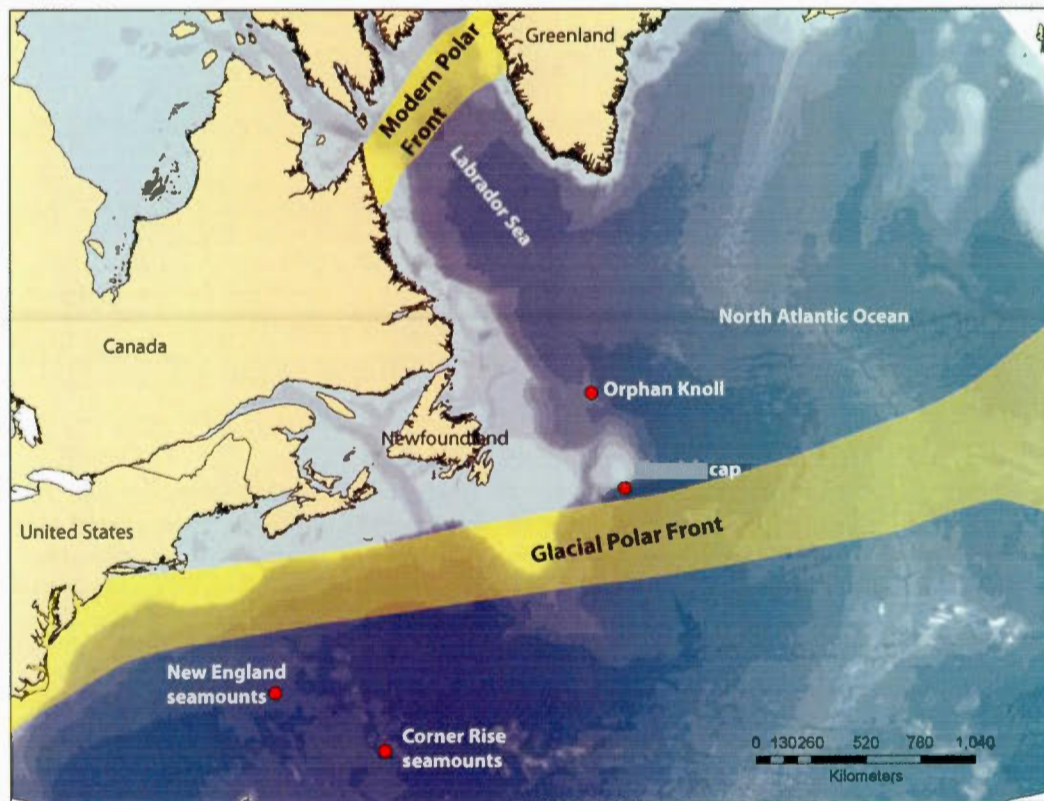


Figure 1.19 position of the polar front during Last Glacial period modified from Thiagarajan et al. (2013) and the actual position of the polar front in the Labrador Sea, data from Montserrat et al. (2011). Zone where *D. dianthus* were collected are pointed with red plots. New England and Corner Rise seamounts were investigated by Thiagarajan et al. (2013), Orphan Knoll and Flemish cap deep-sea corals graveyards were investigated during Hudson cruise in 2010.

During the Last Glacial Maximum (LGM) paleoproductivity in the Labrador Sea decreased, as the Polar Front was displaced southward (Hillaire-Marcel, Claude *et al.*, 1994 ; Montserrat, Sierro et Flores, 2011). Dinocysts and foraminifera appeared to be less abundant than during the Holocene. Those differences related to changes in the water column structure (de Vernal *et al.*, 2002) and Labrador Current activity could cause changes in food supply for deep-sea corals communities during glacial periods. During glacial intervals, the southward shift of the polar front (see Fig.1.18)

displaced the high primary productivity zone associated with the Polar Front to the south of Newfoundland.

Another environmental parameter that could influence the development of deep-sea corals community is temperature. Smith et al. (Smith, Jodie E. *et al.*, 1997) attributed the sudden loss of *D. dianthus* at Orphan Knoll during the onset of the Younger Dryas interval to a decline in temperature. During glacial intervals, ocean surface temperature decreased (Bond, Heinrich, Broecker, Labeyrie, McManus, Andrews, Huon, Jantschik, Clasen et al., 1992 ; McManus, Bond, Broecker, Johnsen, Labeyrie et al., 1994). However during those climatic transitions, temperature changes in the deep ocean were less than changes in the upper ocean part (Sosdian et al., 2009). Furthermore *D. dianthus* communities have been found at a wide range of latitudes and depths. Those organism can live in large depth range between 35 to 2500 meters depth (Cairns, 1994), and have a very large thermal tolerance of -1°C to 28°C (Stanley Jr et al., 1988). Cores from the Labrador sea reconstruct Last Glacial Maximum (LGM) temperature as 2° to -0.5° C (de Vernal *et al.*, 2002). Thus temperature seems an unlikely explanation for the lack of *D. dianthus* accumulation at Orphan Knoll during glacial intervals.

Another environmental parameter which could affect corals growth is the variation of water turbidity. With the increase of the amount of sediment in water, caused by continental erosion, *D. dianthus* possibility of finding food can be affected (Roberts, J. M. *et al.*, 2009). This parameter is controlled by current activity and erosion of the continent. During glacial period most of Canada was covered by ice sheets. When Heinrich event occurs the amount of sediment in water increase abruptly (Heinrich, 1988). The end of the Younger Dryas is marked by a very important Heinrich event (Andrews, J., Jennings, Kerwin, Kirby, Manley, Miller, Bond et al., 1995). This could explain why we don't find occurrence of deep-sea corals in O.K. from the end of the Younger Dryas to $9,703 \pm 161$ years. This hypothesis can't be verified

because of the small population of aged corals in our study. Another problem with this hypothesis is the slow rate of sediment accumulation in the NW Atlantic, particularly at Orphan Knoll, where Holocene sediment is 40 cm maximum thickness (Piper, 2005).

Another important environmental parameter for deep-sea corals growth is dissolved dioxygen concentration. This parameter varies in relation with primary productivity and convection of water masses. For example, deep-water coral accumulation in the Mediterranean may have been locally or regionally interrupted by anoxia (Fink, Wienberg, Hebbeln, McGregor, Schmiedl, Taviani et Freiwald, 2012). During the LGM colder temperature and changes in current activities caused a stratification of the water column in the Labrador Sea (de Vernal *et al.*, 2002) which could have caused a period of hypoxia or anoxia. Cores from O.K. and elsewhere in the NW Atlantic, however, do not contain black organic-rich mud or other direct evidence of hypoxia (Piper, 2005). Thus low oxygen concentrations are a possible, but unlikely, explanation for the lack of coral accumulation at the Orphan Knoll during glacial intervals.

1.6 Conclusion

A coral graveyard accumulation of *D. dianthus* at Orphan Knoll indicates that corals there accumulated mostly during interglacial intervals, with little or no accumulation during glacial intervals. Age distribution of deep-sea corals at Orphan Knoll follows the sequence of interglacial/glacial periods. Among the samples analyzed, three main periods were suitable for the development of deep-sea corals communities. During MIS 7a, MIS 5 (c to d) and during the Holocene environmental parameters permit the development of corals. The availability or absence of food directly related to primary productivity in Labrador Sea is the most important parameter which could explain the temporal occurrence of coral communities in Orphan Knoll. Glacial-interglacial

productivity shifts at O.K. could have been caused by southward displacement of the high primary productivity zone associated with the position of the polar front during glacial intervals.

During those *D. dianthus* skeletons accumulation episode in Orphan Knoll deep-sea graveyard, corals have been degraded mainly by micro and macro bioerosion. Those processes are the most related to the age of the sample. This can be explained by the obliteration of encrustation and breakage signal by bioeroders. The main difference between shallow and deep marine environment is on the duration of the degradation processes, longer in the deep-sea due to the slow burial rate. But because they are faster in shallow marine environment their results are very similar between the two environments. Because of the differential time needed to reach their saturation values, encrustation and breakage processes recording have been degraded by bioerosion. In the case of taphonomic reconstitution, those processes will be underestimated in a deep-sea environment.

1.7 References

- Anagnostou, E., Sherrell, R.M., Gagnon, A., LaVigne, M., Field, M.P. et McDonough, W.F. (2011). Seawater nutrient and carbonate ion concentrations recorded as P/Ca, Ba/Ca, and U/Ca in the deep-sea coral *Desmophyllum dianthus*. *Geochimica et Cosmochimica Acta*, 75(9), 2529-2543.
- Andrews, J., Jennings, A.E., Kerwin, M., Kirby, M., Manley, W., Miller, G., Bond, G. et MacLean, B. (1995). A Heinrich-like event, H-0 (DC-0): Source (s) for detrital carbonate in the North Atlantic during the Younger Dryas Chronozone. *PALEOCEANOGRAPHY*, 10(5), 943-952.
- Andrews, J., Tedesco, K., Briggs, W. et Evans, L. (1994). Sediments, sedimentation rates, and environments, southeast Baffin Shelf and northwest Labrador Sea, 8-26 ka. *Canadian Journal of Earth Sciences*, 31(1), 90-103.

- Auster, P.J. (2005). Are deep-water corals important habitats for fishes? *Cold-water corals and ecosystems* (p. 747-760) : Springer.
- Auster, P.J., Moore, J., Heinonen, K.B. et Watling, L. (2005). A habitat classification scheme for seamount landscapes: assessing the functional role of deep-water corals as fish habitat *Cold-water corals and ecosystems* (p. 761-769) : Springer.
- Boerboom, C.M., Smith, J.E. et Risk, M.J. (1998). Bioerosion and micritization in the deep sea coral *Desmophyllum cristagalli*. [doi: 10.1080/08912969809386572]. *Historical Biology*, 13(1), 53-60.
<http://dx.doi.org/10.1080/08912969809386572>
- Bond, G., Heinrich, H., Broecker, W., Labeyrie, L., McManus, J., Andrews, J., Huon, S., Jantschik, R., Clasen, S. et Simet, C. (1992). Evidence for massive discharges of icebergs into the North Atlantic ocean during the last glacial period.
- Cai, W.-J., Chen, F., Powell, E.N., Walker, S.E., Parsons-Hubbard, K.M., Staff, G.M., Wang, Y., Ashton-Alcox, K.A., Callender, W.R. et Brett, C.E. (2006). Preferential dissolution of carbonate shells driven by petroleum seep activity in the Gulf of Mexico. *Earth and Planetary Science Letters*, 248(1), 227-243.
- Cairns, S.D. (1994). *Scleractinia of the temperate North Pacific*. : Smithsonian Institution Press.
- Callender, W.R., Staff, G.M., Parsons-Hubbard, K.M., Powell, E.N., Rowe, G.T., Walker, S.E., Brett, C.E., Raymond, A., Carlson, D.D. et White, S. (2002). Taphonomic trends along a forereef slope: Lee Stocking Island, Bahamas. I. Location and water depth. *PALAIOS*, 17(1), 50-65.
- Chen, J.H., Edwards, R.L. et Wasserburg, G.J. (1986). ^{238}U , ^{234}U and ^{232}Th in seawater *Earth and Planetary Science Letters*, Vol. 80, pp. 241-251.
- Cherns, L. et Wright, V.P. (2009). Quantifying the impact of early diagenetic aragonite dissolution on the fossil record. *Palaios*, 24, 756-771.

- Colin, C., Frank, N., Copard, K. et Douville, E. (2010). Neodymium isotopic composition of deep-sea corals from the NE Atlantic: implications for past hydrological changes during the Holocene. *Quaternary Science Reviews*, 10.1016, 1-9.
- Copard, K., Colin, C., Henderson, G.M., Scholten, J., Douville, E., Sicre, M.A. et Frank, N. (2012). Late Holocene intermediate water variability in the northeastern Atlantic as recorded by deep-sea corals. [doi: 10.1016/j.epsl.2011.09.047]. *Earth and Planetary Science Letters*, 313–314(0), 34-44.
- Costello, M.J., McCrea, M., Freiwald, A., Lundälv, T., Jonsson, L., Bett, B.J., van Weering, T.C., de Haas, H., Roberts, J.M. et Allen, D. (2005). Role of cold-water *Lophelia pertusa* coral reefs as fish habitat in the NE Atlantic *Cold-water corals and ecosystems* (p. 771-805) : Springer.
- de Vernal, A., Hillaire-Marcel, C., Peltier, W.R. et Weaver, A.J. (2002). Structure of the upper water column in the northwest North Atlantic: Modern versus Last Glacial Maximum conditions. *PALEOCEANOGRAPHY*, 17(4), 1050.
- Donahue, D., Jull, A. et Toolin, L. (1990). Radiocarbon measurements at the University of Arizona AMS facility. *Nuclear Instruments and Methods in Physics Research Section B: Beam Interactions with Materials and Atoms*, 52(3), 224-228.
- Edinger, E., Burr, G., Pandolfi, J. et Ortiz, J. (2007). Age accuracy and resolution of Quaternary corals used as proxies for sea level. *Earth and Planetary Science Letters*, 253(1), 37-49.
- Edinger, E.N. et al., e. (2010). *NSERC ship-time cruise report; ROPOS mission onboard the CCGS Hudson*.
- Edinger, E.N. et Sherwood, O.A. (2012). Applied taphonomy of gorgonian and antipatharian corals in Atlantic Canada: experimental decay rates, field observations, and implications for assessing fisheries damage to deep-sea

- coral habitats. *Neues Jahrbuch für Geologie und Paläontologie-Abhandlungen*, 265(2), 199-218.
- Edinger, E.N., Wareham, V.E. et Haedrich, R.L. (2007). Patterns of groundfish diversity and abundance in relation to deep-sea coral distributions in Newfoundland and Labrador waters. *Bulletin of Marine Science*, 81(Supplement 1), 101-122.
- Edwards, R.L., Chen, J.H. et Wasserburg, G.J. (1987). 238U, 234U, 230Th, 232Th systematics and the precise measurement of time over the past 500,000 years. *Earth and Planetary, Science Letters*, 81, 175-192.
- Edwards, R.L., Chen, J.H. et Wasserburg, G.J. (1987b). 238U-234U-230Th-232Th systematics and the precise measurement of time over the past 500,000 years. *Earth and Planetary Science Letters*, Vol. 81, pp. 175-192.
- Efremov, I. (1940). Taphonomy : new branch of paleontology. *Pan-American Geologist*, 74, 81-93.
- Eisele, M., Frank, N., Wienberg, C., Hebbeln, D., López Correa, M., Douville, E. et Freiwald, A. (2011). Productivity controlled cold-water coral growth periods during the last glacial off Mauritania. [doi: 10.1016/j.margeo.2010.12.007]. *Marine Geology*, 280(1-4), 143-149.
- Estrada Alvarez, L.M., Edinger, E.N. et Pandolfi, J.M. (2004). *Taphonomy of modern corals from Madang Lagoon Papua New Guinea. Canadian Paleontology Conference Proceedings*, Actes du colloque, 2004,
- Fallon, S., Fifield, L. et Chappell, J. (2010). The next chapter in radiocarbon dating at the Australian National University: status report on the single stage AMS. *Nuclear Instruments and Methods in Physics Research Section B: Beam Interactions with Materials and Atoms*, 268(7), 898-901.
- Fink, H.G., Wienberg, C., Hebbeln, D., McGregor, H.V., Schmiedl, G., Taviani, M. et Freiwald, A. (2012). Oxygen control on Holocene cold-water coral development in the eastern Mediterranean Sea. *Deep Sea Research Part I: Oceanographic Research Papers*, 62, 89-96.

- Flessa, K.W., Cutler, A.H. et Meldahl, K.H. (1993). Time and taphonomy: quantitative estimates of time-averaging and stratigraphic disorder in a shallow marine habitat. *Paleobiology*, 266-286.
- Foerster, G., Beuck, L., Haeussermann, V. et Freiwald, A. (2005). Shallow-water *Desmophyllum dianthus* (Scleractinia) from Chile; characteristics of the biocoenoses, the bioeroding community heterotrophic interactions and (paleo)-bathymetric implications Erlangen Earth conference series (p. 937-977). United States : Springer-Verlag Berlin Heidelberg : New York, NY, United States.
- Frank, N., Freiwald, A., Correa, M.L., Wienberg, C., Eisele, M., Hebbeln, D., Van Rooij, D., Henriot, J.-P., Colin, C. et van Weering, T. (2011). Northeastern Atlantic cold-water coral reefs and climate. *Geology*, 39(8), 743-746.
- Freiwald, A. et Roberts, J.M. (2005) Cold-Water Corals and Ecosystems. Dans Communication présentée à /au Erlangen Earth Conference Series (p. 32) Netherland : Springer.
- Freiwald, A. et Wilson, J.B. (1998). Taphonomy of modern deep, cold-temperate water coral reefs. [doi: 10.1080/08912969809386571]. *Historical Biology*, 13(1), 37-52. <http://dx.doi.org/10.1080/08912969809386571>
- Friedman, G.M. (1964). Early diagenesis and lithification in carbonate sediments. *Journal of Sedimentary Research*, 34(4), 777-813.
- Fürsich, F.T. (1978). The influence of faunal condensation and mixing on the preservation of fossil benthic communities. *Lethaia*, 11(3), 243-250.
- Fürsich, F.T. et Aberhan, M. (1990). Significance of time-averaging for palaeocommunity analysis. *Lethaia*, 23(2), 143-152.
- Fürsich, F.T. et Pandey, D.K. (1998). Genesis and environmental significance of Upper Cretaceous shell concentrations from the Cauvery Basin, southern India. [doi: DOI: 10.1016/S0031-0182(98)00099-6]. *Palaeogeography, Palaeoclimatology, Palaeoecology*, 145(1-3), 119-139.

- Ghaleb, B. et Hillaire-Marcel, C. (2006). *^{230}Th vs. ^{14}C age of a pre-YD deep coral from Orphan Knoll (Labrador Sea). AGU Fall Meeting Abstracts, Actes du colloque, 2006,*
- Ginsburg, R.N. (1954). *Early diagenesis and lithification of shallow-water carbonate sediments in south Florida.* : SEPM.
- Greenan, B., Yashayaev, I., Head, E., Harrison, W., Azetsu-Scott, K., Li, W., Loder, J. et Geshelin, Y. (2010). *Interdisciplinary oceanographic observations of Orphan Knoll. SCIENTIFIC COUNCIL MEETING, Actes du colloque, 2010,*
- Greenstein, B.J. et Pandolfi, J.M. (1997). Preservation of community structure in modern reef coral life and death assemblages of the Florida Keys: implications for the Quaternary fossil record of coral reefs. *Bulletin of Marine Science*, 61(2), 431-452.
- Heinrich, H. (1988). Origin and consequences of cyclic ice rafting in the northeast Atlantic Ocean during the past 130,000 years. *Quaternary Research*, 29(2), 142-152.
- Hill, T., LaVigne, M., Spero, H., Guilderson, T., Gaylord, B. et Clague, D. (2012). Variations in seawater Sr/Ca recorded in deep-sea bamboo corals. *PALEOCEANOGRAPHY*, 27(3)
- Hillaire-Marcel, C., Vernal, A.d., Bilodeau, G. et Wu, G. (1994). Isotope stratigraphy, sedimentation rates, deep circulation, and carbonate events in the Labrador Sea during the last~ 200 ka. *Canadian Journal of Earth Sciences*, 31(1), 63-89.
- Hillaire-Marcel, C., Vernal, A.d., Lucotte, M., Mucci, A., Bilodeau, G., Rochon, A., Vallières, S. et Wu, G. (1994). Productivité et flux de carbone dans la mer du Labrador au cours des derniers 40 000 ans. *Canadian Journal of Earth Sciences*, 31(1), 139-158. <http://dx.doi.org/doi:10.1139/e94-012>

- Keen, C. (1978). Cruise Report CSS Hudson 78 020, June 27 to July 19, 1978. *Atl. Geosc. Centre, Bedford Inst. Oceanogr., Int. Rep.* 1, 15.
- Kidwell, S.M. et Bosence, D.W. (1991). Taphonomy and time-averaging of marine shelly faunas. *Taphonomy: releasing the data locked in the fossil record*. Plenum, New York, 115-209.
- Kidwell, S.M. et Flessa, K.W. (1996). The quality of the fossil record: populations, species, and communities 1. *Annual Review of Earth and Planetary Sciences*, 24(1), 433-464.
- Kowalewski, M. (1996). Time-averaging, overcompleteness, and the geological record. *Journal of Geology*, 104(3), 317-326. Récupéré de geh
- Kowalewski, M. et Bambach, R.K. (2008). *The limits of paleontological resolution*. : Springer.
- Lescinsky, H.L., Edinger, E. et Risk, M.J. (2002). Mollusc shell encrustation and bioerosion rates in a modern epeiric sea: taphonomy experiments in the Java Sea, Indonesia. *PALAIOS*, 17(2), 171-191.
- McManus, J., Bond, G., Broecker, W., Johnsen, S., Labeyrie, L. et Higgins, S. (1994). High-resolution climate records from the North Atlantic during the last interglacial. *Nature*, 371(6495), 326-329.
- Meredyk, S., Piper, D., Edinger, E. et Ruffman, A. (2012b). *Composition, probable origin, and recent coral fauna of enigmatic mounds on Orphan Knoll, Northwest Atlantic Ocean*. GAC-MAC annual meeting, Actes du colloque, 2012b, St. John's, NL
- Montserrat, A.-G., Sierro, F.J. et Flores, J.A. (2011). Arctic front shifts in the subpolar North Atlantic during the Mid-Pleistocene (800–400 ka) and their implications for ocean circulation. *Palaeogeography, Palaeoclimatology, Palaeoecology*, 311(3–4), 268-280.
<http://dx.doi.org/http://dx.doi.org/10.1016/j.palaeo.2011.09.004>

- Nothdurft, L. et Webb, G. (2009). Earliest diagenesis in scleractinian coral skeletons: implications for palaeoclimate-sensitive geochemical archives. *Facies*, 55(2), 161-201. <http://dx.doi.org/10.1007/s10347-008-0167-z>
- Olszewski, T.D. (2004). Modeling the influence of taphonomic destruction, reworking, and burial on time-averaging in fossil accumulations. *PALAIOS*, 19(1), 39-50.
- Parsons-Hubbard, K.M., Callender, W.R., Powell, E.N., Brett, C.E., Walker, S.E., Raymond, A.L. et Staff, G.M. (1999). Rates of burial and disturbance of experimentally-deployed molluscs; implications for preservation potential. *PALAIOS*, 14(4), 337-351.
- Parsons, K.M. et Brett, C.E. (1991). Taphonomic processes and biases in modern marine environments. *The processes of fossilization*, 22-65.
- Parsons, K.M., Powell, E.N., Brett, C.E., Walker, S.E. et Callender, W.R. (1997). *Shelf and slope experimental taphonomy initiative (SSETI) : Bahamas and gulf of Mexico. Proc 8th Int Coral Reef Sym*, Actes du colloque, 1997,
- Piper, D.J.W. (2005). *Hudson 2004-024 Cruise Report: Geohazards on the continental margin off Newfoundland.* : Geological Survey of Canada, Open File.
- Powell, E., Staff, G., Davies, D. et Callender, W.R. (1989). Macrobenthic death assemblages in modern marine environments: formation, interpretation, and application. *Reviews in Aquatic Sciences*, 1, 555-589.
- Powell, E.N., Parsons-Hubbard, K.M., Callender, W.R., Staff, G.M., Rowe, G.T., Brett, C.E., Walker, S.E., Raymond, A., Carlson, D.D. et White, S. (2002). Taphonomy on the continental shelf and slope: two-year trends—Gulf of Mexico and Bahamas. *Palaeogeography, Palaeoclimatology, Palaeoecology*, 184(1), 1-35.
- Powell, E.N., Parsons-Hubbard, K.M., Callender, W.R., Staff, G.M., Rowe, G.T., Brett, C.E., Walker, S.E., Raymond, A., Carlson, D.D., White, S. et Heise, E.A. (2002). Taphonomy on the continental shelf and slope: two-year trends —

- Gulf of Mexico and Bahamas. [doi: 10.1016/S0031-0182(01)00457-6].
Palaeogeography, Palaeoclimatology, Palaeoecology, 184(1–2), 1-35.
- Roberts, J.M., Wheeler, A., Freiwald, A. et Cairns, S. (2009). *Cold-water corals: the biology and geology of deep-sea coral habitats*. : Cambridge University Press,.
- Roberts, J.M., Wheeler, A.J. et Freiwald, A. (2006). Reefs of the deep: the biology and geology of cold-water coral ecosystems. *Science*, 312(5773), 543-547.
- Rollion-Bard, C., Blamart, D., Cuif, J.-P. et Juillet-Leclerc, A. (2003). Microanalysis of C and O isotopes of azooxanthellate and zooxanthellate corals by ion microprobe. *Coral Reefs*, 22(4), 405-415.
- Ruffman, A. (1989). *Devonian Shelf-depth Limestone Dredged from Orphan Knoll: A 1971 Discovery and A Reassessment of the Hudson 78-020 Dredge Hauls from Orphan Knoll*. : G.S.C.
- Scott, D. (1992). *Multivariate Density Estimation: Theory, Visualization, and Practice* : John Wiley & Sons, New York.
- Sheather, S.J. et Jones, M.C. (1991). A reliable data-based bandwidth selection method for kernel density estimation. *Journal of the Royal Statistical Society. Series B (Methodological)*, 683-690.
- Sherwood, O.A., Heikoop, J.M., Scott, D.B., Risk, M.J., Guilderson, T.P. et McKinney, R.A. (2005). Stable isotopic composition of deep-sea gorgonian corals *Primnoa* spp.: a new archive of surface processes. *Marine Ecology Progress Series*, 301, 135-148.
- Sherwood, O.A., Jamieson, R.E., Edinger, E.N. et Wareham, V.E. (2008). Stable C and N isotopic composition of cold-water corals from the Newfoundland and Labrador continental slope: Examination of trophic, depth and spatial effects. [doi: 10.1016/j.dsr.2008.05.013]. *Deep Sea Research Part I: Oceanographic Research Papers*, 55(10), 1392-1402.
- Silverman, B.W. (1986). *Density estimation for statistics and data analysis*. (Vol. 26) : CRC press.

- Smith, J.E. (1993). *Late Quaternary paleoclimatic reconstruction using the deep-sea coral *Desmophyllum cristagalli**.
- Smith, J.E., Risk, M.J., Schwarcz, H.P. et McConnaughey, T.A. (1997). Rapid climate change in the North Atlantic during the Younger Dryas recorded by deep-sea corals. [10.1038/386818a0]. *Nature*, 386(6627), 818-820.
- Sosdian, S. et Rosenthal, Y. (2009). Deep-sea temperature and ice volume changes across the Pliocene-Pleistocene climate transitions. *Science*, 325(5938), 306-310.
- Staff, G.M., Callender, W.R., Powell, E.N., Parsons-Hubbard, K.M., Brett, C.E., Walker, S.E., Carlson, D.D., White, S., Raymond, A. et Heise, E.A. (2002). Taphonomic Trends Along a Forereef Slope: Lee Stocking Island, Bahamas. II. Time. *PALAIOS*, 17(1), 66-83.
- Stanley Jr, G.D. et Cairns, S.D. (1988). Constructional azooxanthellate coral communities: an overview with implications for the fossil record. *PALAIOS*, 233-242.
- Strasser, A. et Strohmenger, C. (1997). Early diagenesis in Pleistocene coral reefs, southern Sinai, Egypt: response to tectonics, sea-level and climate. *Sedimentology*, 44(3), 537-558.
- Stuiver, M., Reimer, P.J. et Reimer, R. (2005). *CALIB 5.0*.
- Thiagarajan, N., Gerlach, D., Roberts, M.L., Burke, A., McNichol, A., Jenkins, W.J., Subhas, A.V., Thresher, R.E. et Adkins, J.F. (2013). Movement of deep-sea coral populations on climatic timescales. *PALEOCEANOGRAPHY*
- Tomasovych, A. et Schlögl, J. (2008). Analyzing variations in cephalopod abundances in shell concentrations : the combined effects of production and density-dependent cementation rates. *Palaeogeography Palaeoclimatology Palaeoecology*, 23, p. 648–666.
- Vogel, J.S., Nelson, D. et Southon, J.R. (1987). Carbon-14 background levels in an accelerator mass spectrometry system. *Radiocarbon*, 29(3), 323-333.

- Walker, S.E., Parsons-Hubbard, K., Powell, E. et Brett, C.E. (2002). Predation on experimentally deployed molluscan shells from shelf to slope depths in a tropical carbonate environment. *PALAIOS*, 17(2), 147-170.
- Walker, S.E., Parsons Hubbard, K., Powell, E.N. et Brett, C.E. (1998). Bioerosion or bioaccumulation? Shelf-slope trends for EPI-and endobionts on experimentally deployed gastropod shells. *Historical Biology*, 13(1), 61-72.
- Wood, R. (2011). Taphonomy of reefs through time *Taphonomy* (p. 375-409) : Springer.
- Zuschin, M., Stachowitsch, M. et Stanton, R.J. (2003). Patterns and processes of shell fragmentation in modern and ancient marine environments. [doi: DOI: 10.1016/S0012-8252(03)00014-X]. *Earth-Science Reviews*, 63(1-2), 33-82.

CHAPITRE II

CONCLUSION

La dégradation des squelettes de *D. dianthus* prélevés dans le cimetière sous marin d'Orphan Knoll est principalement causée par des processus biologique. En raison du long temps de résidence des échantillons à l'interface eau/sédiment, ces processus vont se poursuivre jusqu'à saturation du signal taphonomique. Néanmoins la confrontation des degrés d'altération des différents paramètres affectant les squelettes permet de relier les processus taphonomiques à l'âge des spécimens. Les paramètres liés à la bioérosion (micro et macro) provoquant la perte de détails ainsi que des traces d'*entobia* et de *gnathichnus* sont ceux qui atteignent la valeur de saturation le plus tard. Ils peuvent donc être reliés à l'âge du spécimen. L'encrouement principalement causé par les serpulides et les bryozoaires atteint la valeur de saturation relativement rapidement et son enregistrement est par la suite dégradé par l'action des organismes érodeurs. Les fortes valeurs de ce paramètre caractérisent donc plus spécialement des spécimens récents datés de l'Holocène. En raison du faible hydrodynamisme dans la zone d'étude, les cassures vont affecter les squelettes principalement lors de leur chute de la falaise au cimetière. L'enregistrement de ces cassures va par la suite être dégradé notamment par l'action des micro-bioérodeurs. Les spécimens présentant des valeurs élevés dans ce paramètre vont donc eux aussi généralement appartenir à la population Holocène. Le dépôt d'oxydes de manganèse est lié au temps de résidence à l'interface eau/sédiment. Cependant les méthodes de colorimétrie et d'analyse d'image ne permettent pas de différencier les individus en fonction de leur âge. Seul les

individus ayant été enfouis précocement (D46 et D47) et ceux âgés entre 70 et 1200 ans sont dépourvus d'encroûtement d'oxydes de manganèse.

Afin de bien aborder l'étude des spécimens de coraux profonds récoltés dans un cimetière sous marin, la compréhension des paramètres environnementaux ayant contraint l'accumulation des squelettes est primordiale. L'analyse des processus taphonomique en relation avec la distribution des âges des spécimens, contrôlés par ces paramètres, peut discriminer les différentes populations d'âge du cimetière. Le choix des spécimens à analyser pour les études géochimique devra tenir compte de ces données. L'impact des différents processus taphonomique et notamment les encroûtements dûs aux organismes calcitiques et de manganèse devront aussi être pris en compte pour toutes les procédures de nettoyage des échantillons afin d'éviter toute contamination. Les informations taphonomique sont cruciales pour comprendre la perte d'informations liées à la dégradation des spécimens dans cet environnement à faible taux d'enfouissement.

La datation des squelettes de *Desmophyllum dianthus* provenant du cimetière sous-marin d'Orphan Knoll a montré que ces conditions de faible taux de sédimentation engendrait un faible taux d'enfouissement des squelettes. Le temps de résidence du spécimen D5 étant de 181000 ans, l'accumulation de ces fossiles est un processus à long terme. Ces datations ont permis de regrouper les spécimens en deux populations : la population de l'Holocène comprenant les spécimens récoltés vivants jusqu'à ceux datés de 10000 ans BP, la population du stade isotopique 5 datée entre 97000 et 111000 ans BP et un seul spécimen du stade isotopique 7 daté à 181000 ans BP. Plusieurs hypothèses visant à expliquer cette distribution de l'âge des échantillons ont été avancées. Parmi celles-ci, l'hypothèse de l'influence des variations de productivité primaire dûe au déplacement vers le sud du front polaire pendant les périodes glaciaires semble la plus probable. De plus cette hypothèse semble confirmée par les travaux de (Frank, Freiwald, Correa, Wienberg, Eisele, Hebbeln, Van Rooij, Henriët,

Colin et van Weering, 2011 ; Thiagarajan, Gerlach, Roberts, Burke, McNichol, Jenkins, Subhas, Thresher et Adkins, 2013). L'accumulation de squelettes de *D. dianthus* dans les formations d'Orphan Knoll et de Flemish cap n'est donc pas un phénomène continu. C'est un processus lié aux conditions environnementales favorisant la croissance des communautés de coraux profonds.

Les analyses de diffraction aux rayons X ont mis en évidence que les squelettes de *D. dianthus* originellement aragonitique comprennent pour les échantillons fossiles une part de moins de 5% de calcite. Les processus de recristallisation des squelettes coralliens tropicaux interviennent précocement et parfois même du vivant de l'individu (Nothdurft et Webb, 2009). Les processus de micritisation sont eux aussi connus chez *Desmophyllum dianthus* (Boerboom, Smith et Risk, 1998). Des analyses en cathodoluminescence seraient intéressantes pour en comprendre l'impact sur les analyses géochimiques. Parmi celles-ci, l'analyse de la composition en Nd ainsi que la méthode des lignes effectuée sur la composition en isotopes stables et décrite par (Hill, Spero, Guilderson, LaVigne, Clague, Macalello et Jang, 2011 ; Smith, Schwarcz, Risk, McCONNAUGHEY et Keller, 2000) pourrait permettre de valider la similarité des environnements et notamment des conditions hydrographiques entre le MIS 7, le MIS 5 et l'Holocène. Enfin effectuer une étude comparative sur la taphonomie en milieu profond dans d'autres zones géographiques permettrait d'affiner les résultats présentés ici et d'augmenter nos connaissances sur la dégradation des restes organiques dans ces milieux particuliers.

2.1 Références

- Boerboom, C.M., Smith, J.E. et Risk, M.J. (1998). Bioerosion and micritization in the deep sea coral *desmophyllum cristagalli*. [doi: 10.1080/08912969809386572]. *Historical Biology*, 13(1), 53-60.
<http://dx.doi.org/10.1080/08912969809386572>
- Frank, N., Freiwald, A., Correa, M.L., Wienberg, C., Eisele, M., Hebbeln, D., Van Rooij, D., Henriët, J.-P., Colin, C. et van Weering, T. (2011). Northeastern Atlantic cold-water coral reefs and climate. *Geology*, 39(8), 743-746.
- Hill, T., Spero, H., Guilderson, T., LaVigne, M., Clague, D., Macalello, S. et Jang, N. (2011). Temperature and vital effect controls on bamboo coral (Isididae) isotope geochemistry: A test of the “lines method”. *Geochemistry, Geophysics, Geosystems*, 12(4)
- Nothdurft, L. et Webb, G. (2009). Earliest diagenesis in scleractinian coral skeletons: implications for palaeoclimate-sensitive geochemical archives. *Facies*, 55(2), 161-201. <http://dx.doi.org/10.1007/s10347-008-0167-z>
- Smith, J.E., Schwarcz, H.P., Risk, M.J., McCONNAUGHEY, T.A. et Keller, N. (2000). Paleotemperatures from deep-sea corals: overcoming ‘vital effects’. *PALAIOS*, 15(1), 25-32.
- Thiagarajan, N., Gerlach, D., Roberts, M.L., Burke, A., McNichol, A., Jenkins, W.J., Subhas, A.V., Thresher, R.E. et Adkins, J.F. (2013). Movement of deep-sea coral populations on climatic timescales. *PALEOCEANOGRAPHY*

APPENDICE A

SÉLECTION DES ÉCHANTILLONS GRÂCE À DES CRITÈRES TAPHONOMIQUES

Une méthode est proposée dans les appendices suivants pour aborder l'étude d'un cimetière sous-marin à coraux profonds. Cette méthode se propose tout d'abord un moyen de documenter et décrire les spécimens sur des critères taphonomiques.

A.1 Description des paramètres

La description taphonomique des spécimens de *Desmophyllum dianthus* se base sur l'évaluation de 4 paramètres selon une échelle semi-quantitative graduée de 0 à 4 (abaque 1 à 4) :

- la perte de détails résulte de l'action corrosive de micro organismes sur le squelette. Elle se traduit par la perte progressive des structures sur les différentes parties du squelette : base, épithéca et septa (Fig.1.A1) ;
- les traces de macro-bioérosion résultent de l'action d'organismes bio-corrodeurs. Elle se traduit par la présence de perforations (*Entobia* spp) dues principalement à l'action de spongiaires et de traces de broutage (*Gnathichnus* spp) dues à l'action d'échinodermes (Fig.1.6) ;
- l'encroutement résulte de l'action d'organismes benthiques utilisant le squelette comme habitat ou substrat. Il se traduit par la présence de tubes calcitiques dues à l'action de serpulides, de squelettes de bryozoaires calcifiés, de *D. dianthus* juvéniles ou d'organismes à corps mou comme des éponges ou des tuniqués ;

- les cassures résultent de l'action de processus physiques (choc ou chute) suite à la fragilisation du squelette par les processus de corrosions.

Un abaque permettant d'attribuer une valeur pour chaque paramètre aux différents spécimens est proposé dans les pages suivantes.

Ces paramètres sont évalués à la loupe binoculaire et à l'œil nu. Les spécimens sont photographiés sous statif de reproduction afin d'homogénéiser les conditions lumineuses entre les clichés des différents échantillons. Les clichés comprenant si possible 4 vues : 2 vues longitudinales, 1 vue basale et une vue sommitale, sont utilisés pour mesurer les valeurs de Cyan, Magenta, Jaune et Noir dues à l'encroutement d'oxydes de manganèse grâce à Illustrator®. Les valeurs CMJN sont extraites de 25 points choisis aléatoirement sur le cliché le plus représentatif de l'échantillon. La moyenne de ces valeurs est utilisée pour définir la couleur d'un échantillon.



Figure A.1 Clichés de *D. dianthus*, scale barr = 0.5 mm. A) Septa de l'échantillon D57 comprenant : C=cassure de niveau 1 et R= rugosité. B) Epithéca de l'échantillon D47 comprenant : O=ornementation. C) Vue d'ensemble de l'échantillon D57 montrant les différentes parties du corail : S=Septa, E=épithéca et B=base.

Tableau A.1 Abaque d'évaluation de la perte de détails






| Valeur | Description | Photo |
|--------|---|---|
| 0 | Préservation parfaite des détails du squelette Septa entières et rugosité visible à la loupe binoculaire à leurs surface Ornementations de l'épithéca préservées |  |
| 1 | Septa entières Disparition des rugosités à la surface des septa Ornementations de l'épithéca moins visibles |  |
| 2 | Disparition totale des rugosités des septa et de l'ornementation de l'épithéca Dégradation des septa secondaires Septa principales préservées |  |
| 3 | Disparition totale des rugosités des septa et de l'ornementation de l'épithéca Disparition des septa secondaires Septa principales réduites d'au moins 50% |  |
| 4 | Disparition totale des rugosités des septa et de l'ornementation de l'épithéca Disparition des septa secondaires et principales |  |

Tableau A.2 Abaque d'évaluation de la macro-bioérosion

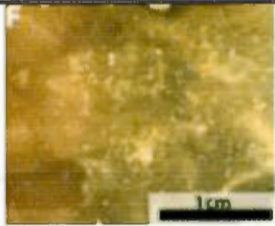
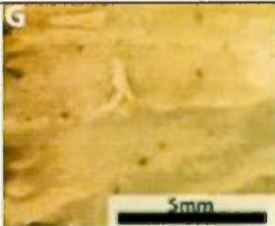
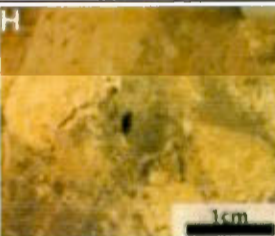


| Valeur | Description | Photo |
|--------|--|---|
| 0 | Absence |  |
| 1 | Rare Traces d' <i>Entobia</i> micrométriques |  |
| 2 | Présent Traces d' <i>Entobia</i> millimétrique et de galeries non jointive millimétriques Traces de broutage (<i>Gnathichnus isp</i>) localisées |  |
| 3 | Commun Traces d' <i>Entobia</i> millimétrique et galeries jointives centimétriques Traces de broutage (<i>Gnathichnus isp</i>) localisées |  |
| 4 | Abondant Traces d' <i>Entobia</i> millimétrique et galeries jointives centimétrique Traces de broutages (<i>Gnathichnus isp</i>) communes |  |

Tableau A.3 Abaque d'évaluation de l'encrouement par des organismes

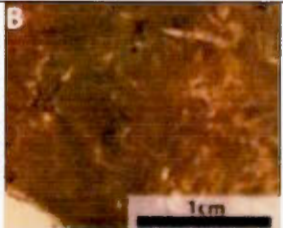








| Valeur | Description | Photo |
|--------|--|---|
| 0 | Absence d'encrouement |  |
| 1 | Faible présence d'encrouement Tubes de Serpulides millimétriques Affecte une zone de l'échantillon |  |
| 2 | Présence d'encrouement Tubes de Serpulides centimétriques Peut recouvrir plusieurs zones de l'échantillon |  |
| 3 | Présence d'encrouement Tubes de Serpulides centimétriques et continues Recouvre plusieurs zones de l'échantillon |  |
| 4 | Forte présence d'encrouement Tubes de Serpulides centimétriques et continues Affecte l'ensemble de l'échantillon |  |

Tableau A.4 Abaque d'évaluation de la cassure

| Valeur | Description | Photo |
|--------|--|---|
| 0 | Absence de cassures |  |
| 1 | Cassures millimétriques généralement situées sur les septa Fragments secondaire de taille millimétrique |  |
| 2 | Cassures des septa Multiples fragments secondaire de septa de taille millimétrique à centimétrique |  |
| 3 | Cassures centimétriques sur l'ensemble du squelette Fragments centimétrique avec un fragment principale aisément reconnaissable |  |
| 4 | Squelette très fragmenté Plusieurs fragments principaux difficilement reconnaissable |  |

A.2 Enregistrement des données

Les valeurs attribuées aux différents paramètres sont enregistrées sur la base de données FileMaker pro®. Cette base de donnée permet de donner différentes valeurs en fonction de la partie du spécimen étudiée (base, épithéca et septa). Cette méthode permet de préciser notamment quelles sont les parties manquantes du spécimen. Dans le cas où les valeurs d'un paramètre sont différentes pour les différentes parties, seule la valeur la plus élevée est utilisée pour l'évaluation taphonomique du spécimen car correspondant au maximum de dégradation subie. À noter cependant que dans le cas de l'évaluation du paramètre "cassure" cette différenciation est impossible car l'évaluation de ce paramètre prend en compte l'intégralité du spécimen.

A.3 Discrimination des différentes populations

Les datations absolues sur les échantillons ont permis de distinguer deux populations de coraux dans le cimetière sous-marin d'Orphan Knoll. Une première population comprenant des échantillons datés entre 0 et 10000 ans BP correspondant à l'Holocène et une autre population comprenant des échantillons datés entre 97000 et 110000 ans BP correspondant au Pléistocène supérieur.

Ainsi que montré dans le chapitre 1, les paramètres macro-perforation et perte de détails sont les plus corrélés avec l'âge du spécimen. Un spécimen obtenant de fortes valeurs dans ces paramètres a de forte chance d'appartenir aux populations du MIS 5 ou du MIS 7. Les échantillons présentant de fortes valeurs dans les paramètres cassure et encroutement ont de forte chance d'appartenir à la population Holocène. Des échantillons présentant de faibles valeurs pour les quatre paramètres ont soit été récoltés vivants ou ont subi un enfouissement rapide et peuvent donc appartenir à toutes les populations.

APPENDICE B

MÉTHODE DE NETTOYAGE ET DATATION U/Th

B.1 Nettoyage :

B.1.1 Nettoyage physique :

Pour le prélèvement ainsi que pour le nettoyage physique il est recommandé d'utiliser un dremel. Les parties les plus simples à prélever sont les septas. Des échantillons de taille centimétrique y ont été prélevés. Les échantillons ont subi un premier nettoyage mécanique au dremel afin d'enlever une partie de la matière organique ainsi que l'essentielle de la couche d'oxydes de manganèse. Puis ces échantillons ont été plongés dans un bain à ultra-sons dans de l'eau distillée. Ils ont ensuite été découpés en fragments millimétriques et nettoyés à nouveau au dremel afin de retirer les dernières traces d'oxyde de manganèse observées à la loupe binoculaire (avec x20 de magnification).

B.1.2 Nettoyage chimique :

Les échantillons ont ensuite subi un nettoyage chimique en plusieurs étapes décrite dans le Tableau B.1.

Les échantillons ont été passés 12h à l'étuve à 50°C afin de les sécher. Puis les échantillons ont été broyés grâce à un mortier en agate et placés dans un contenant hermétique.

Tableau B.1 procédures de nettoyage chimique

| Étape | Description | But | Durée |
|-------|---|---|------------|
| 1 | Bain à ultra-sons avec une solution d'ascorbique à 0.5M ramenée à pH=7 par ajout de NaOH 2M | Éliminer les traces résiduelles d'oxydes de manganèse | 10 minutes |
| 2 | Bain à ultra-sons dans de l'eau distillée | Rinçage et suppression du sédiment restant | 15 minutes |
| 3 | Bain à ultra sons dans solution avec 50% d'eau de javel | Elimination de la matière organique résiduelle | 10 minutes |
| 4 | Bain à ultra-sons dans de l'eau distillée | Rinçage | 15 minutes |

B.2 Datation U/Th :

B.2.3 Préparation du traceur :

La méthodologie qui a été suivi est celle décrite mise au point par Chen *et al.* (1986) et Edwards *et al.* (1987b). Le traceur que nous avons utilisé est composé d'isotopes U/Th non naturels : ^{236}U , ^{233}U et ^{229}Th . Il a été pesé grâce à une balance de précision et évaporé dans des savilex.

B.2.4 Récupération chimique de l'Uranium et du Thorium :

Les échantillons ont été pesés puis dissout avec le traceur dans du HNO_3 15M. La solution obtenue a été séchée. Puis diluée à nouveau en HNO_3 15M, 12 gouttes de

FeCl_3 y ont été rajoutées, puis de l'ammoniac et de l' H_2O afin de créer le précipité $\text{Fe}(\text{OH})_3$ pour piéger les éléments lourds. Ce précipité a ensuite été récupéré par centrifugation et évaporé.

B.2.5 Séparation de l'Uranium et du Thorium :

Le précipité a été dissout en HCl 6M puis passé dans une colonne de séparation, préparée avec une résine AG1x8 200-400 mesh et conditionnée en HCl 6M.

Afin d'éliminer les autres éléments présents, les 6 solutions contenant respectivement l'Uranium et le Thorium des 3 échantillons, ont été passées par différentes colonnes de séparation suivant les procédures décrites par Cheng (2000) et mises au point par Chen *et al.* (1986) et Edwards *et al.* (1987b).

B.2.6 Mesure au spectromètre de masse :

Les fractions séparées contenant l'uranium et le thorium ont été déposées séparément, entre deux fines couches de graphite colloïdal, sur des filaments simples en rhénium. Les rapports isotopiques ont été mesurés sur un spectromètre de masse *TRITON plus* (TIMS). Les rapports isotopiques des différentes solutions ont été mesurés grâce au compteur d'ions du spectromètre de masse.

Lors de l'analyse de l'uranium, les rapports $^{238}\text{U}/^{236}\text{U}$, $^{238}\text{U}/^{235}\text{U}$, $^{236}\text{U}/^{235}\text{U}$, $^{235}\text{U}/^{234}\text{U}$, $^{236}\text{U}/^{234}\text{U}$ et $^{236}\text{U}/^{233}\text{U}$ sont mesurés en quatre cycles de séquences d'analyses successives au compteur d'ions. Les rapports $^{233}\text{U}/^{238}\text{U}$ et $^{234}\text{U}/^{238}\text{U}$ corrigés sont ensuite traités afin de compenser l'apport du spike (méthode de la dilution isotopique). Les concentrations des isotopes sont calculées en fonction des rapports atomiques mesurés, des poids de l'échantillon et du spike et de la concentration connue du spike.

Au cours de l'analyse du thorium les rapports $^{232}\text{Th}/^{229}\text{Th}$, $^{229}\text{Th}/^{230}\text{Th}$ et $^{232}\text{Th}/^{230}\text{Th}$ sont mesurés. Les rapports sont traités par la méthode de la dilution isotopique et les concentrations sont calculées de la même manière que pour l'uranium.

B.3 Références :

- Chen, J.H., Edwards, R.L. et Wasserburg, G.J. (1986). ^{238}U , ^{234}U and ^{232}Th in seawater *Earth and Planetary Science Letters*, Vol. 80, pp. 241-251.
- Cheng, H., Adkins, J., Edwards, R.L. et Boyle, E.A. (2000). U-Th dating of deep-sea corals. [doi: 10.1016/S0016-7037(99)00422-6]. *Geochimica et Cosmochimica Acta*, 64(14), 2401-2416.
- Edwards, R.L., Chen, J.H. et Wasserburg, G.J. (1987b). ^{238}U - ^{234}U - ^{230}Th - ^{232}Th systematics and the precise measurement of time over the past 500,000 years. *Earth and Planetary Science Letters*, Vol. 81, pp. 175-192.

BIBLIOGRAPHIE

- Anagnostou, E., Sherrell, R.M., Gagnon, A., LaVigne, M., Field, M.P. et McDonough, W.F. (2011). Seawater nutrient and carbonate ion concentrations recorded as P/Ca, Ba/Ca, and U/Ca in the deep-sea coral *Desmophyllum dianthus*. *Geochimica et Cosmochimica Acta*, 75(9), 2529-2543.
- Andrews, J., Jennings, A.E., Kerwin, M., Kirby, M., Manley, W., Miller, G., Bond, G. et MacLean, B. (1995). A Heinrich-like event, H-0 (DC-0): Source (s) for detrital carbonate in the North Atlantic during the Younger Dryas Chronozone. *PALEOCEANOGRAPHY*, 10(5), 943-952.
- Andrews, J., Tedesco, K., Briggs, W. et Evans, L. (1994). Sediments, sedimentation rates, and environments, southeast Baffin Shelf and northwest Labrador Sea, 8-26 ka. *Canadian Journal of Earth Sciences*, 31(1), 90-103.
- Auster, P.J. (2005). Are deep-water corals important habitats for fishes? *Cold-water corals and ecosystems* (p. 747-760) : Springer.
- Auster, P.J., Moore, J., Heinonen, K.B. et Watling, L. (2005). A habitat classification scheme for seamount landscapes: assessing the functional role of deep-water corals as fish habitat *Cold-water corals and ecosystems* (p. 761-769) : Springer.
- Boerboom, C.M., Smith, J.E. et Risk, M.J. (1998). Bioerosion and micritization in the deep sea coral *desmophyllum cristagalli*. [doi: 10.1080/08912969809386572]. *Historical Biology*, 13(1), 53-60.
<http://dx.doi.org/10.1080/08912969809386572>
- Bond, G., Heinrich, H., Broecker, W., Labeyrie, L., McManus, J., Andrews, J., Huon, S., Jantschik, R., Clasen, S. et Simet, C. (1992). Evidence for massive

discharges of icebergs into the North Atlantic ocean during the last glacial period.

- Cai, W.-J., Chen, F., Powell, E.N., Walker, S.E., Parsons-Hubbard, K.M., Staff, G.M., Wang, Y., Ashton-Alcox, K.A., Callender, W.R. et Brett, C.E. (2006). Preferential dissolution of carbonate shells driven by petroleum seep activity in the Gulf of Mexico. *Earth and Planetary Science Letters*, 248(1), 227-243.
- Cairns, S.D. (1994). *Scleractinia of the temperate North Pacific*. : Smithsonian Institution Press.
- Callender, W.R., Staff, G.M., Parsons-Hubbard, K.M., Powell, E.N., Rowe, G.T., Walker, S.E., Brett, C.E., Raymond, A., Carlson, D.D. et White, S. (2002). Taphonomic trends along a foreereef slope: Lee Stocking Island, Bahamas. I. Location and water depth. *PALAIOS*, 17(1), 50-65.
- Chen, J.H., Edwards, R.L. et Wasserburg, G.J. (1986). 238U, 234U and 232Th in seawater *Earth and Planetary Science Letters*, Vol. 80, pp. 241-251.
- Cherns, L. et Wright, V.P. (2009). Quantifying the impact of early diagenetic aragonite dissolution on the fossil record. *Palaios*, 24, 756-771.
- Colin, C., Frank, N., Copard, K. et Douville, E. (2010). Neodymium isotopic composition of deep-sea corals from the NE Atlantic: implications for past hydrological changes during the Holocene. *Quaternary Science Reviews*, 10.1016, 1-9.
- Copard, K., Colin, C., Henderson, G.M., Scholten, J., Douville, E., Sicre, M.A. et Frank, N. (2012). Late Holocene intermediate water variability in the northeastern Atlantic as recorded by deep-sea corals. [doi: 10.1016/j.epsl.2011.09.047]. *Earth and Planetary Science Letters*, 313–314(0), 34-44.
- Costello, M.J., McCrea, M., Freiwald, A., Lundälv, T., Jonsson, L., Bett, B.J., van Weering, T.C., de Haas, H., Roberts, J.M. et Allen, D. (2005). Role of cold-water *Lophelia pertusa* coral reefs as fish habitat in the NE Atlantic *Cold-water corals and ecosystems* (p. 771-805) : Springer.

- de Vernal, A., Hillaire-Marcel, C., Peltier, W.R. et Weaver, A.J. (2002). Structure of the upper water column in the northwest North Atlantic: Modern versus Last Glacial Maximum conditions. *PALEOCEANOGRAPHY*, 17(4), 1050.
- Donahue, D., Jull, A. et Toolin, L. (1990). Radiocarbon measurements at the University of Arizona AMS facility. *Nuclear Instruments and Methods in Physics Research Section B: Beam Interactions with Materials and Atoms*, 52(3), 224-228.
- Edinger, E., Burr, G., Pandolfi, J. et Ortiz, J. (2007). Age accuracy and resolution of Quaternary corals used as proxies for sea level. *Earth and Planetary Science Letters*, 253(1), 37-49.
- Edinger, E.N. et al., e. (2010). *NSERC ship-time cruise report; ROPOS mission onboard the CCGS Hudson*.
- Edinger, E.N. et Sherwood, O.A. (2012). Applied taphonomy of gorgonian and antipatharian corals in Atlantic Canada: experimental decay rates, field observations, and implications for assessing fisheries damage to deep-sea coral habitats. *Neues Jahrbuch für Geologie und Paläontologie-Abhandlungen*, 265(2), 199-218.
- Edinger, E.N., Wareham, V.E. et Haedrich, R.L. (2007). Patterns of groundfish diversity and abundance in relation to deep-sea coral distributions in Newfoundland and Labrador waters. *Bulletin of Marine Science*, 81(Supplement 1), 101-122.
- Edwards, R.L., Chen, J.H. et Wasserburg, G.J. (1987). 238U, 234U, 230Th, 232Th systematics and the precise measurement of time over the past 500,000 years. *Earth and Planetary, Science Letters*, 81, 175-192.
- Edwards, R.L., Chen, J.H. et Wasserburg, G.J. (1987b). 238U-234U-230Th-232Th systematics and the precise measurement of time over the past 500,000 years. *Earth and Planetary Science Letters*, Vol. 81, pp. 175-192.
- Efremov, I. (1940). Taphonomy : new branch of paleontology. *Pan-American Geologist*, 74, 81-93.

- Eisele, M., Frank, N., Wienberg, C., Hebbeln, D., López Correa, M., Douville, E. et Freiwald, A. (2011). Productivity controlled cold-water coral growth periods during the last glacial off Mauritania. [doi: 10.1016/j.margeo.2010.12.007]. *Marine Geology*, 280(1–4), 143-149.
- Estrada Alvarez, L.M., Edinger, E.N. et Pandolfi, J.M. (2004). *Taphonomy of modern corals from Madang Lagoon Papua New Guinea. Canadian Paleontology Conference Proceedings*, Actes du colloque, 2004,
- Fallon, S., Fifield, L. et Chappell, J. (2010). The next chapter in radiocarbon dating at the Australian National University: status report on the single stage AMS. *Nuclear Instruments and Methods in Physics Research Section B: Beam Interactions with Materials and Atoms*, 268(7), 898-901.
- Fink, H.G., Wienberg, C., Hebbeln, D., McGregor, H.V., Schmiedl, G., Taviani, M. et Freiwald, A. (2012). Oxygen control on Holocene cold-water coral development in the eastern Mediterranean Sea. *Deep Sea Research Part I: Oceanographic Research Papers*, 62, 89-96.
- Flessa, K.W., Cutler, A.H. et Meldahl, K.H. (1993). Time and taphonomy: quantitative estimates of time-averaging and stratigraphic disorder in a shallow marine habitat. *Paleobiology*, 266-286.
- Foerster, G., Beuck, L., Haeussermann, V. et Freiwald, A. (2005). Shallow-water *Desmophyllum dianthus* (Scleractinia) from Chile; characteristics of the biocoenoses, the bioeroding community heterotrophic interactions and (paleo)-bathymetric implications Erlangen Earth conference series (p. 937-977). United States : Springer-Verlag Berlin Heidelberg : New York, NY, United States.
- Frank, N., Freiwald, A., Correa, M.L., Wienberg, C., Eisele, M., Hebbeln, D., Van Rooij, D., Henriët, J.-P., Colin, C. et van Weering, T. (2011). Northeastern Atlantic cold-water coral reefs and climate. *Geology*, 39(8), 743-746.

- Freiwald, A. et Roberts, J.M.(2005) Cold-Water Corals and Ecosystems. Dans
Communication présentée à /au Erlangen Earth Conference Series (p. 32)
Netherland : Springer.
- Freiwald, A. et Wilson, J.B. (1998). Taphonomy of modern deep, cold-temperate
water coral reefs. [doi: 10.1080/08912969809386571]. *Historical Biology*,
13(1), 37-52. <http://dx.doi.org/10.1080/08912969809386571>
- Friedman, G.M. (1964). Early diagenesis and lithification in carbonate sediments.
Journal of Sedimentary Research, 34(4), 777-813.
- Fürsich, F.T. (1978). The influence of faunal condensation and mixing on the
preservation of fossil benthic communities. *Lethaia*, 11(3), 243-250.
- Fürsich, F.T. et Aberhan, M. (1990). Significance of time-averaging for
palaeocommunity analysis. *Lethaia*, 23(2), 143-152.
- Fürsich, F.T. et Pandey, D.K. (1998). Genesis and environmental significance of
Upper Cretaceous shell concentrations from the Cauvery Basin, southern
India. [doi: DOI: 10.1016/S0031-0182(98)00099-6]. *Palaeogeography*,
Palaeoclimatology, *Palaeoecology*, 145(1-3), 119-139.
- Ghaleb, B. et Hillaire-Marcel, C. (2006). *230Th vs. 14C age of a pre-YD deep coral
from Orphan Knoll (Labrador Sea). AGU Fall Meeting Abstracts*, Actes du
colloque, 2006,
- Ginsburg, R.N. (1954). *Early diagenesis and lithification of shallow-water carbonate
sediments in south Florida.* : SEPM.
- Greenan, B., Yashayaev, I., Head, E., Harrison, W., Azetsu-Scott, K., Li, W., Loder,
J. et Geshelin, Y. (2010). *Interdisciplinary oceanographic observations of
Orphan Knoll. SCIENTIFIC COUNCIL MEETING*, Actes du colloque,
2010,
- Greenstein, B.J. et Pandolfi, J.M. (1997). Preservation of community structure in
modern reef coral life and death assemblages of the Florida Keys:

- implications for the Quaternary fossil record of coral reefs. *Bulletin of Marine Science*, 61(2), 431-452.
- Heinrich, H. (1988). Origin and consequences of cyclic ice rafting in the northeast Atlantic Ocean during the past 130,000 years. *Quaternary Research*, 29(2), 142-152.
- Hill, T., LaVigne, M., Spero, H., Guilderson, T., Gaylord, B. et Clague, D. (2012). Variations in seawater Sr/Ca recorded in deep-sea bamboo corals. *PALEOCEANOGRAPHY*, 27(3)
- Hillaire-Marcel, C., Vernal, A.d., Bilodeau, G. et Wu, G. (1994). Isotope stratigraphy, sedimentation rates, deep circulation, and carbonate events in the Labrador Sea during the last~ 200 ka. *Canadian Journal of Earth Sciences*, 31(1), 63-89.
- Hillaire-Marcel, C., Vernal, A.d., Lucotte, M., Mucci, A., Bilodeau, G., Rochon, A., Vallières, S. et Wu, G. (1994). Productivité et flux de carbone dans la mer du Labrador au cours des derniers 40 000 ans. *Canadian Journal of Earth Sciences*, 31(1), 139-158. <http://dx.doi.org/doi:10.1139/e94-012>
- Keen, C. (1978). Cruise Report CSS Hudson 78 020, June 27 to July 19, 1978. *Atl. Geosc. Centre, Bedford Inst. Oceanogr., Int. Rep. 1*, 15.
- Kidwell, S.M. et Bosence, D.W. (1991). Taphonomy and time-averaging of marine shelly faunas. *Taphonomy: releasing the data locked in the fossil record*. Plenum, New York, 115-209.
- Kidwell, S.M. et Flessa, K.W. (1996). The quality of the fossil record: populations, species, and communities 1. *Annual Review of Earth and Planetary Sciences*, 24(1), 433-464.
- Kowalewski, M. (1996). Time-averaging, overcompleteness, and the geological record. *Journal of Geology*, 104(3), 317-326. Récupéré de geh
- Kowalewski, M. et Bambach, R.K. (2008). *The limits of paleontological resolution*. : Springer.

- Lescinsky, H.L., Edinger, E. et Risk, M.J. (2002). Mollusc shell encrustation and bioerosion rates in a modern epeiric sea: taphonomy experiments in the Java Sea, Indonesia. *PALAIOS*, 17(2), 171-191.
- McManus, J., Bond, G., Broecker, W., Johnsen, S., Labeyrie, L. et Higgins, S. (1994). High-resolution climate records from the North Atlantic during the last interglacial. *Nature*, 371(6495), 326-329.
- Meredyk, S., Piper, D., Edinger, E. et Ruffman, A. (2012b). *Composition, probable origin, and recent coral fauna of enigmatic mounds on Orphan Knoll, Northwest Atlantic Ocean. GAC-MAC annual meeting, Actes du colloque, 2012b, St. John's, NL*
- Montserrat, A.-G., Sierro, F.J. et Flores, J.A. (2011). Arctic front shifts in the subpolar North Atlantic during the Mid-Pleistocene (800–400 ka) and their implications for ocean circulation. *Palaeogeography, Palaeoclimatology, Palaeoecology*, 311(3–4), 268-280.
<http://dx.doi.org/http://dx.doi.org/10.1016/j.palaeo.2011.09.004>
- Nothdurft, L. et Webb, G. (2009). Earliest diagenesis in scleractinian coral skeletons: implications for palaeoclimate-sensitive geochemical archives. *Facies*, 55(2), 161-201. <http://dx.doi.org/10.1007/s10347-008-0167-z>
- Olszewski, T.D. (2004). Modeling the influence of taphonomic destruction, reworking, and burial on time-averaging in fossil accumulations. *PALAIOS*, 19(1), 39-50.
- Parsons-Hubbard, K.M., Callender, W.R., Powell, E.N., Brett, C.E., Walker, S.E., Raymond, A.L. et Staff, G.M. (1999). Rates of burial and disturbance of experimentally-deployed molluscs; implications for preservation potential. *PALAIOS*, 14(4), 337-351.
- Parsons, K.M. et Brett, C.E. (1991). Taphonomic processes and biases in modern marine environments. *The processes of fossilization*, 22-65.

- Parsons, K.M., Powell, E.N., Brett, C.E., Walker, S.E. et Callender, W.R. (1997). *Shelf and slope experimental taphonomy initiative (SSETI) : Bahamas and gulf of Mexico. Proc 8th Int Coral Reef Sym*, Actes du colloque, 1997,
- Piper, D.J.W. (2005). *Hudson 2004-024 Cruise Report: Geohazards on the continental margin off Newfoundland.* : Geological Survey of Canada, Open File.
- Powell, E., Staff, G., Davies, D. et Callender, W.R. (1989). Macrobenthic death assemblages in modern marine environments: formation, interpretation, and application. *Reviews in Aquatic Sciences*, 1, 555-589.
- Powell, E.N., Parsons-Hubbard, K.M., Callender, W.R., Staff, G.M., Rowe, G.T., Brett, C.E., Walker, S.E., Raymond, A., Carlson, D.D. et White, S. (2002). Taphonomy on the continental shelf and slope: two-year trends—Gulf of Mexico and Bahamas. *Palaeogeography, Palaeoclimatology, Palaeoecology*, 184(1), 1-35.
- Powell, E.N., Parsons-Hubbard, K.M., Callender, W.R., Staff, G.M., Rowe, G.T., Brett, C.E., Walker, S.E., Raymond, A., Carlson, D.D., White, S. et Heise, E.A. (2002). Taphonomy on the continental shelf and slope: two-year trends – Gulf of Mexico and Bahamas. [doi: 10.1016/S0031-0182(01)00457-6]. *Palaeogeography, Palaeoclimatology, Palaeoecology*, 184(1–2), 1-35.
- Roberts, J.M., Wheeler, A., Freiwald, A. et Cairns, S. (2009). *Cold-water corals: the biology and geology of deep-sea coral habitats.* : Cambridge University Press,.
- Roberts, J.M., Wheeler, A.J. et Freiwald, A. (2006). Reefs of the deep: the biology and geology of cold-water coral ecosystems. *Science*, 312(5773), 543-547.
- Rollion-Bard, C., Blamart, D., Cuif, J.-P. et Juillet-Leclerc, A. (2003). Microanalysis of C and O isotopes of azooxanthellate and zooxanthellate corals by ion microprobe. *Coral Reefs*, 22(4), 405-415.

- Ruffman, A. (1989). *Devonian Shelf-depth Limestone Dredged from Orphan Knoll: A 1971 Discovery and A Reassessment of the Hudson 78-020 Dredge Hauls from Orphan Knoll.* : G.S.C.
- Scott, D. (1992). *Multivariate Density Estimation: Theory, Visualization, and Practice* : John Wiley & Sons, New York.
- Sheather, S.J. et Jones, M.C. (1991). A reliable data-based bandwidth selection method for kernel density estimation. *Journal of the Royal Statistical Society. Series B (Methodological)*, 683-690.
- Sherwood, O.A., Heikoop, J.M., Scott, D.B., Risk, M.J., Guilderson, T.P. et McKinney, R.A. (2005). Stable isotopic composition of deep-sea gorgonian corals *Primnoa* spp.: a new archive of surface processes. *Marine Ecology Progress Series*, 301, 135-148.
- Sherwood, O.A., Jamieson, R.E., Edinger, E.N. et Wareham, V.E. (2008). Stable C and N isotopic composition of cold-water corals from the Newfoundland and Labrador continental slope: Examination of trophic, depth and spatial effects. [doi: 10.1016/j.dsr.2008.05.013]. *Deep Sea Research Part I: Oceanographic Research Papers*, 55(10), 1392-1402.
- Silverman, B.W. (1986). *Density estimation for statistics and data analysis.* (Vol. 26) : CRC press.
- Smith, J.E. (1993). *Late Quaternary paleoclimatic reconstruction using the deep-sea coral *Desmophyllum cristagalli*.*
- Smith, J.E., Risk, M.J., Schwarcz, H.P. et McConnaughey, T.A. (1997). Rapid climate change in the North Atlantic during the Younger Dryas recorded by deep-sea corals. [10.1038/386818a0]. *Nature*, 386(6627), 818-820.
- Sosdian, S. et Rosenthal, Y. (2009). Deep-sea temperature and ice volume changes across the Pliocene-Pleistocene climate transitions. *Science*, 325(5938), 306-310.

- Staff, G.M., Callender, W.R., Powell, E.N., Parsons-Hubbard, K.M., Brett, C.E., Walker, S.E., Carlson, D.D., White, S., Raymond, A. et Heise, E.A. (2002). Taphonomic Trends Along a Forereef Slope: Lee Stocking Island, Bahamas. II. Time. *PALAIOS*, 17(1), 66-83.
- Stanley Jr, G.D. et Cairns, S.D. (1988). Constructional azooxanthellate coral communities: an overview with implications for the fossil record. *PALAIOS*, 233-242.
- Strasser, A. et Strohmenger, C. (1997). Early diagenesis in Pleistocene coral reefs, southern Sinai, Egypt: response to tectonics, sea-level and climate. *Sedimentology*, 44(3), 537-558.
- Stuiver, M., Reimer, P.J. et Reimer, R. (2005). *CALIB 5.0*.
- Thiagarajan, N., Gerlach, D., Roberts, M.L., Burke, A., McNichol, A., Jenkins, W.J., Subhas, A.V., Thresher, R.E. et Adkins, J.F. (2013). Movement of deep-sea coral populations on climatic timescales. *PALEOCEANOGRAPHY*
- Tomasovych, A. et Schlogl, J. (2008). Analyzing variations in cephalopod abundances in shell concentrations : the combined effects of production and density-dependent cementation rates. *Palaeogeography Palaeoclimatology Palaeoecology*, 23, p. 648–666.
- Vogel, J.S., Nelson, D. et Southon, J.R. (1987). Carbon-14 background levels in an accelerator mass spectrometry system. *Radiocarbon*, 29(3), 323-333.
- Walker, S.E., Parsons-Hubbard, K., Powell, E. et Brett, C.E. (2002). Predation on experimentally deployed molluscan shells from shelf to slope depths in a tropical carbonate environment. *PALAIOS*, 17(2), 147-170.
- Walker, S.E., Parsons Hubbard, K., Powell, E.N. et Brett, C.E. (1998). Bioerosion or bioaccumulation? Shelf-slope trends for EPI-and endobionts on experimentally deployed gastropod shells. *Historical Biology*, 13(1), 61-72.
- Wood, R. (2011). Taphonomy of reefs through time *Taphonomy* (p. 375-409) : Springer.

Zuschin, M., Stachowitsch, M. et Stanton, R.J. (2003). Patterns and processes of shell fragmentation in modern and ancient marine environments. [doi: DOI: 10.1016/S0012-8252(03)00014-X]. *Earth-Science Reviews*, 63(1-2), 33-82.